METHANE ADSORPTION INTO SANDSTONES AND ITS ROLE IN GAS RECOVERY FROM DEPLETED RESERVOIRS.

HAYATU BASHIR
(B.Eng., M.Sc.)

PhD Thesis **2018**

Methane Adsorption into Sandstones and its Role in Gas Recovery from Depleted Reservoirs.

HAYATU BASHIR
(B.Eng., M.Sc.)

School of Computing, Science and Engineering
University of Salford,
Manchester, UK

Submitted in Partial Fulfilment of the Requirements of the Degree of Doctor of Philosophy, April 2018

Declaration

I declare that this thesis is a presentation of my original research work. Wherever contributions of others are involved, every effort is made to indicate this clearly. This study has not been previously submitted for a degree or a similar award at any institution. The work was done under the supervision of Dr Yu Wayne Wang, at the University of Salford, Manchester, United Kingdom.

Abstract

Depleted gas reservoirs represent the most viable option for research and development and are the most preferred method for Enhanced gas recovery and sequestration application. The adsorption process acts as a displacement mechanism in the enhanced gas recovery, therefore investigating this process will lead to a better understanding of methane recovery in the EGR-CO_2 process. Despite many pilot studies on EGR-CO_2 in depleted reservoirs, no projects have moved to commercial phase, due to both technical and economic issues. This research demonstrated the role of adsorption as a mechanism for gas displacement in the EGR-CO_2 process by investigating the interaction of the mineral components of sandstones (i.e. Quartz, Plagioclase, feldspar and clays), with methane (CH_4), the effect of pressure and the interaction between water/brine and methane (CH_4) gas in a competitive sorption environment for sandstones and their constituents.

The first series of tests were conducted using commercial helium pycnometer to quantify the effect of experimental parameters (pressure, contact time) and water on void volume of sandstone core samples. The average of the measured void volume using helium was 8.017cm^3 for *Bandera* and 4.5171cm^3 for the *Scioto* sandstones with a deviation of less than 0.002 cm^3 and 0.001 cm^3 indicating little dependence on pressure in void volume measurement. Water content of 5.62 wt. % and 5.48wt. % for both samples respectively can reduce the dry capacity by as much as 12.53% and 11.20%.

Subsequently, a manometric adsorption apparatus was self-fabricated specifically for this research to quantify the methane adsorption capacity of sandstone cores samples. The experiments were conducted using dry sandstone core samples. Methane (CH_4) adsorption capacity of sandstones was investigated using dry sandstone samples. The methane (CH_4) adsorption capacity varied for the different sandstone types, which for the present studies *Bandera* and *Scioto* are considered. The *Scioto* sandstone has the largest CH_4 adsorption capacity of the tested samples with a maximum amount of adsorbed CH_4 of 0.110 mmol/g while the *Bandera* sandstone had significantly less CH_4 sorption capacity with a maximum amount of adsorbed CH_4 of 0.089 mmol/g. Using X-ray diffraction (XRD) results, the *Scioto* sample had the highest total amount of clays present (22%) compared to *Bandera* (14%) and had the highest adsorption capacity. The previous analyses imply that high content of clay minerals in the *Scioto* sample relative

to the *Bandera* provides extra surface area for adsorption of methane (CH_4). As a result, it can be concluded that there exists a correlation between methane (CH_4) adsorption capacity and surface area of clay present in the samples.

Finally, the methane (CH_4) adsorption capacity of sandstones saturated with water or brine at a particular water/ brine content (33, 65 and 91%) was investigated. The analysis showed that for water saturated core samples the CH_4 adsorption capacity decreased by 47.21, 54.47 and 60.89 % for *Scioto* and 10.26, 24.36, and 38.03% for *Bandera* relative to dry core samples. The loss of methane adsorption capacity was due to increase in water content (33, 65 and 91%) and was much lower than that of dry samples at the same experimental pressure (0 - 400 psia). The presence of brine in sandstone samples caused an overall decrease in methane adsorption capacity of 30.17,43.57 and 69.83% for *Scioto* and 28.90, 42.58 and 52.85% for *Bandera* compared to dry samples. These results indicate that methane adsorption of clay minerals found in a combined state with sandstone rock fabric as the case in real reservoirs will be influenced by its structural, physical, geotechnical, and geological properties.

Experimental data verification were conducted using the repeatability and best fit method. Two replicate runs were conducted to investigate the reproducibility of the isotherm measurements. The average data deviation was 0.33 and 0.42 for dry Scioto and Bandera samples respectively, while the deviations were 3.85 and 3.59 for samples saturated with water and brine respectively between the first and repeat experiments. Excellent repeatability of experimental data for both sandstone samples (*Scioto* and *Bandera*) was observed.

Dedication

*This work is dedicated to "**ALMIGHTY ALLAH**", the originator, the true innovator, the source and owner of all knowledge*

Acknowledgements

First and foremost, I'd like to thank Allah the Almighty for giving me such a wisdom and capability to reach such a milestone accomplishment, and to his messenger, Prophet Muhammad (Peace be upon him) for his guidance and teaching of morality which guided me throughout this period.

I'd also like to extend my profound gratitude to my excellent team of supervisors, Dr Yu Wang, Dr Abubakar Jibrin Abbas, Dr Martin Burby and Dr Edmund Chadwick for their constant support, kindness and guidance, without which nothing could have been possible during this study. I'd also like to acknowledge the effort of Mr Alan Maplin for his help and support in the laboratory during the cause of conducting most of my experiments for this study. I am profoundly grateful to my sponsor, Petroleum Technology Development Fund (PTDF), for considering me worthy of a PhD Sponsor.

I'd also like to acknowledge and thank my Father, Engineer Bashir Abdullahi and my Mother, Hajia Hauwa Bashir for their unconditional support and inspiration throughout my life, without which, nothing could have been possible in my career. I am short of word in expressing my exact gratitude for you except with these novel verses in the Qur'an (Isra 17: 23-24) "And lower unto them the wing of submission and humility through mercy, and say: My Lord! Bestow on them your mercy as they did bring me up when I was young." (Isra 17:23-24).

Prominently, I must acknowledge the unconditional love and care I enjoyed from my lovely wife (Nabila) and daughter (Fatima Zarah), whose support, encouragement and patience is no doubt instrumental to everyday achievement I have throughout the cause of this study. A special thanks to my in-laws for their continuous support and guidance. May Allah reward you abundantly.

To my beloved siblings to mention, in particular, Mukhtar, Naja'atu, Hadiza, Namadina, Mustapha, Ibrahim, Asiya, Billy for their immense care and support both in Kind and Morally. To my family members, nonetheless, to the families of my Aunty (Hajjia Turai Yar'adua), uncle (Alhaji Mukhtar Maimaje) for their endless support and encouragement, May Allah bless you all in abundance.

Last but not the least, I'd like to extend my gratittude to the so many friends and family members that supported me, notably; those we have shared so many times of educational hustle for their contribution both academically and socially to mention but few, Sa'id Kori, Aminu Abba, Abdulkadir Sani, Aliyu Tukur, Aminu Abba, Murtala Mohammed, Umar Iliyasu, Abdullahi Aneco, Ramadan Bonadour, Ibrahim surajo, Salihu Maiwalima, Dr. Abubakar Shinkafi among many others. Also to my friends Abdullahi Abdulazeez, Gidado Mainasara, Faisal Jafar, Ibrahim Shika, Yusuf Dandume, samaila Abdullahi gobir, and all others whose names were not mentioned for their commitment, solidarity and being there always for me.

List of Publications

Journal Papers

Bashir. H, Wang. Y, Abbas. A (2016). On void volume Determination in Clay Rich Shale. Journal of International Journal of Latest Trends in Engineering and Technology, Volume 7, Issue 2:216 - 220. DOI: http://dx.doi.org/10.21172/1.72.535.

Bashir. H, Wang. Y, Burby, M (2016). A comparative evaluation of adsorption in clay-dominated shale. Journal of International Journal of Latest Trends in Engineering and Technology. Volume 7, Issue 2: 269-281. DOI: http://dx.doi.org/10.21172/1.72.545.

Bashir. H, Wang. Y, Abbas. A (2016). Two-phase flow in clay-rich shale. Journal of Petroleum Engineering & Technology. Volume 6, Issue 3: 44–53p. ISSN: 2321-5178.

Bashir. H, Wang. Y, Abbas. A (2016). Construction/assembling of a low-cost adsorption apparatus for cored clay shales**.** Journal of Petroleum Engineering & Technology. Volume 6, Issue 3: 54–60p. ISSN: 2321-5178.

Bashir. H, Wang. Y, Abbas. A (2016). Chemical potential of water from Monte Carlo simulation: the fundamentals**.** Research and Review: Journal of Physics. Volume 5, Issue 3: 16–27p. ISSN: 2347-9973.

Conference paper presentation

Bashir. H, Wang. Y, A. Abbas, Burby, M (2016). Theoretical fit of adsorption isotherm in cored clay shale. In 4th international conference on Petroleum engineering. Crowne Plaza, Heathrow, London, UK, August 15-17, 2016.

Table of Contents

List of Tables

List of Figures

List of symbols

Symbol	Physical Quantity
Psia	Pound per square inch absolute
MPa	Mega Pascal
^{0}C	Degree Celsius
Mpa	Mega Pascal
Cm	Centimetre
In	Inches
P	Pressure
r	radius
L	Length
π	Pi
V_b	Bulk Volume
V_v	Void volume
V_g	Grain volume
V_c	Sample Chamber Volume
V_r	Reference Chamber Volume
V_v	Valve Displacement Volume
P_1	Absolute Initial Reference Volume Pressure
P_2	Absolute Expanded Pressure
Pa	Absolute Atmospheric Pressure Initially in Sample Chamber
PL	Langmuir Pressure
VL	Langmuir volume
V_{ads}	Volume of methane adsorbed
T	Temperature
m	Mass of gas
n	No of moles
V_{free}	Volume of free gas
$m_{ads}{}^{excess}$	Excess adsorption capacity
n_{total}	Total no of moles
x	Amount of adsorbed
k and n	Freundlich empirical constants
K_R, a_R, and g	Redlich-Peterson isotherm constants
CH_4	Methane
CO_2	Carbon dioxide
Mins	Minutes
Hrs	Hours
$m^{He}{}_{trans}$	Helium transferred
V_{Rc}	Volume of reference cell

$\rho_{Rc}{}^{He}$	Density of helium in reference cell
$\rho_{sc}{}^{He}$	Density of helium in sample cell
ΔV_{ads}	Change in adsorbed volume
ΔV_{sw}	Changes in volume due to swelling
ΔV_{rec}	Changes in volume due to reaction
Wt %	Weight percent
%RH	Percentage relative humidity
DA	Dubinin–Astakhov Isotherm
BET	Brunauer–Emmett–Teller Isotherm
m_{dry}	Mass of the dry sample
m_{wet}	Mass of the wet sample
w_c	Water content
SE	Sum of squares due to error
RMSE	Root mean squared error
R^2	Coefficient of multiple determination
Gigatonnes Carbon	GtC
Enhanced gas recovery and sequestration	EGR-CO_2

CHAPTER 1

1 INTRODUCTION

1.1 Research Background

Securing the energy supply of the future will require the application of innovative approaches to overcome existing energy crisis. These challenges, which include a shortage of hydrocarbons, increasing crude oil prices, logistical problems and increased carbon dioxide emissions, have compelled stakeholders in the gas and oil industry to develop innovative approaches when exploiting natural resources (Max., 2013). On the other hand, there has been growing interest from governments around the world about the impact of discharging CO_2 into the atmosphere, which contributes to global warming (Stein et al., 2010). So far, the solutions proposed as sustainable to overcome this energy crisis include using renewable energy source, efficient fuel consumption, and biomass fuel source (Ampomah et al., 2015). Among the prior sustainable technologies is EGR-CO_2 (Enhanced gas recovery and sequestration). This process is regarded as an efficient and effective method that can be adopted for the reduction of CO_2 emission into the atmosphere (IPCC. 2005, Hester and Harrison. 2010, Baines and Worden. 2004; Dai et al., 2014; Bachu. 2015, Ampomah et al., 2015). Enhanced gas recovery and sequestration (EGR-CO_2) is a process that combines Carbon Capture and Sequestration (CCS) with Enhanced gas recovery. It is used to recover natural gas mainly methane by injecting CO_2 in natural gas reservoirs. Recovery of natural gas is highly efficient, leaving a significant amount of void space and surface area to store CO_2 (Stevens et al., 2001). Despite the viability of producing methane from gas reservoirs by injecting CO_2 using a process were CO_2 replaces methane using adsorption mechanism in the gas reservoir by Enhanced gas recovery and sequestration (EGR-CO_2), significant amounts of methane remain unrecoverable, retained through interactions with minerals in gas reservoirs. Releasing the trapped CH_4 through these processes requires understanding adsorption interaction of sandstone and its components (i.e. clay) with methane (CH_4) and developing strategies that will permanently enhance the retention of Carbon dioxide (CO_2). Moreover, precise

knowledge of methane (CH_4) induced interactions between CH_4, water or saline formation fluid and reservoir rock, and of the impact of gas adsorption on these two-phase reservoirs is critical to the optimisation of these reservoir types.

An essential starting parameter, determined in the laboratory, is the methane (CH_4) storage potential of core samples, being the sum of the adsorption and void volume. Accurate determination of void volume is a critical step in an adsorption isotherm experiment since the amount of adsorbed gas is calculated using the previously calculated void volume data. However, the parameters affecting both the adsorption capacity and void volume calculation of sandstones are not entirely understood.

The assessment of the adsorption capability of a microporous solid involves the quantification of a certain amount of adsorbant in this case, a gas present at the surface of the adsorbent at different pressures under a certain temperature to obtain an adsorption isotherm. It is then fitted to a theoretical model to analyse certain parameters (Adsorption volume, pressure). In general, the adsorption capacity of these materials depends on:

- The distribution of pore sizes in the material (Ross & Bustin., 2007; Heller and Zoback., 2015),
- The molecular size of the adsorbate gas (Sing et al., 1985; Roquerol et al., 1999; Ross & Bustin., 2007, Anovitz and Cole., 2015, Aljaman et al., 2010).
- The combined interfacial forces and energy of the surface material and the adsorbate gas (Langmuir., 1916; Brunauer et al., 1938).

Due to the importance of adsorption mechanism for gas storage, numerous authors (Ross & Bustin., 2007; Ji et al., 2012; Liu et al., 2013, Heller and Zoback, 2014) have made valuable contributions to the literature through both laboratory studies and modelling to characterize adsorption of various rocks found abundantly in different categories of geological formation. Many theoretical isotherm models (Langmuir., 1916; Brunauer et al., 1938, Freundlich., 1906; Redlich and Peterson., 1959) have been formulated and used for fitting experimental data. Among them, the Langmuir isotherm, which is the most widely implemented, represents the adsorption of a monolayer of molecules on the surface of a material considering an ideal surface (Langmuir, 1916). The assumptions of the Langmuir model (Do., 1998) are:

- The surface is homogeneous, and the adsorption energy is constant over all sites.
- Adsorption on the surface is localised, and adsorbed atoms or molecules are adsorbed at individual, restricted sites.
- Each site can accommodate only one molecule or atom.

The assumptions in Langmuir isotherm are simple and might not hold for depleted sandstone gas reservoirs of interests, and CO_2 storage purpose (Li et al., 2015). There are a lot of literature on methane(CH_4) adsorption measurements with respect to CO_2 capture storage and sequestration for coal (Salmachi., 2013; Holloway., 2013; Zhang et al., 2016; Paschke & Dreisbach., 2013), and shale gas reservoirs (Godec et al., 2013,2014; Boosari et al.,2015). However, for Powdered clay (Ji et al., 2012; Liu et al., 2013; Heller and Zoback, 2011, 2014) only a few exist with sketchy details. On the other hand, reports on methane (CH_4) adsorption measurements of depleted sandstones gas reservoirs are few. This research aims to contribute to these critically needed and sought for information.

This thesis is composed of two parts: first, a commercial helium pycnometer was used to quantify the effect of experimental parameters (pressure, contact time) and water on void volume of sandstone core samples; secondly, a manometric adsorption apparatus was self-fabricated specifically for this research to quantify the methane adsorption capacity of sandstone cores samples. The experiments were conducted using dry and sandstone core samples saturated with water and brine. The aim of using the wet samples was to investigate the effect of pre adsorbed water or brine at a particular content (33, 65, and 91%) on the methane adsorption capacity of sandstones. Experimental data verification were conducted using the repeatability and best fit method.

1.2 Depleted reservoirs as a means of Enhanced gas recovery and Sequestration (CO_2-EGR)

The first reported natural gas storage using pipeline in depleted gas reservoirs during summer for later utilisation in the winter was in the US in 1915(Jordan., 1959, Davis., 1951). About 339 reservoirs with a capability to store about 211x109 m^3 (7.437 TSCF) of natural gas were in existence in 26 states in the United States by 1979; these gas reservoirs had a seasonal withdrawal of $1.1x10^9$ m^3 (39.7 BSCF). The main types of reservoirs used for these operations were depleted gas reservoirs, which provided about 80% of storage capacity with the remaining 20% provided by aquifer-filled reservoirs at a pressure range of 300 to 4,000 psi (Mamora et al., 2002). There are about 630 underground ground storage facilities worldwide with the United States having 394 underground storage facilities out of which 37 were classified as marginal (there was no injections or withdrawals, or withdrawals only were made) at the end of 2005 (EIA., 2006). 410 underground natural gas storage facilities were in operation in 1998, with an increase to 418 operational sites in 2001. However, between 1998 and 2005, 26 new sites were placed in service, and 42 facilities were depleted or abandoned while in Europe around 120 facilities were still in operation as at 2006 (EIA., 2006). Depleted oil/gas fields (478 or 76%) are the major types of reservoirs that have been utilised for Underground gas storage (UGS), with aquifers (80 or 13%) outnumbering those in salt caverns (66 or 11%) (Evan and West. 2008). The storage capacity available in depleted gas reservoirs worldwide for CCS is estimated to be 140 Gigatonnes Carbon (Sobers et al., 2004). Studies (IEA GHG Programme in 1993) evaluate an extra storage capacity of about 670 Gigatonnes Carbon (GtC) CO_2 (assuming the volume of recovered hydrocarbons could be replaced by carbon dioxide) in abandoned gas reservoirs (Taber et al., 2012). Currently considered storage options (Figure 1.1) for CO_2 in geological media include:

- Injection into depleted oil and gas fields
- Deep aquifers
- Using CO_2 for enhanced gas recovery (EOR)
- Enhanced coal bed methane recovery (ECBM)
- Deep unmineable coal seams

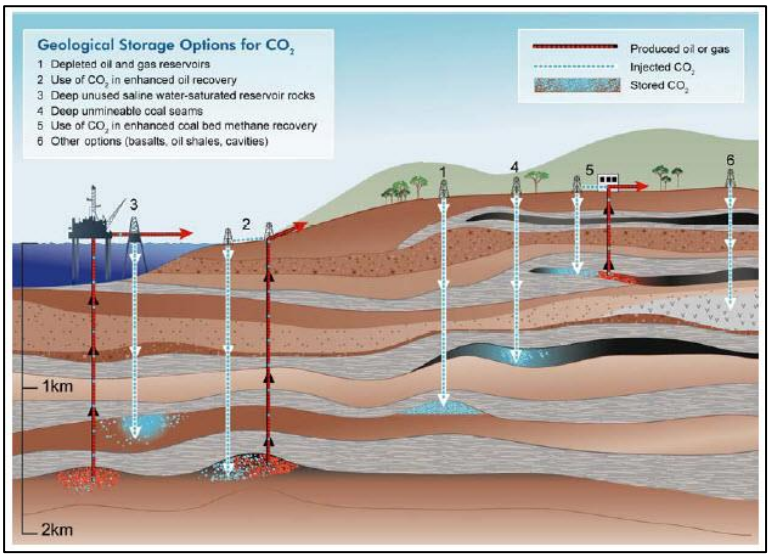

Figure 1.1: Geological storage opportunities (IPCC, 2005)

Depleted gas reservoirs represent the most viable option for research and development and are the most preferred method for Enhanced gas recovery and sequestration application (Holloway, 2004; Jenkins et al., 2012). Research and development projects using depleted gas reservoirs include; Five Metric tonnes(Mt) of acid gas (CO_2 and H_2S) safely stored in depleted gas reservoirs in Canada (Bachu & Haug., 2005), the European Union-funded, Ketzin, (Schilling et al., 2009), Total, Lacq, (Aimard et al., 2007) in Germany and France respectively. These demonstration prototypes are projected to increase the scientific understanding of the processes and impact of enhanced gas recovery and carbon dioxide sequestration (EGR-CO_2). The scientific analyses of which are made readily accessible and ally the public, which may otherwise block the implementation of this technology (Jenkins et al., 2012).

As a possibility for mitigating greenhouse gas emission, the use of depleted gas reservoirs in capturing and long-term storage of massive amounts of carbon dioxide (Figure 1.2) using technologies such as EGR-CO_2 (Gniese et al., 2013) provides a long-term solution to reducing CO_2 emissions to the atmosphere.

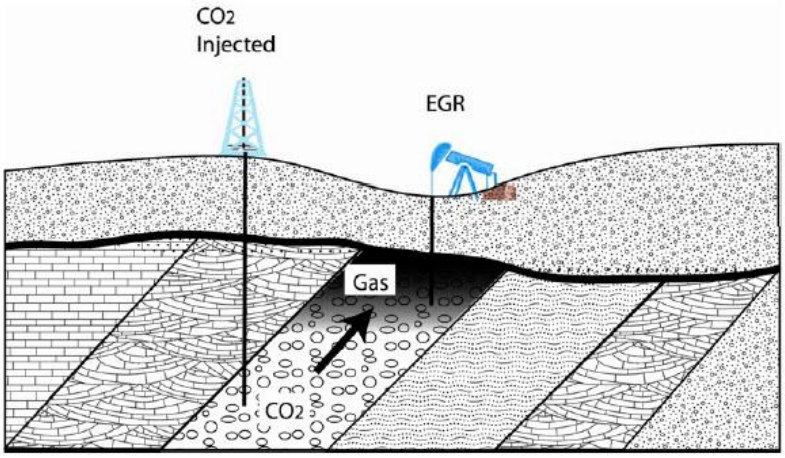

Figure 1.2: Schematic of enhanced gas recovery and CO_2 Sequestration (Gniese et al., 2013).

They are the most efficient among other systems for isolating greenhouse gas emissions (Benson & Cook., 2005; Bachu et al., 2007; Loizzo et al., 2009; IEA, 2009). These types of deep geological formations have advantages (Pawar et al., 2006; Van der Meer et al., 2006) such as;

- The geological structure and physical properties of these reservoirs are well understood.
- They have adequate integrity and safety to trap reservoir gases.
- Storage costs are compensated by the saving of using some of the existing infrastructure and wells for handling CO_2 storage operations and by the sale of the additional gas recovered in the case of enhanced gas recovery (Azin et al., 2008).

An efficient way of decreasing CO_2 emissions into the atmosphere would be to implement the methods outlined by the U.S. Department of Energy, which involves recycling CO_2 from sources of broad emission and thus injecting it into depleted gas reservoirs. In Europe and North America, thousands of gas fields are approaching or are already past their productive economic duration. These gas reservoirs are depleted or have already been abandoned. Many of these formations could act as active sequestration sites for CO_2 disposal (Taber et al., 2012). The injection of CO_2 into geological formations (oil reservoirs) has been practised for years to improve oil recovery (Stalkup., 1984, Jarrell et al., 2002, Stein et al., 2010). However, the effect depends on the efficiency and suitability of the different types of reservoirs, i.e.

depleting/depleted oil and gas fields, deep saline aquifers, the deep ocean, coal seams. Relative to storage in saline aquifers, CO_2 injection in depleted gas reservoirs will enhance methane production, where the increased revenues generated can be used to offset the costs of CO_2 Sequestration. Furthermore, the risk of leakage is low, as the in-place methane has proven that adsorption, retention and seal have been there effectively for millions of years (Godec et al., 2013). For Oil reservoirs, the presence of water either injected during the recovery processes or invaded because of reservoir pressure decline, decreases the available storage for Carbon dioxide (CO_2). The CO_2 storage capacity in water as dissolved gas is much less than that of CO_2 as supercritical gas in empty pores. Meanwhile, the residual oil saturation after most tertiary recovery methods is still as high as 30% (Schumacher. 1980). It has been found that compared to the depleted natural gas reservoir with a similar pore volume a depleted oil reservoir can store significantly less CO_2 (Wang et al., 2009). The reasons for the reduced storage is due to two primary reasons (Mamora et al., 2002):

- The gas recovery (about 65% of initial gas-in-place) is typically about twice that of oil (average 35% of initial oil in place). In addition, gas density – in-situ gradient about 0.08 psi/ft. is significantly less than that of oil, which is typically about 90.27 psi/ft. There is, therefore, less hydrocarbon remaining in a gas reservoir than in an oil reservoir under the same recovery process.

- Methane gas is 30 times more compressible than oil or water. At 200 psia (1.38 MPa), the isothermal compressibility of natural gas is typically about $500x10^{-6}$ psia ($3.46x10^{-6}$ MPa) versus $15x10^{-6}$ psia ($1.37x10^{-7}$ MPa) for oil and $3x10^{-6}$ psia ($2.48x10^{-8}$ MPa) for water.

Coal seams have a higher affinity to adsorb gaseous carbon dioxide than methane (Cracknell et al., 1996; Dreisbach et al., 1999; Kurniawan et al., 2006; Liu and Wilcox., 2012). Carbon dioxide (CO_2) in coal seams can displace methane, at the same time enhancing Coalbed methane (CBM) recovery (Paschke & Dreisbach., 2013; Gensterblum, 2013). However, a depth of less than 1000 m (Metz et al., 2005; Mazumder et al., 2006) restricts them.

Saline formations are sedimentary rocks saturated with formation waters or highly mineralized brines, which have a relatively high affinity for CO_2. Their storage capacities are significantly greater than those of gas reservoirs, and are more likely to be found close to large CO_2 point sources. However, these sites are still relatively poorly understood regarding their properties and characteristics compared to gas fields.

Geologic sequestration literature (Bachu et al., 1994; Freund and Ormerod., 1997; Holloway., 1997, 2004; Hitchonetal., 1999; Bachu., 2000; Busch et al., 2008; Hovorka et al., 2009) shows that the main sequestration sites include:

- Depleted hydrocarbon reservoirs such as depleted oil and gas repositories.
- Brine-bearing "saline" formations & Ocean storage, at approximately 3,000-meter depth.
- Unmineable coal seams.
- Natural and human-made caverns, unused porous and permeable reservoir rocks, if the CO_2 can be maintained at supercritical conditions by injecting it deep underground (800-1000 meters minimum).

These sequestration sites have received attention but have been limited by time constraints and considerable logistical problems (Ehlig-Economides and Economides, 2009). By far the best and most practical option among these choices for bulk carbon dioxide injection is an abandoned gas reservoir depleted without active water drive (Li et al., 2005; Ehlig-Economides and Economides, 2009).

1.3 Research Problem Statement

Thousands of gas fields are currently in production; most of them are past their economic output and will become depleted in the coming decades (Bolourinejad, 2015). These fields are close to abandonment or have already been abandoned. An Estimated capacity of as much as 140 Gigatonnes Carbon (GtC) can be sequestered into depleted or abandoned natural gas reservoirs, with about 10 to 25 Gigatonnes Carbon (GtC) in the United States alone (Oldenburg et al., 2001). Emissions from the combustion of fossil fuels, especially of carbon dioxide (CO_2) into the atmosphere, have caused global warming and adverse climate fluctuations and is becoming a source of global concern.

The amount of gas in depleted reservoirs at abandonment pressure is of interest since it has to do with the mechanics of the storage reservoirs. Abandonment pressure varies for different gas fields, with values ranging from 50 – 100 psia or 0.34 – 0.69 MPa (Okwananke et al., 2011) or range of 50.76 and 116.03psia or 0.35 and 0.80 MPa (MacRoberts, 1962; Okwananke et al., 2011, Yekeen Adeboye & Sulaimon 2011, Mathias et al., 2014). Singh et al., (2011, 2012) considered an initial pressure of 580.151psia or 4.0 MPa, Han et al., 2012 considered an initial pressure of 999.31psia (6.89 MPa), Mukhopadhyay et al., 2012 presented numerical simulations concerning CO_2 injection into a depleted gas reservoir at 72.5189 psi or 0.50 MPa. Afanasyev, 2013 assumed a minimum initial pressure of 652.67psia (4.50 MPa) and Ziabaksh-Ganji & Kooi, 2014 assumed an initial pressure of 870.226 psi (5.90 MPa). Most previous work relating to Enhanced gas recovery and CO_2 sequestration in depleted gas reservoirs used simulation with investigated pressures ranges higher than 1450.38 psi or 10.0 MPa (Andre et al., 2010; Mathias et al., 2013), and mainly investigated the effect of CO_2 injection on depleted gas reservoirs. The effect of methane (CH_4) adsorption at abandonment pressure of depleted reservoirs is yet to be evaluated.

Several investigators found positive correlations between clay content and adsorption capacity (Gasparik et al., 2012; Ji et al., 2012; Schettler and Parmely., 1991; Merkel et al., 2015). Compared with extensive studies of CO_2 adsorption in depleted reservoirs, less attention has been paid to CH_4 adsorption of clay minerals, although clay minerals are a critical component of sandstone. This lack of research may be because it is assumed that clay minerals have higher hydrophilicity and low porosity; consequently, it is expected that clay minerals would encounter difficulty in the adsorption of methane (CH_4). However, recent studies (Cheng and Huang., 2004; Lu et al., 1995; Ross and Bustin., 2009) have shown the ability of clay minerals for methane (CH_4) adsorption. Although the above-mentioned studies examined the CH_4 absorption capacity of clay minerals, unfortunately, the CH_4 adsorption mechanisms, including CH_4 adsorption sites and influencing factors, remain unclear (Liu et al., 2013). Advanced imaging techniques have revealed the amount of microporous clays (Kaolinite, illite, Chlorite) can vary in sandstones from very little to high; which have high adsorption capability due to their large surface area. As a result, adsorption is an important mechanism of sandstone

reservoirs for gas storage. The clay content in depleted sandstone gas reservoirs exhibits methane (CH_4) gas storage capacity at the depleted adsorption sites.

The use of helium as an inert gas to determine the buoyancy or void volume of samples, in gravimetric and manometric/volumetric adsorption methods respectively is widely utilised in adsorption measurements (Gensterblum., 2013; Wang et al., 2013; Gasparik et al., 2014; Rexer et al., 2014). The use of Helium as an inert gas for void volume measurement has been a subject of debate between researchers (Charles et al., 1969; Sing et al., 1985; Lu et al., 1993, 1995; Roquerol et al., 1999; Krooss et al., 2002; Goodman et al., 2004, Zhang et al., 2011; Mohammed et al., 2009; Sakruvos et al., 2009; Gasparik et al., 2013, 2014). The impact of helium adsorption on the void volume measurements of microporous adsorbents (clay-shale, sandstones, powdered pure clay) is a still a contentious issue. In the literature, there is no unanimous agreement among the different authors. In the laboratory, errors in void volume measurements affect the accuracy of adsorption analysis. These errors in measured void volume occur not from the efficiency and accuracy of the measuring devices but because of the primary measurements of experimental parameters. The sources of error involved in void volume determination when using helium for void volume evaluation as suggested by researchers (Ross and Bustin, 2007; Muhammed et al., 2009) include:

- Selection of helium as an appropriate inert gas (Sing et al., 1985; Lu et al., 1993, 1995; Roquerol et al., 1999, Krooss et al., 2002; Goodman et al., 2004; Ross & Bustin., 2007; Zhang et al., 2011).
- Averaging the void volume values for multiple pressure steps (Chareonsuppanimit et al., 2012; Gasparik et al., 2012, 2014, Heller and Zoback., 2014; Rani et al., 2015).
- Contact time (Ross and Bustin, 2007; Gasparik et al., 2013).
- The presence of water (Ekrem et al., 2003; Ross & Bustin., 2007; Muhammed et al., 2009).

Methane (CH_4) gas adsorption capacities are typically reported on a dry basis, neglecting water or brine content and adsorption onto clay surfaces. The presence of water in reservoirs has negative impact on adsorption capacity (Don & Ann., 1981; Hovorka et al., 2009; Fischer et al., 2010; Yu et al., 2012) of the sandstone in gas

reservoirs. Researchers with interest in gas reservoirs have a general agreement that water has adverse effect on methane adsorption of reservoirs in general (Gasparik et al., 2013; Ross and Bustin., 2007; Tan et al., 2014; Yuan et al., 2014; Merkel et al., 2015). The ratio of adsorbed and free gas is strongly dependent on the water saturation of the sandstone, but quantitative impact analyses are not available in the literature. While the impact of water on methane adsorption using powdered clay minerals have been investigated (Ji et al., 2012; Heller and Zoback, 2011, 2014; Jin and Foozabadi, 2014; Liu et al., 2013), studies on the impact of water on the methane adsorption capacity of water or brine saturated sandstones are few. Notwithstanding, the effect of water on the adsorption behaviour of methane and on enhanced gas recovery and sequestration, is still not sufficiently understood.

In the case of the absence of sufficient data to characterise methane (CH_4) adsorption capacity of sandstones, it will be hypothesised that clays in sandstone will behave like coal, which preferentially adsorbs carbon dioxide (CO_2) compared to methane (CH_4). However, the contribution of methane(CH_4) adsorption in depleted sandstone reservoirs has always been neglected, in spite of that, it could provide insight of the adsorption displacement process of Enhanced gas recovery and Carbon dioxide Sequestration in depleted reservoirs. So far, the following questions of critical interest have not been fully answered or understood:

1. What factors will influence the process of evaluating the void volume?
2. How reliable are the current method using helium to quantify the void volume as part of the adsorption quantification process in sandstone?
3. Which parameters control gas storage of sandstone core samples at depleted reservoir pressure?
4. What role does methane (CH_4) adsorption play in depleted reservoirs during the displacement process of EGR-CO_2 (Carbon Sequestration and Enhanced gas recovery) Process?
5. How does the presence of water and brine affect methane (CH_4) adsorption of sandstones?

This study helps in addressing this knowledge gap. First, experimental studies of the interactions between sandstones and its components (i.e. Clays) with CH_4 were designed to study the effect of pressure, contact time and water on void volume as part of the methane adsorption capacity measurement. Secondly, the impact of adsorption mechanism at equilibrium and abandonment pressure of gas reservoirs was studied by measuring the adsorption capacity of dry and sandstone core samples saturated with water or brine.

This study particularly provides researchers with a detailed analysis of methane (CH_4) adsorption data of sandstones from the initial void volume measurement to the methane adsorption capacity of dry, and sandstones core samples with preadsorbed water and brine, such that effect of adsorbed methane in sandstone depleted reservoirs could be accounted for while increasing gas recovery. Researchers will gain an understanding of CH_4 adsorption process, which can be contrasted with data from carbon dioxide (CO_2) adsorption to understand how the displacement process by adsorption can be optimised to improve the enhanced gas recovery and sequestration (EGR-CO_2) implementation process. It is the hope of the author that the contribution in knowledge from this research will help when developing strategies for permanently enhancing the retention of Carbon dioxide (CO_2) in depleted reservoirs.

1.4 Research objectives:

1. Conduct an experimental study on the effect of pressure, equilibrium time and water content on void volume measurement.
2. Evaluate methane adsorption of sandstones using a self-assembled manometric adsorption set up;
3. Apply existing adsorption theoretical isotherms (Langmuir, Freundlich, Redlich Paterson) using experimental data to find the best-fit isotherm which describes adsorption sandstone reservoirs.

1.5 Research Contributions

This work aims to contribute to the investigation of adsorption at solid–gas interfaces of sandstones in gas reservoirs and Increase the knowledge of the role of methane(CH_4) adsorption as a displacement process in CO_2-EGR (Carbon Sequestration and Enhanced gas recovery), especially in depleted reservoirs. This will lead to the understanding of the physical mechanism of adsorption in depleted reservoirs since the study of adsorption is necessary to optimise the CO_2-EGR processes. The following research questions of critical interest are answered by this thesis in order to contribute to knowledge:

a. Can helium be used as an inert gas in void volume estimation?

b. What factors will influence the process of evaluating the void volume?

c. How does the presence of water and brine affect the methane (CH4) adsorption capacity of sandstones?

d. Which parameters control adsorbed gas storage of sandstone core at the simulated temperature and variable pressure?

e. The effect of methane adsorption in sandstones and its role in depleted reservoirs during the displacement process of CO2-EGR (Carbon Sequestration and Enhanced gas recovery).

The first question regarding the use of Helium as an inert gas for sandstone specifically was, what fraction of the void volume of the sandstone core sample could be considered available for the free gas phase? The results regarding reliability indicate that:

Helium can be used to determine the void volume of sandstones accurately. However, using other gases for examples argon has the potential to be adsorbed therefore leading to inaccurate void volume determination (Rani et al., 2015; Moghadam, 2013).The averaging of pressure shows constancy of average void volume with pressure in sandstone core sample indicating helium adsorption at the surface of the investigated samples was not in observable quantity and can be neglected. This means helium was not adsorbed in both sandstone core samples at the investigated pressure (15 - 115 Psia or 0.10 – 0.79 MPa). If helium were adsorbed, then the graphical plot of void volume as a function of experimental pressure would behave like an adsorption isotherm. It can be concluded that reported negative adsorption (Ross and Bustin. 2007, Merey. 2009)

caused by overestimation of void volume by helium comparable to methane at high pressure is not applicable to sandstones at investigated experimental pressure ranges (i.e., 15 – 115Psia or 0.10 – 0.79 MPa).

Secondly, considering the dramatic effect of water on the void volume estimation and the fact that free gas storage calculations for adsorbed methane are usually performed using void volume measured on dry samples. These observations imply that most calculations are massively overestimating the void volume of sandstones. Experimental investigation showed that water content of 5.62 wt. % and 5.48wt. % for both sandstone samples respectively can reduce the dry capacity by as much as 12.53% and 11.20%. This implies that in both cases if formation water is present in sufficient quantities, it occupies adsorption sites and pore throats of sandstone surface and pore spaces, in turn creating less space for the helium molecule and may restrict helium diffusion, as suggested by the less void volume value in water-saturated samples.

Thirdly, if the water in pore spaces takes up a significant fraction of the sandstone pore volume, how accurately is the sandstone gas storage capacity estimated using the conventional helium pycnometry methods? This question was answered by showing that the current industry standard disregards the volume consumed by the water in pore spaces, thus inadvertently overestimating the pore volume available for free-gas storage. We demonstrated that with Equation (3.10) a correct volume is calculated. Thus, using any other than the water saturated void volume data would yield unrealistically high values for storage calculations.

The second question regarding the factors that influence the void volume was answered through:

a. Averaging void volume at various experimental pressure steps;
b. Monitoring the contact time of sandstone cores as a function void volume and;
c. Saturating core samples with water at certain water content.

It has been shown that the pressure ranges investigated show close results regarding the measured void volume value with data scattering about an average of 8.017cm^3 for *Bandera* and 4.5171cm^3 for the *Scioto* samples. These values corresponds to both experimental and numerical works, which imply there was negligible pressure dependence.

Equilibrium time was attained after a contact time between helium and sandstone samples of 240mintes (Four hours). The investigation revealed that longer contact times between gas and sandstone core samples yield better void volume data, this is because as equilibrium time increased, helium could access minute sizes of pores because of its small molecular diameter. This is because adequate time must be allowed for samples to be completely saturated with gas, due to the time-dependent diffusive transport of helium.

The experimental investigation indicates that water content of 5.62 wt. % and 5.48wt. % for both samples respectively can reduce the dry capacity by as much as 12.53% and 11.20%. Therefore, when quantifying storage in sandstones, which is water-wet, corrections must be made in calculations to account for water in its various forms (adsorbed form and in pore space) or errors might arise.

The question about the parameters controlling adsorbed gas storage at the simulated depletion conditions was answered by investigating the effect of adsorption at equilibrium and abandonment pressures and comparing the results with carbon dioxide adsorption capacity. Firstly, For the *Bandera* sandstone, the maximum adsorbed volume at 1250 psia (8.62 MPa) was 0.089 mmol/g. For the *Scioto* sample, the maximum adsorbed volume at the maximum adsorbed volume at 1250 psia (8.62 MPa) was 0.110 mmol/g. The amount of methane uptake increases with an increase in the pressure for experimental equilibrium adsorption data, but when the adsorbent monolayer is saturated the amount of adsorption approaches to a limit gradually. This indicates that the types of isotherm is a type 1 isotherm.

For sandstone core samples at abandonment pressure of depleted reservoirs, the experimental adsorption capacity at very low pressures up to 500 psia (3.45 MPa) remains concave, indicating the availability of adsorption sites. The result for maximum adsorption capacities of methane result at depleted reservoir pressure were 0.61 and 0.82mmol/g. This indicates that the adsorption rate of CH_4 depends strongly on pressure. The result of this investigation is favourable indicating that available sites can be filled up by a gas with more adsorption capability, i.e. CO_2.

Clay minerals in sandstone core samples are composed of different particle sizes, For example, the abundance of micro- and mesopores in the size range of 10s of nanometres

in chlorite and illite interstratified clay. The high internal surface area with pores of 1–2 nm radius between crystal layers and variable micro pore volume in sandstone samples (mainly kaolinite, illite and chlorite) utilised in this investigation will provide an overall increase in adsorption capacity. The *Scioto* sample had the highest total amount of clays present (22%) compared to *Bandera* (14%) and had the highest adsorption capacity. This implies that high content of clay minerals in the Scioto sample relative to the Bandera provide extra surface area for adsorption of methane(CH_4) therefore contributing to the overall sorption capacity of the samples.

Experiments were conducted at a variable water and brine content (33, 65 and 91%) to investigate the effect of the presence of water and brine on methane (CH_4) adsorption capacity of sandstones. These studies revealed the qualitative and quantitative impact of water and brine on the methane sorption characteristics:

Detailed analyses of the experimental data show that sandstone core samples saturated with water have an overall decrease in adsorption capacity of 47.21, 54.47 and 60.89% for *Scioto* and 10.26, 24.36, and 38.03% for *Bandera* with increasing water content (33, 65 and 91%) and were much lower than the adsorption capacity of dry samples at the same variable pressure (0 – 400 psia or 2.76 MPa). For sandstone samples saturated with brine, an overall decrease in the methane adsorption capacity of 30.17, 43.57 and 69.83% for *Scioto* and 28.90, 42.58 and 52.85% was observed for the *Bandera* when compared to dry samples. At 20% brine salinity saturation, there was an additional loss of methane adsorption capacity compared to samples saturated with water of 47.21, 54.47, 60.89% for *Scioto* and 10.26, 24.36, 38.03% for *Bandera*.

Two adsorption types control the interaction of water with sandstone rocks; a) physisorption onto polar surfaces and b) chemisorption onto clay surfaces, which results in a substantial water adsorption capacity due to extra electric charges formed on their surface by isomorphous substitution. At 20% sodium chloride (NaCl) low salinity brine will alter the *Bandera* sandstone wettability toward strongly water-wet conditions, while the surface charge of *Scioto* sandstone will be strongly affected by low-salinity water and the zeta potential of illite and chlorite clays will be significantly decreased.

The main reasons leading to the significant reduction in adsorption capacity are the hydrophilic nature of clay minerals. The water would occupy the hydrophilic adsorption

sites in clay minerals and block the access of methane molecules to clay minerals by filling the pore throat. Hence, hydrophilic nature of clay minerals must be considered to adequately describe the adsorption capacity of sandstone rocks under water-saturated condition. For this reason, the amount of gas adsorption under reservoir conditions evaluated based on gas adsorption measurements in the laboratory using dry cores samples might be overestimated because of the water or brine content in depleted gas reservoirs. Therefore, to accurately describe the gas adsorption amount in these gas reservoirs, the influence of water content both in adsorbed and in free gas storage volume should be taken into consideration.

It can be concluded that the sorption capacity of CH_4 decreases with increasing water content. Typically, gas adsorption capacity measurements are done on dry core samples, because the presence of water would substantially reduce the measured gas adsorption capacity. Based on the water content, all of the sandstone core samples at a certain amount of water content (33, 65 and 91%) proved that methane (CH_4) sorption capacity would be significantly reduced due to the presence of water or brine.

1.6 Structure of Research thesis

The overall description of this thesis including its significance is divided into five main chapters:

Chapter 1 – Introduction

The chapter introduces the general purpose and objective of research work. It explains the concept of gas adsorption including definition, analytical models and error functions.

Chapter 2- Literature review

The chapter has a significant role in supporting this research. It presents a review of the impact of parameters on void volume, the adsorption mechanism in sandstone reservoirs and the impact of water and brine.

Chapter 3 – Material and Methods

The chapter covers the detailed experimental set up, description and design involved. It also provide set up schematics, fabrication details and assemblies of experimental apparatus.

Chapter 4 – Main Results and Discussions

The chapter discusses the results of rigorous experimental work conducted in chapter 3 to investigate the influence of a range of process parameters on void volume measurement and to quantify the methane adsorption capacity of dry, water and brine saturated sandstone samples. Experimental Data verification was conducted by using repeatability experiments, and theoretical isotherms were fit to experimental data using nonlinear regression to analyse experimental data sets.

Chapter 5 – Conclusion and Recommendation

The chapter provides conclusions of the findings made from the research, benefits of the results and recommendations for future studies.

CHAPTER 2

2 ADSORPTION FUNDAMENTALS AND THEORY

2.1 Helium Void volume

The amount or volume of space, in which free or non-adsorbed gas is stored and is present in the sample cell (SC) during adsorption experimental setup, is termed the void volume (Ross and Bustin., 2007). Accurate determination of void volume is a critical step in an adsorption isotherm experiment since the amount of adsorbed gas is calculated using the previously calculated void volume data (Rani et al., 2015). However, errors have been observed in experimental data from the void volume step (Mohammed et al., 2009; Sakurovs et al., 2008; Gasparik et al., 2014). Different methods (Helium Pycnometer, Volumetric and Manometric methods) and an inert probing gas i.e. Helium of known volume (mole) are used to determine this free gas volume. The process of which is referred to as Helium void volume or pycnometry. The inert gas is allowed to fill in the sample cell volume containing the sample in a core or crushed form.

Researchers (Lu et al., 1993, 1995; Krooss et al., 2002; Goodman et al., 2004; Zhang et al., 2011) have shown that the inert gas is not adsorbed onto the microporous samples at a room temperature. The gas pressure in the void volume increases as the inert gas occupies the total adsorbent volume (i.e. pore space). This procedure is repeated many times, and in successive steps, as the gas is filled with higher pressure. The void volume is calculated for each step and then averaged. The average void volume is used for subsequent adsorption calculation.

2.2 Adsorption Fundamentals

Adsorption is a process whereby gas molecules (adsorbate) attach to the surface of a substrate known as the adsorbent (Zhang et al., 2013). Because of surface energy, a film of the adsorbate is formed at the surface of the adsorbent (Gregg and Sing., 1982). The surface energy is the excess energy applied on the adsorbate compared to the bulk adsorbate material under free and open states. There are two types of adsorption:

- Physisorption (physical adsorption), which is predominantly due to attractive van der Waals' intermolecular forces.
- Chemisorption (chemical adsorption), in which a chemical bond is formed.

In general, the gas adsorption that commonly occurs in sandstones is physical adsorption, with a corresponding heat of adsorption of less than 20 kJ/mole (Atkin. 2006). The process is exothermic, reducing free energy and the entropy of the adsorbed gas. In this process, when the gas adsorbate, the methane (CH_4) in this case, is in contact with the solid adsorbent, the sandstone surface, after a period the adsorbent and adsorbate will reach an equilibrium at the end, a state depending on gas pressure, temperature and the material properties of the adsorbent and adsorbate, which can be expressed using a state function, i.e.: $V_{ads} = f(P, T)$, where V_{ads} is the equilibrium adsorbed amount of methane in unit of mmol/g or SCF/ton, P is the gas pressure, T is the temperature.

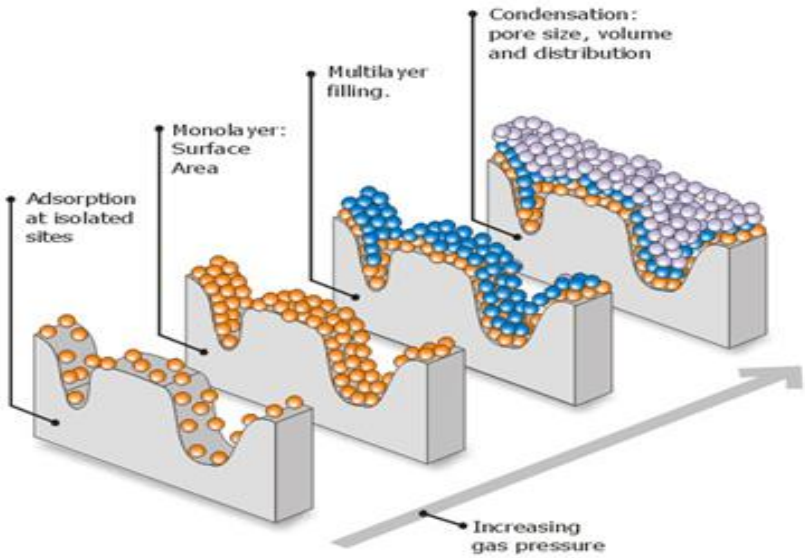

Figure 2.1: Principles of adsorption on a solid surface (Micrometrics, 2012)

Figure 2.1 shows isolated sites begin to adsorb gas at low pressure (stage 1), and as pressure increases, a monolayer coverage of molecules is formed at the surface (stage 2). As pressure continues to increase, a multilayer may form depending upon the gas and solid (stage 3) and finally as equilibrium is reached, the surface area will be completely saturated with gas molecules (stage 4). There are different ways to quantify gas adsorption in an experiment. If pressure is varied and the temperature is kept

constant, the relationship between the adsorbate volume and the adsorbate gas pressure at equilibrium is termed adsorption isotherm, i.e.: V_{ads} = f (P). If pressure is kept constant, but temperature varies, i.e.: (V_{ads} = (f (T), the relationship is called adsorption isobar. If the amount of adsorbate is kept constant, but temperature or pressure varied respectively, i.e.: P = f (T), the relation is called adsorption isosteric. In practice, the adsorption isotherm is widely used for adsorption assessment rather than the adsorption isobar or isosteric. Table 2.1 lists out the main symbols/terms and their definition for the adsorption process.

Table 2.1: Important definitions for gas adsorption

Definition/symbol	Description
n	The no of moles of gas in both bulk and adsorbed form.
V	The total volume of the present in the sample cell (including the volume occupied by the adsorbent). It is known by calibrating the instrument.
V_v	The amount or volume of space, in which free or non-adsorbed gas is stored and is present in the sample cell (SC) during adsorption experimental setup. It is the volume impenetrable to the adsorptive gas and is measured by a helium pycnometer.
V_g	Grain volume is the volume of the rock grains or solids (not including the pore volume).
V_b	Bulk volume is the volume that the rock occupies, sometimes called matrix volume.
m	Mass of the adsorbent
V_{vd}	Dead volume. The space within control instruments such as valves and fitting.
Adsorptive	Components in the bulk fluid phase before adsorption.
Adsorbent	Bulk solid phase.
Adsorbate	Adsorbed gas molecules on the solid surface

2.2.1 Gibbs Surface Excess

The Gibbs surface excess is a model proposed by Josiah Willard Gibbs, which is widely applied to measure the adsorbed phase of gas molecules in contact with an adsorbent surface. It assumes the original surface of an adsorbent as an idealised surface of zero thickness (Gibbs., 1928; Sircar., 1999), because of the difficulty to determine the structure of the adsorbed phase (absolute adsorption) experimentally. Figure 2.2 illustrates this model using a geometric plane surface parallel to the adsorbent surface, using a single gas phase at constant pressure and temperature (p, *T*) in contact with a solid adsorbent (m).

In Figure 2.2, the layer model represents adsorption in a real system while the Gibbs representation describes the idealised system. In a real system, the gas/adsorbate density(ρ) decreases with increasing distance (z) until it reaches the constant gas bulk density. In the layer model, three zones are distinguished: adsorbent (zone I), adsorbed layer (zone II), and adsorptive gas (zone III).

The zone III is at a sufficient distance from the adsorbent, where the solid surface has little influence on the gas molecules, and the equilibrium gas density depends on pressure and temperature there. Zone II has one side bonded to the solid surface while the other end of the bulk gas phase. The force field of the solid surface applied on the gas causes the increase of gas density towards the surface. The local density of this layer depends on the distance from the solid surface.

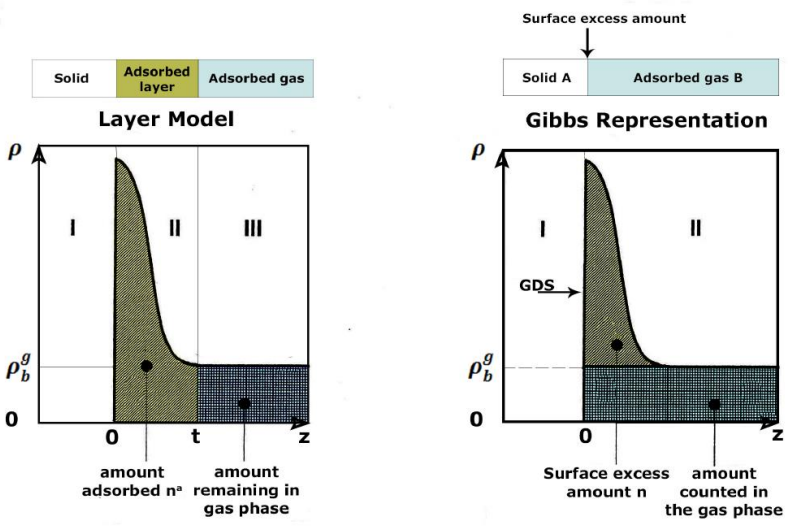

Figure 2.2: The layer and Gibbs representation (Rouquerol et al, 1998)

Using the Gibbs approach, the system is divided into two regions using a geometrical plane surface parallel to the adsorbent surface. The Gibbs dividing surface placed on the solid surface is shown in Figure 2.2, In the Gibbs representation, the sum of the free bulk (V_{free}) gas volume and adsorbed (V_{ads}) equals the total void volume (V_v) as shown (Eqn. 1.1):

$$V_v = V_{free} + V_{ads} \quad (1.1)$$

Therefore, the surface excess amount, n, illustrated in Figure 2.2 is the difference between the total amount of adsorbate gas in the material surface and the amount of gas present in the bulk phase. In this thesis, the surface excess (Eqn. 1.2) is defined as ${n_{ads}}^{excess}$, n_{inj} is the total amount of adsorbate and V_v is the volume of gas present in the bulk phase, the surface excess can then be calculated using:

$$\mathrm{n_{ads}}^{\mathrm{excess}} = \mathrm{n_{inj}} - \rho_{\mathrm{g}}(\mathrm{P,T})\mathrm{V_v} \quad (1.2)$$

n_{inj} is the total amount of gas transferred successively through the reference volume into the sample cell containing the sample, and the void volume ($_{void}$) is determined by helium expansion measurement before the adsorption experiment.

2.2.2 Adsorption Isotherm

Adsorption isotherms are graphs that describes the adhesion of molecules to a solid surface as a function of pressure at a fixed temperature. It is a mathematical plot of the solid adsorbent capacity against its pressure. For pure gases, experimental physical adsorption isotherms have shapes that are classified into five types as discussed below. Each of these types is observed in practice but by far the most common are types I, II and IV. The types of adsorption isotherms are shown in Figure 2.3 (Gregg and Sing., 1982):

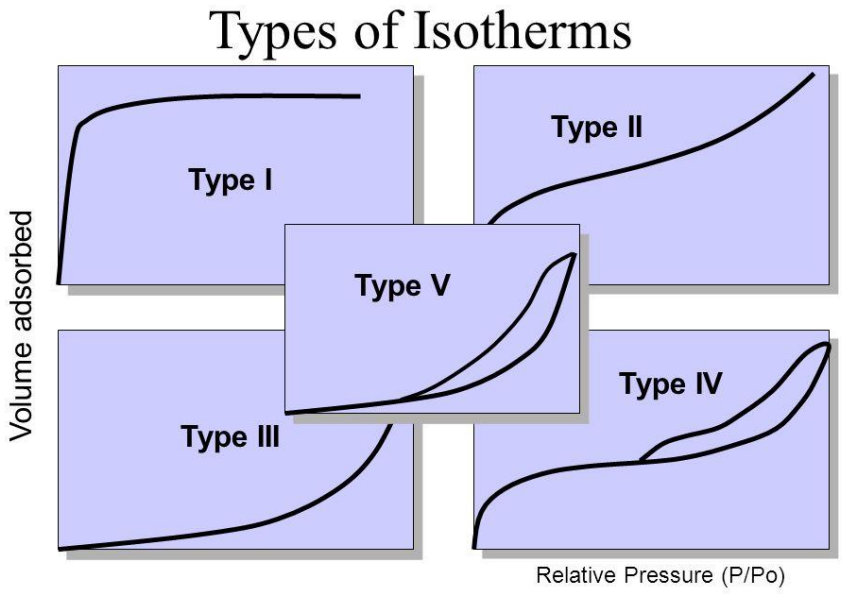

Figure 2.3: Types of adsorption isotherm (Gregg and Sing., 1985)

- The monolayer is formed on the surface of adsorbent in Type I (Gregg and Sing., 1982). The appearance of a nearly horizontal plateau is an indication of a tiny horizontal pore surface area, and this is typical of microporous solids.

- Type II is ubiquitous for the case of physical adsorption with multilayer formation. At a low relative pressure, it is concave, and then linear for a small pressure range where monolayer coverage is complete. Then, it becomes convex to the relative pressure axis. Multilayer's thickness increases progressively with an increase in relative pressure (Gregg and Sing., 1982).

- Both Type III and Type V isotherms are characterised by being convex to the relative pressure axis. As seen in Figure 2.3, Type III Isotherm's convexity continues throughout the isotherm. However, Type V isotherm reaches a plateau at a high relative pressure. The convexity of the isotherm indicates that the already adsorbed molecules tend to enhance the adsorption of other molecules. In nonporous or highly microporous adsorbents, Type III isotherms are standard. On the other hand, Type V isotherms are observed in the case of mesoporous or microporous adsorbents for the adsorption of both polar and nonpolar adsorbent (Gregg and Sing., 1982). The convexity of the isotherm is the indication of

cooperative adsorption, which means that the already adsorbed molecules tend to enhance the adsorption of other molecules. In other words we can say that it support the adsorbate-adsorbate interaction.

- Type IV isotherms are observed in the case of mesoporous adsorbents. At low relative pressures, the shape of isotherms follows the same path as Type II. Then, the slope starts decreasing at a higher pressure. At saturation vapour pressure, the isotherm levels off to a constant value of adsorption. The portion of isotherm that is parallel to the pressure axis is attributed to pore filling by the capillary condensation (Gregg and Sing., 1982). The shape of the type IV isotherm is similar to that of type II at the start but differs at the higher relative pressure region where it displays a hysteresis loop. The hysteresis is attributed to capillary cracks from which adsorbate molecules do not desorb as readily as they adsorb. This is due to vapour pressure lowering over the concave meniscus formed by condensed liquid in the pores (Sing et *al*., 1985).

2.3 Theoretical adsorption Isotherms Fitting

Different adsorption isotherm models have been analysed by researchers (Kumar et al., 2007; Mohammed, 2007; Foo and Hammed, 2009; Chen et al., 2012, 2015; Osmari et al., 2013) to assess their ability to fit experimental data. These model are either two or three-parameter models (Foo and Hammed, 2010). Some models were modified by incorporating more parameters into the original form of the model (McKay and Porter., 1997; Al-Asheh et al., 2003; Liu and Wang., 2008). Besides, to use the theoretical assumptions behind these mathematical equations, several error deviation functions have been used to measure the goodness of fit of the models (Mohammed, 2007). These error functions are criteria that evaluate the error distribution between the experimental data and the predictive values of isotherm models (Foo and Hammed, 2010). Researchers (McKay and Porter., 1997; Allen et al., 2003; Ho and Wang., 2004; Ho., 2004; Wang and Qin., 2005; Parimal et al., 2010) select one, two or several criteria to determine the best performance for all functions (Ho et al., 2002; Ringot et al., 2007; Allen et al., 2003; Chen et al., 2012).

Published studies have compared the performances of linear and non-linear regressions of adsorption isotherms (Kumar and Sivanesan, 2005, 2006; Kumar, 2006; Bolster and Hornberger, 2007; Parimal et al., 2010). However, the non-linear regression procedure provides better fits and can be performed for different models with the same set of adjustable variables, allowing for more direct comparison of distinct model fits (osmari et al., 2013). Search for the best-fit adsorption isotherm using the non-linear method is the most widely used technique to predict the optimum isotherm. Currently, non-linear regression method is found to be the best way in selecting the optimum isotherm (Ho., 2004; Kumar, 2006, 2007; Kumar and Porkodi, 2006; Ho et al., 2005). The coefficient of determination, r^2 is the most widely used error function to minimise the error distribution between the experimental equilibrium data and isotherms (Ho., 2004; Kumar. 2006, 2007; Kumar and Porkodi, 2006; Ho et al., 2005).

2.4 Analytical models for adsorption

Accurate representation of the adsorption of gas onto a solid depends upon a good description of the equilibrium between the two phases. By plotting the adsorption capacity (mmol/g) against pressure (psia) graphically, it is possible to depict the equilibrium adsorption isotherm. The adsorption isotherm must be established to evaluate the capacity of an adsorption system (Cheng et al., 2012). There are many theories relating to adsorption equilibrium. However, the models used in this research were the Freundlich, Langmuir, and Redlich–Peterson. The mathematical equations of these models and their associated parameters are illustrated below:

2.4.1 Langmuir Isotherm

The Langmuir isotherm (Eqn. 2.3) is an empirical model originally developed to describe one layer or monolayer adsorption (Langmuir. 1916). The assumptions of the Langmuir model (Yang 1997; Do., 1998) are; 1). The surface is homogeneous, that is the adsorption energy is constant over all sites; 2). Adsorption on the surface is localised, that is adsorbed atoms or molecules are adsorbed at individual, restricted sites; 3). Each site can accommodate only one molecule or atom. It is expressed as:

$$V = {V_L p}/{p_L + P} \qquad (2.3)$$

Where, V is adsorption equilibrium capacity (SCF/tonne); V_L is the Langmuir volume, and P_L is the Langmuir Pressure (psia). This model is the most widely used to describe adsorption dynamics, but due to it, not adequately describing multi-layer adsorption or temperature differentials other isotherms were developed.

2.4.2 Freundlich Isotherm

Freundlich presented the earliest known adsorption isotherm equation (Freundlich. 1906). This empirical model can be applied to monolayer and multilayer adsorption types on different surfaces and is expressed by Equation 2.4:

$$\frac{x}{m} = kP^{\frac{1}{n}} \qquad (2.4)$$

Where x: the amount of adsorbed methane (g), m: the mass of clay adsorbent (g), P: the pressure of methane gas (psia), k and n: are empirical constant characterising adsorption capacity and intensity. For an excellent adsorbent, 1<n<10, and a higher value of n indicates better adsorption and formation of a strong bond between the adsorbate and adsorbent.

2.4.3 Redlich- Paterson Isotherm

Redlich–Peterson isotherm (Eqn. 2.5) is an isotherm featuring both Langmuir and Freundlich isotherms; it is a hybrid developed by Jossens and workers, who modified the three-parameter equation first drawn up by Redlich and Peterson, (1959). At low pressure, it describes the Langmuir isotherm at high pressure it becomes the Freundlich isotherm (Ho et al., 2001). It is expressed mathematically as:

$$q_e = K_R C_e \Big/ 1 + a_R C_e^{\,g} \qquad (2.5)$$

Where, K_R, a_R, and g are the Redlich-Peterson isotherm constants. It comprises of a three-parameter empirical equation that is similar to the Langmuir isotherm, but with the equilibrium concentration in the denominator raised to a 'g' parameter, which is positive and smaller than 1. It also can be easily observed that the Redlich–Peterson isotherm reduces to the Langmuir isotherm when the parameter g is equal to 1. Besides, when the term $a_R C_e^{\,g}$ in the denominator is much higher than 1, the behaviour of the Redlich–Peterson isotherm is similar to the Freundlich isotherm (Osmari et al., 2013).

2.5 Error Functions

For a given combination of adsorbent (solid) and adsorbate (gas), selection and configuration of an appropriate isotherm expression is typically accomplished by regression against experimental data (Roy et al., 1992; Matott and Rabideau., 2007). The MATLAB computer program automates this process and provides a range of post-regression statistical and diagnostic measures. The goodness of fit is an essentially important parameter that estimates how well the curve predicts the experimental data. It is based on the theory that the scale of the difference between the experimental data points and the prediction curve is a good measure of how well the curve fits the data. The following parameters are measured to judge the goodness of fit (Hossain et al., 2013):

2.5.1 The coefficient of multiple determination (r^2),

This statistic measures how successful the fit is in explaining the variation of the data. It is presented in Equation 2.6. Put another way, R-square is the square of the correlation between the response values and the predicted response values:

$$r^2 = \frac{\Sigma(q_{meas} - \overline{q_{calc}})^2}{\Sigma(q_{meas} - \overline{q_{calc}})^2 + \Sigma(q_{meas} - q_{calc})^2} \quad (2.6)$$

Where q_{meas} is the constant obtained from the isotherm model, q_{calc} is the equilibrium capacity obtained from experimental data, and $\overline{q_{calc}}$ is the average of q_{calc}. A value closer to 1 indicates a better fit to experimental data (Karadag et al., 2007; Foo and Hammed, 2009).

2.5.2 The sum of squares due to error (SSE)

A statistic that measures the total deviation of the response values from the fit to the response values and is presented as Eqn.2.7. It is also known as summed square of residuals.

$$\Sigma_{i=1}^{N}(q_{calc} - q_{meas})^2 \quad (2.7)$$

Where, q_{calc} is the theoretical adsorbed gas phase, which have been calculated from one of the isotherm equations and q_{meas} is the experimentally determined adsorption capacity. A value closer to 0 indicates that the model has a smaller random error

component and that the fit will be more useful for prediction (Kumar et al., 2006; Mane et al., 2007; Foo and Hammed, 2009).

2.5.3 The root mean squared error (RMSE)

It is also known as the fit standard error and the standard error of the regression. It is an estimate of the standard deviation of the random component in the data and is presented in Equation 2.8:

$$RMSE=\sqrt{\frac{1}{N}}\ \sum_{i=1}^{n}\left(q_{calc}-q_{meas}\right)^2 \qquad (2.8)$$

Where, q_{calc} and q_{meas} are the calculated and experimental adsorption capacity respectively and N is the number of data points. Just as with SSE, an RMSE value closer to 0 indicates a fit that is more useful for the prediction of the fit (Ho et al., 2002; Hossain et al., 2012, 2013).

2.5.4 Residual plot

It is an important criterion to assess the adequateness of a regression model (Draper and Smith, 1981; Myers, 1986). The distribution between the model predictive errors (residuals) versus predictive values is called the residual plots (Chen et al., 2012).

CHAPTER 3

3 LITERATURE REVIEW

3.1 Introduction

Depleted Sandstone reservoirs are an important resource and have recently attracted attention as a medium for isolating greenhouse gases. The adsorbed state is one of the most important storage mechanism of methane (CH_4) in these reservoirs. Investigating the capacity of adsorbed gas in sandstones is required not only to understand the reservoir but also as a means of optimising the process of enhanced gas recovery and sequestration (Chalmers and Bustin., 2008; Curtis., 2002; Ross and Bustin., 2007, 2008; Strapoc et al., 2010; Zhang et al., 2012; Liu et al., 2013). Enhanced gas recovery and sequestration (EGR-CO_2) operations in depleted gas reservoirs will require reliable predictions of the physical and chemical effects of methane (CH_4) on the sandstone, i.e. a clear understanding of sandstone-CH_4 interaction processes under relevant conditions.

An essential starting parameter, which is determined in the laboratory is the methane (CH_4) storage potential of the core samples being the sum of the adsorption capacity and void volume measurements. When considering microporous solids as a medium to store CH_4, physical adsorption is considered as the primary process. Physical adsorption was also found to be an important process in gas adsorption where clay minerals are present (Busch et al., 2008) for example in sandstone reservoirs.

The Helium void volume i.e. the amount or volume of space, in which free or non-adsorbed gas is stored and is present in the sample cell (SC) during adsorption experimental setup is affected by many parameters. However, this thesis concentrates on the effect of pressure, equilibrium time and water content. Moreover, it is also important to take account of the sample form (crushed, core) and type (pure clay, clay shale, sandstone) used for these tests since each material has different properties.

Methane (CH_4) gas adsorption capacities are typically reported on a dry basis, neglecting water or brine content and adsorption onto clay surfaces. The presence of water in reservoirs has negative impact on adsorption capacity (Don & Ann., 1981;

Hovorka et al., 2009; Fischer et al., 2010; Yu et al., 2012) of the sandstone in gas reservoirs. Methane (CH_4) adsorption on mineral surfaces (especially clays) has been found to be significant (Busch et al., 2008; Weniger et al., 2010a; Wollenweber et al., 2010). Carbon dioxide (CO_2) adsorption capacities are of a high order compared to methane adsorption on clay minerals (Fitzgerald et al, 2005; Ottiger et al, 2008; Pini et al, 2010; Gensterblum, 2013).

The methane (CH_4) adsorption capacity of sandstones, the impact of abandonment pressure (0-500psia) on methane (CH_4) adsorption and the parameters that affect the void volume of sandstones are yet to be investigated. Research on this topic is still in progress and mechanisms are not well understood yet. Therefore, it might be misleading to report CH_4 adsorption capacities based on dry basis alone without the consideration of water, brine and clay mineral surfaces (depending on the respective contents).

In this chapter, a comprehensive literature review of the research topics relevant to this study is presented. The chapter is divided into two sections:

Section 1: focuses on the use of helium as an inert gas for void volume measurements in adsorption experiments of microporous materials, and in doing so examines the effects of averaging pressure, contact time and the presence of water.

Section 2: presents a review of adsorption mechanism in sandstone reservoirs and the impact of water and brine. It considers the abandonment pressure of depleted reservoirs, Methane (CH_4) and Carbon dioxide (CO_2) adsorption in Enhanced gas recovery and sequestration (EGR-CO_2), Methane (CH_4) adsorption of clay-rich rocks and the effect of Water and Brine content on methane (CH_4) adsorption capability.

3.2 SECTION 1: The Impact of parameters on void volume quantification

3.2.1 Helium as an inert gas for void volume quantification

The use of helium as an inert gas to determine the buoyancy or void volume of samples, in gravimetric and manometric/volumetric adsorption methods respectively is widely utilised in adsorption measurements (Gensterblum., 2013; Wang et al., 2013; Gasparik et al., 2014; Rexer et al., 2014). The use of Helium as an inert gas for void volume measurement has been a subject of debate between researchers (Charles et al., 1969; Sing et al., 1985; Lu et al., 1993, 1995; Roquerol et al., 1999; Krooss et al., 2002; Goodman et al., 2004, Zhang et al., 2011; Mohammed et al., 2009; Sakruvos et al., 2009; Gasparik et al., 2013, 2014). The impact of helium adsorption on the void volume measurements of microporous adsorbents (clay-shale, sandstones, powdered pure clay) is a still a contentious issue. In the literature, there is no unanimous agreement among the different authors:

Using helium to define the reference "non-sorption" case is not entirely unambiguous, and several works have indicated that a non-negligible adsorption of helium takes place at ambient temperatures on activated carbons and zeolites (Malbrunot et al., 1997; Sircar., 2001; Gumma and Talu., 2003). However, Researchers (Sing et al., 1985; Roquerol et al., 1999; Ross & Bustin., 2007) argued against the assumed non-adsorption of helium in microporous adsorbent, when measuring the void volume, pointing out it could be a source of uncertainty in experiments. For example, the small kinetic diameter of helium compared to the molecular diameter of other gases is shown in Table 3.1. The smaller molecular size of helium can lead to an overestimate of the void volume (Ross and Bustin, 2007). The error due to molecular sieve effect can be eliminated by using other inert gas such as argon (Ross and Bustin, 2007; Vermylen, 2011), which has molecular diameter of 0.34 nm, comparable to methane. However, Argon has a higher rate of adsorption compared to helium and should be avoided (Rani et al., 2015).

Table 3.1: Molecular diameter of gases compared with helium.

	Gas			
Molecular	Helium	Carbon Dioxide	Nitrogen	Methane
Diameter	0.26	0.33	0.36	0.38

Higher penetration of helium to the finest microporosity (Ross & Bustin., 2007; Aljaman et al., 2010; Anovitz and Cole, 2015) compared to other gases, which is the ability of the helium gas to penetrate smaller pores spaces in microporous materials due to its low molecular size. This ability of helium can overestimate the void volume compared to the void volume available to methane (CH_4), which leads to Negative values in Methane and Carbon dioxide (CH_4 and CO_2) adsorption isotherm (Ross & Bustin., 2007; Moghaddam., 2013; Merey et al., 2016). Furthermore, Helium can be absorbed on inert solids such as silicates and clays (Charles et al., 1969; Ross & Bustin., 2007). Other authors (Walker Jr., 1988; Siemons and Busch., 2007; Sakurovs et al., 2009; Gensterblum., 2013) have provided an overview of the topic.

Helium adsorption is very negligible; it is adsorbed on solid adsorbents at low temperatures and high pressures, but not at room temperature and low-pressure (Tarczewski and Grillet., 1989; Malbrunot et al., 1997; Rani et al., 2015). It has unique properties such as; a low chemical reactivity (inert); an ideal gas (Aljaman et al., 2010; Anovitz and Cole, 2015) and a high diffusivity (Anovitz and Cole, 2015). These properties suggest that Helium is the perfect choice for void volume measurement (Lu et al., 1993, 1995; Krooss et al., 2002; Goodman et al., 2004, Zhang et al., 2011). In clays, shale and coal the magnitude of the helium sorption is expected to be slight (in μmol/g range compared to mmol/g of the typical adsorption capacities for CH_4 or CO_2) and thus considered negligible (Sakurovs et al., 2009; Gasparik et al., 2013; Heller and Zoback, 2014).

Ross & Bustin., (2007) investigated the effects of helium adsorption on the void volume measurement of powdered clay minerals (illite, smectite and kaolinite). The study showed that:

- The measured void volume increases with pressure due to helium adsorption or access to finer pores at higher pressures (up to 725.189 psia or 5 MPa).
- If adsorption of helium were responsible for the variation in void volume measurement with pressure, the general slopes of the helium isotherm curves would plateau at higher pressures rather than being continuous and relatively constant. The previous observation suggests that helium will not be significantly adsorbed as no saturation point is reached.

- The negative values of adsorption isotherm was because of an overestimation of the void volume due to ‘molecular sieving' effect.

However, the increasing trend in void volume with pressure in their results was mainly a consequence of greater accessibility of helium to restricted pores (i.e. a capillary effect) which occurs only at high pressure (upto 5MPa).The adsorption is this research was negative indicating that the void volume was not only the cause of error in their adsorption capacity experiments. The molecular sieve effect is observed in porous materials with the pore size comparable to molecular size. This effect is as a result of Helium (He) molecules having a smaller kinematic diameter compared to other gases (CH_4, CO_2) as shown in Table 3.1. It can access tiny pores that are not accessible to methane (CH_4) gas. Helium adsorption, if present, will be in little range as compared to CH_4 or CO_2 adsorption capacity, which is usually in a high range and hence can be neglected (Sakurovs et al., 2009; Gensterblum., 2013). Moreover, the adsorption of helium at ambient temperature (i.e. 25°C) and low pressure (0 - 2175.57 psia or 0 – 15 MPa) is small.

It has been advocated that helium void volume measurements be modified to account for helium adsorption (Myers and Monsoon, 2002). This procedure is, however, lengthy and tedious because it requires the determination of the Henry constant for adsorption of helium. One inefficient factor of using Helium is due to its virial coefficient, which is smaller than most adsorptive gases, and, it may increase in density near the pore wall surfaces (adsorption) in micropores (Myers and Monsoon, 2003). However, using theoretical density or pycnometer in measuring void volume will solve this problem. Theoretically, the adsorption of helium on a microporous surface is not of importance.

In adsorption experiments, the only methodology that acts as a differentiation standard between experiments on adsorption has to do with the procedure of choosing a gas that can quantify the void volume and a reference state (Myers and Monsoon, 2003). Questions such as; Firstly, how do we differentiate between the adsorbed gas and free gas, and which procedure will lead to a more accurate result? These questions need to be considered in experimental measurements. Furthermore, if gas expansion methods are adopted, which gas should be used and at what reference state? The last two questions have vital importance when determining the void volume (Roquerol et al.,

2009). The answers to these questions depend on the methodology adopted. There are direct and indirect methods available for quantifying the void volume.

A procedure used by Gasparik et al., (2013) to estimate the void volume consists of constructing the total-mass-of transferred- helium versus the equilibrium density of helium. It involves plotting a graph of the total amount of helium transferred (m^{He}_{trans}) successively as a function of helium density (ρ_{sc}^{He}) in the sample cell (Figure 3.1), with the slope of this "helium isotherm" equal to the void volume. The total mass of helium transferred is calculated using Eqn. 3.1:

$$m^{He}{}_{trans} = V_{Rc} \sum_{s=1}^{N} \left[\rho_{Rc}{}^{He}\left(T, P_{2s}{}^{be}\right) - \rho_{Rc}{}^{He}\left(T, P_{2s+1}{}^{ae}\right) \right] \qquad (3.1)$$

Where $m^{He}{}_{trans}$ is the total amount of helium transferred from the reference cell, V_{Rc} is the volume of the reference cell, $\rho_{Rc}{}^{He}$ (T, $P_{2s}{}^{be}$) is the helium density in the sample cell at an initial pressure and before equilibrium(upper script ^{be}) and $\rho_{Rc}{}^{He}$ (T, $P_{2s+1}{}^{ae}$) is the helium density at equilibrium(upper script ^{ae}) at a constant temperature. N and s represent the number of successive injection steps.

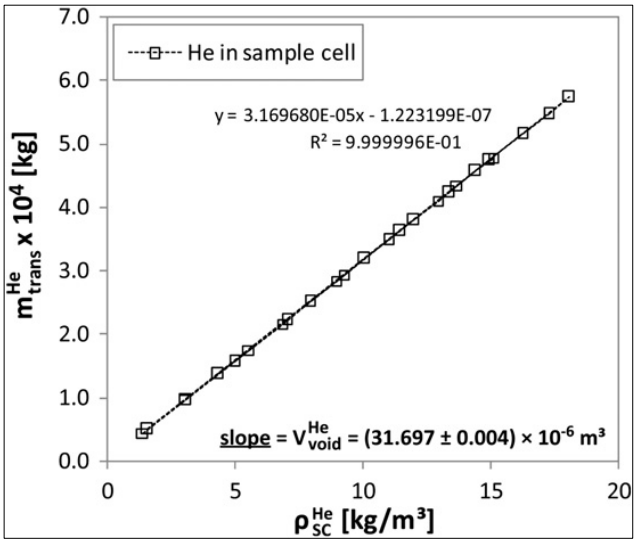

Figure 3.1: Mass of helium transferred versus helium density (Gasparik et al., 2013)

The advantages of this procedure (Gasparik et al., 2013) are that:

- It does not require any individual data point elimination or selection (e.g. outliers, data scatter as the equilibrium pressure approaches the maximum pressure value).
- The slope is independent of the initial pressure value.
- It mimics the evaluation of the excess isotherm in which the total amount of adsorptive gas transferred into the sample cell is measured. It is, moreover, analogous to the measurement of the "helium isotherm" in the gravimetric method to obtain the sample volume for the buoyancy correction.

However, this procedure is lengthy and the choice of Equation of State will have a significant influence on the calculated sorption quantity. Preferred reliable predictions of void volume should be jointly with other sources of error as suggested by Ross and Bustin such as: 1) averaging the void volume values for multiple pressure steps; and 2) selection of an appropriate inert gas (Ross and Bustin, 2007).

Several other attempts have been used to incorporate potential further changes of the volume of the solid adsorbent like swelling, water adsorption and reaction with microporous adsorbent:

Khosrokhavar et al. (2012) and Moghaddam. (2013) suggested modification in void volume calculations (Eqn. 3.2) to account for the volume occupied by adsorbed helium, swelling of the sample due to its infinite weight, and the reaction of adsorbed gas with the microporous solid:

$$V^{N}_{void} = V^{0}_{void} - \sum_{i=1}^{N} \Delta V_{ads} - \sum_{i=1}^{N} \Delta V_{sw} - \sum_{i=1}^{N} \Delta V_{rec} \qquad (3.2)$$

Where, N is the number of experimental steps, ΔV_{ads} is the volume adsorbed on the clay surface; ΔV_{sw} is the effect of swelling and the reaction of adsorbed gas with the microporous surface (ΔV_{rec}). The authors claimed that the void volume determined with Helium may overestimate the void volume accessible to CH_4. Then the void volume can change at every time step due to the finite volume of the adsorbed phase, swelling of the clays and possible reactions of the introduced gas with the minerals. However, the void volume measurements in their research was validated with Argon and Helium and they report not observing any change in void volume before and after introducing the CH_4 to the sample.

The application of helium as an inert gas is still the only and most accurate for void volume determination. So far, this approach provides an important and useful generalised procedure for void volume determination as reported in many recently published papers (Lu et al., 1993, 1995; Krooss et al., 2002; Goodman et al., 2004; Badalyan & Pendleton., 2008; Mohammed et al., 2009; Zhang et al., 2011; Khosrokhavar et al., 2012; Gasparik et al., 2013; Moghaddam., 2013; Rani et al., 2015). The helium expansion method is the only accurate and efficient method available for now, and is used generally as a "standard" procedure for measuring adsorption on the surface of adsorbent solids (Gasparik et al., 2013). Nevertheless, it is also important to take account of the sample form (crushed, core) and type (pure clay, clay shale, sandstone) used for these tests since each of these materials have different properties.

3.2.2 Effect of averaging pressure on void volume measurement

Errors were observed in the experimental data when quantifying adsorption capacity, some of which have been attributed to the inaccuracy of void volume measurement (Sakurov et al., 2008; Gasparik et al., 2014). At pressures, 0 - 2175.57 psia or 0 - 15.0 MPa (Chareonsuppanimit et al., 2012; Gasparik et al., 2012, 2014; Heller and Zoback., 2014; Rani et al., 2015), the average void volume change as a function of pressure is little for coal, shale and pure powdered clay minerals (kaolinite, illite, Smectite). However, the experiment by Ross and Bustin (2007) did not agree with that of others because of gas capillary effect and helium adsorption at higher pressures with the natural microporous materials.

Chareonsuppanimit et al., (2012) observed that the void volume calculated from helium injections varied less than 0.3 cm^3 for an average reading of 60 cm^3. The helium void volume measurements were performed at the same temperature as the gas adsorption isotherms (328.2 K) and over a range of pressures from 0 - 12.4 MPa (1800 psia) in intervals of 1.4 MPa (200 psia). The helium adsorption was considered negligible at these conditions and we modified our apparatus to reduce, as much as possible, the void volume in the equilibrium cell. An injection pressure of 7 MPa (about 1000 psia) was used since this gives the optimal overall performance for a fixed pressure, experimental apparatus. Our apparatus modifications resulted in a 34% reduction in void volume, and this lowered the expected uncertainties in adsorption by more than two-fold.

Heller and Zoback, (2014) also observed similar results (Figure 3.2) reporting average void volume data of 14.956ml with a deviation of 0.0045ml for Eagle Ford shale sample at pressure up to 1400 psia or 9.65 MPa.

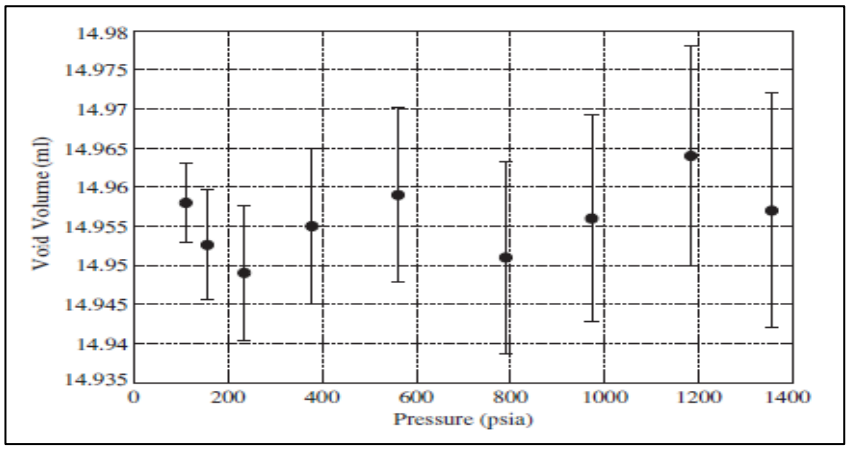

Figure 3.2: Void volume versus Pressure for Eagle Ford sample (Heller and Zoback, 2014)

Rani et al (2015) compared the void volume in a volumetric adsorption study using two shale types, KG and Salanpur, from India at 40˚C and 1334.35 psia (9.2 MPa). Using Argon and helium, they observed that, in the case of helium, void volume was independent of pressure, while for argon, they found a correlation between pressures and void volume measurement (Figure 3.3). They concluded that the reason for this relationship between pressure and void volume is due to argon adsorption and molecular sieving effect.

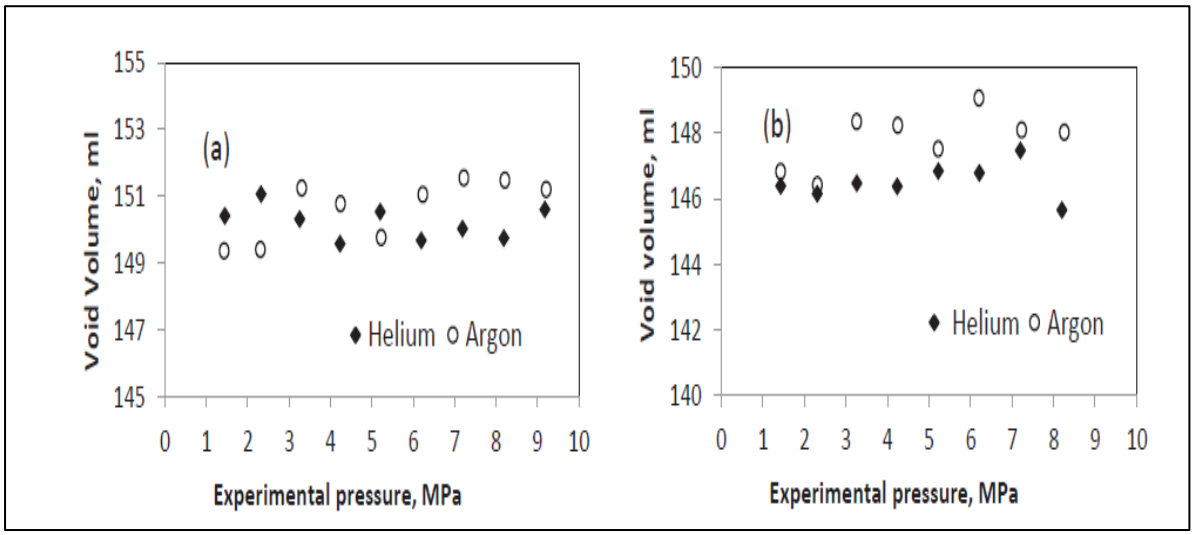

Figure 3.3: Void volume measurements for Krishna Godavari (KG) and Salanpur shale using Argon and helium (Rani et al., 2015)

However, this result is not agreeable to the suggestion by Ross and Bustin, 2007 and Vermylen, 2011 that the error due to the molecular sieve effect can be eliminated by using other inert gas such as argon to determine the void volume. With a molecular diameter of 0.34 nm, argon is comparable to methane and it is suggested that error due to molecular sieving will be reduced. Generally, helium is used as the inert gas for void volume determination. Helium has a smaller kinetic diameter (0.265 nm) compared to methane (0.380 nm).

Ross and Bustin, (2007) observed that at a pressure of 36.25 to 725.19 psia (0.25 to 5Mpa), the total void volume increased as a function of incremental pressure for powdered clay minerals. They calculated the void volume by mass balance using the Equation 3.3:

$$V_v = \frac{P_2 - P_3}{P_3 - P_1} \qquad (3.3)$$

Where with appropriate correction for non-ideality, V_v is the void volume, P_1 is the initial sample cell pressure, P_2 is the pressure in the reference cell after charging with helium and P_3 is the pressure in the sample cell and reference cell after expansion. By comparing plots of helium void volume measurement versus pressure for clay minerals (Kaolinite, Smectite and illite) with quartz as shown in Figure 3.4; they observed that the total void volume increased for pure clay minerals compared with a constant value for quartz. However, the assumptions of constant void volume for quartz in the research

was not obvious compared to that of clay minerals which increased with increasing pressure.

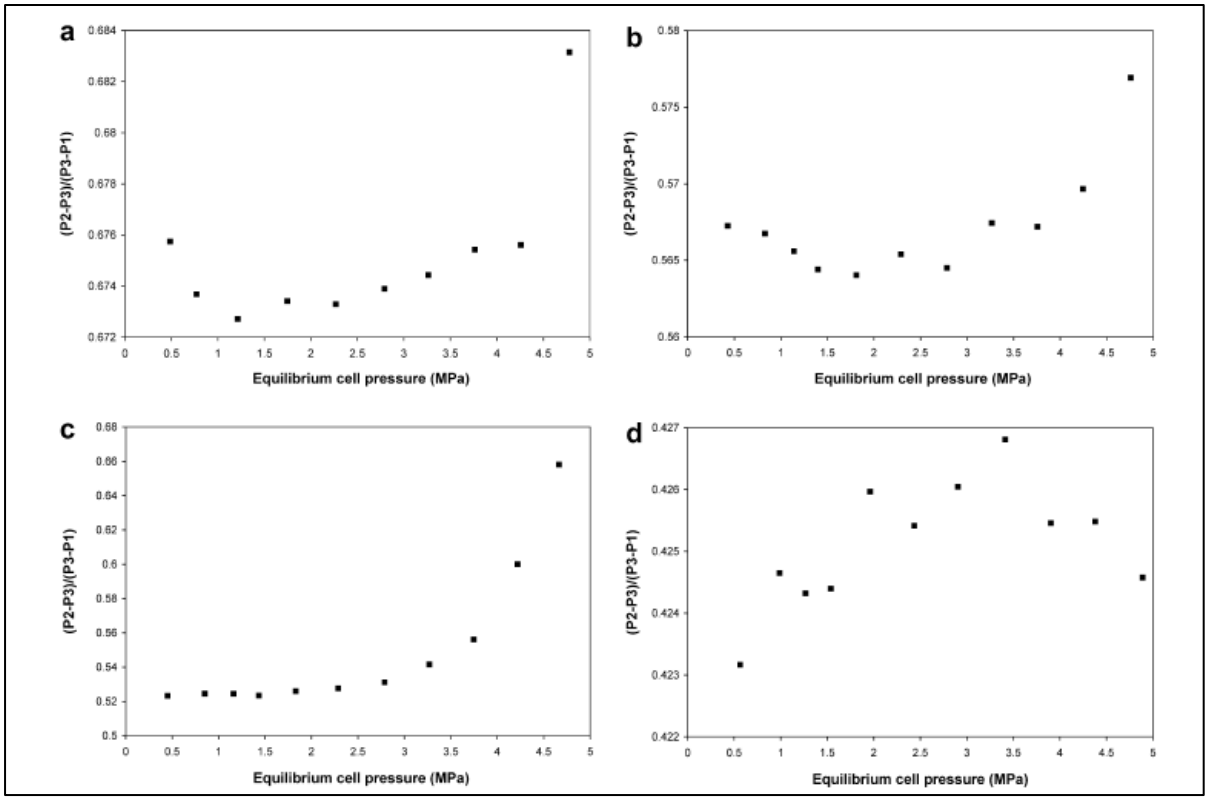

Figure 3.4: Comparison of measured void volume for major constituents of shale/mud rock samples (all on dry basis). (a) Kaolinite; (b) smectite; (c) illite; (d) quartz (Ross and Bustin, 2007)

They conclude that the uniform pore size of quartz leads to the total void volume remaining constant compared with the inconsistent structure of shale and clay minerals in which there was an apparent total void volume increase with variable pressure.

3.2.3 Effect of Contact Time on void volume measurements

The contact time influences the void volume measurement due to the time-dependant diffusive nature (Mair et al., 1998) of helium. However, only two researchers (Gasparik et al., 2013, Ross and Bustin, 2007) conducted experiments to analyse the impact of contact or equilibrium time on void volume measurement.

Gasparik et al, (2013) observed that an equilibrium period of at least 500 min (> 8 hrs), must be given when measuring the void volume in organic shale due to their low permeability.

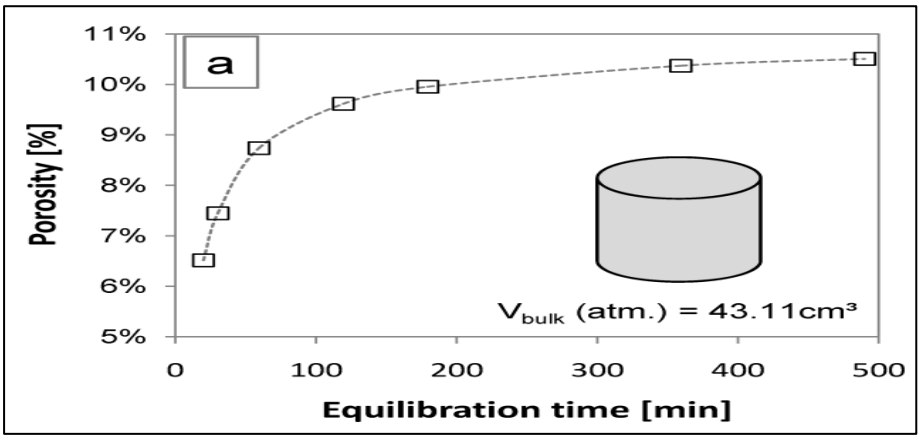

Figure 3.5: Measured shale porosity as a function of equilibrium time (Gasparik et al., 2013)

From Figure 3.5, as equilibrium time increased the total sample porosity increased until it tends to stabilise at 500 minutes. This observation indicates that insufficient contact time, for example, less than 30 min, could result in a significant underestimation of the apparent porosity.

Ross and Bustin, (2007) investigated the effect of contact time on accurate void volume estimation on shale and pure clay minerals (Kaolinite, illite, Smectite). They observed that diffusion of helium into sample volume is a function of time from calculated excess helium capacities using different calibration times.

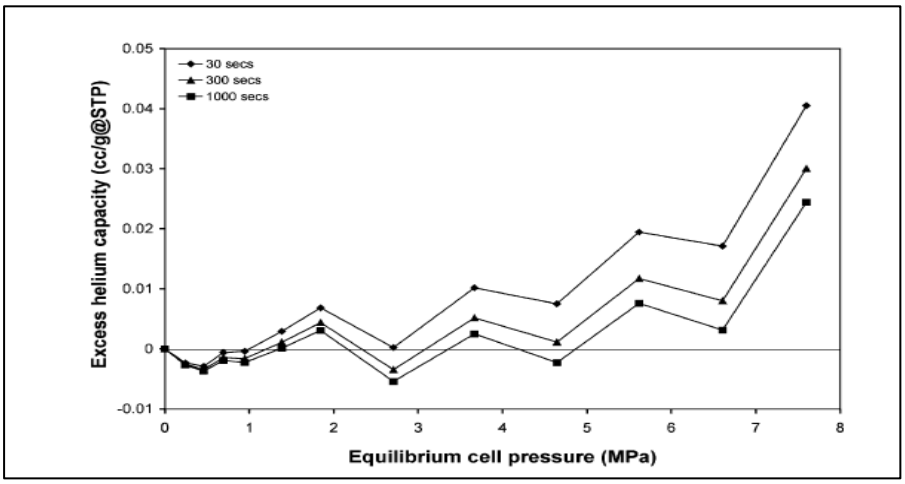

Figure 3.6: Calculated helium isotherms of a shale sample using various contact time (Ross and Bustin, 2007).

They concluded that using shorter time in void volume measurements produces smaller void volume since the samples will not be saturated due to less time for helium to

diffuse and occupy the sample (Figure 3.6). However, with longer contact time (i.e. 1000 s), the gas molecule has higher accessibility to sample pore spaces.

3.2.4 Effect of water content on void volume measurement

Errors in measured void volumes due to the presence of water in pore spaces and surface area of core or crushed samples remain a challenge for storage capacity estimation.

Ross and Bustin, (2007) used shale and mudrock samples to investigate the effect of moisture on void volume. They conclude that the occupation of adsorption sites and pore-throats by water creates less space for the helium molecule to occupy and may restrict helium diffusion, as suggested by the less significant increase in void volume in moist samples from their results.

Muhammed et al., (2009) evaluated errors in helium void volume determination, assuming that the sample under investigation is at its equilibrium saturation state with water i.e. assuming that no water-rich phase exist. The water is adsorbed completely by the sample in the volume of the sample cell (V_{cell}) and has a volume of Water (V_{ads}). This assumption is based on available experimental data on helium solubility in water and considering that, the Helium void volume does not vary with change in pressure as reviewed in section 3.2.2. They applied the equation (Eqn. 3.4) below to determine the void volume of a water saturated adsorbent:

$$V_{void}^{helium} = V_{container} - (V_{adsorbent} + V_{water}^{ads}) \qquad (3.4)$$

Where V_{void}^{helium} is the measured void volume, $V_{container}$ is the volume of the sample cell, V_{water}^{ads} is the water adsorbed in a sample and $V_{adsorbent}$ is the solid adsorbent capacity. Adsorbents with water present in their void spaces have a correction that accounts for the fact that the void volume measurements in the presence of water will lead to errors i.e. underestimating the volume. The correction for this experimental error is to subtract the amount of gas soluble in the water from the amount adsorbed (calculated in the usual manner for dry adsorbents). Errors in this correction is expected to be greatest in magnitude for gases that are highly soluble in water, such as CO_2 (Mohammed et al., 2009).

At the macro scale, Gasparik et al, (2014) proved that trace amounts of water (usually in ppm range) in high-purity gases could affect void volume estimations. They conclude that the presence of water in adsorption experiment requires attention because the total amount of water in the system container does not change with pressure (assuming dry injection gas).

So far, most literature related to the effect of water on void volume measurement are mostly theoretical formulations that only consider the effect of adsorbed water. Unfortunately, few experimental studies have investigated the effect of water on the void volume measurement using sandstone as part of adsorption capacity experiments.

3.3 Summary

- The sources of error involved in void volume measurements when using helium as suggested by researchers (Ross and Bustin, 2007; Muhammed et al., 2009) include; Selection of helium as an appropriate inert gas, averaging the void volume values for multiple pressure steps, Contact time and the presence of water.
- Helium expansion method is the only accurate and efficient method available for now, and is used generally as a "standard" procedure for measuring adsorption on the surface of adsorbent solids.
- Sample form (crushed, core) and type (pure clay, clay shale, sandstone) used for these tests need to be taken into account since each of these materials have different properties. Moreover, most of the research on void volume measurements were related to either powdered clay or shale.
- Literature review showed that proper experimental techniques and a void volume of high precision are critical for obtaining an accurate adsorption quantification.
- Methodology adopted in research determines the accuracy and precision of experimental dataset while helium accessibility to sample pore space mainly determined by helium adsorption and its accessibility to the void volume.
- Water occupies adsorption sites in surface, pore throats of microporous solids creating less space for the helium molecule to occupy, and may restrict helium diffusion.

3.4 SECTION 2: Adsorption mechanism in sandstone reservoirs and the effect of water and brine

3.4.1 Abandonment pressures of Depleted gas reservoirs

Depletion is a stage in the lifetime of a reservoir when hydrocarbons production diminishes to sub-economic levels even though significant hydrocarbons remain in the reservoir, some of which may be recovered with appropriate workovers on wells or assisted recovery technique (Hovorka et al., 2009). The abandonment pressure is the minimum pressure of the reservoir at abandonment or depletion.

Recent studies have shown that the abandonment pressure is a key connection point between the methane (CH_4) gas recovery efficiency and CO_2 sequestration. From the angle of economic development, if the abandonment pressure is too high, the gas recovery will reduce (Godec et al., 2014), the injection pressure also must be high enough to inject CO_2 into depleted gas formation, on the contrary, if the abandonment pressure is too small, the gas recovery and CO_2 storage capacity will be enhanced. However, too little abandonment means too low abandonment gas rate. Thus, the development cost will sharply increase (Tian et al., 2016).

The amount of gas in depleted reservoirs at abandonment pressure is of interest since it has to do with the mechanics of the storage reservoirs. Abandonment pressure varies for different gas fields, with values ranging from 50 – 100 psia or 0.34 – 0.69 MPa (Okwananke et al., 2011) or range of 50.76 and 116.03psia or 0.35 and 0.80 MPa (MacRoberts, 1962; Okwananke et al., 2011, Yekeen Adeboye & Sulaimon 2011, Mathias et al., 2014). Singh et al., (2011, 2012) considered an initial pressure of 580.151psia or 4.0 MPa, Han et al., 2012 considered an initial pressure of 999.31psia (6.89 MPa), Mukhopadhyay et al., 2012 presented numerical simulations concerning CO_2 injection into a depleted gas reservoir at 72.5189 psi or 0.50 MPa. Afanasyev, 2013 assumed a minimum initial pressure of 652.67psia (4.50 MPa) and Ziabaksh-Ganji & Kooi, 2014 assumed an initial pressure of 870.226 psi (5.90 MPa).

Most previous work relating to Enhanced gas recovery and CO_2 sequestration in depleted gas reservoirs used simulation with investigated pressures ranges higher than 1450.38 psi or 10.0 MPa (Andre et al., 2010; Mathias et al., 2013), and mainly investigated the effect of CO_2 injection on depleted gas reservoirs. The effect of

methane (CH_4) adsorption at abandonment pressure of depleted reservoirs is yet to be evaluated.

3.4.2 Methane (CH_4) and carbon dioxide (CO_2) adsorption in Enhanced gas recovery and sequestration (EGR-CO_2)

Sandstones in gas reservoirs are composed of clays that serve as adsorption sites, which have high gas storage capacity (Sondergeld et al., 2010). The adsorption characteristics of clays in sandstone are necessary for the exact determination of gas reserves in depleted reservoirs, i.e. of the optimisation of primary and secondary recovery procedures (Sandor, 1977). The determination of adsorption capacity of sandstone is a complicated task because sandstones have a complex mineral composition, particle size also changes within a wide range (Berczi et al., 1970). Clays as important component of sandstone will contribute significantly to gas storage in sandstone reservoirs.

Numerous research have been conducted regarding CO_2 storage in depleted reservoirs and various mechanism have been reported. Even though an understanding of, as well as an ability to predict these different physical and chemical processes are needed for successful storage projects to be designed. These mechanisms with the exception of adsorption process are not the focus of this research and have been reviewed in brief.

The process of CO_2 injection into an underground reservoir initiates various trapping modes in sequence. The initial trapping method is physical (stratigraphic and residual), followed by chemical (solubility and mineral) trapping as time progresses (IPCC., 2005; Jung and Wan., 2012; Luo et al., 2012; Bolourinejad et al., 2013; Goater et al., 2013; Hellevang et al., 2013). These mechanisms have been extensively investigated using numerical modelling and laboratory experiment (Gunter et al., 1993, 1997; Xu et al., 2003, 2005; Gaus et al., 2005; Knauss et al., 2005; White et al., 2005; Zerai et al., 2006; Ide et al., 2007; Hesse et al., 2008; Saadatpoor., 2009; Gaus, 2010; Pentland et al., 2011; Lu et al., 2012). Carbon dioxide can be retained in geologic formations by the following four mechanisms (Hitchon., 1996; Dooley., 2006; Mazumder et al., 2006): first, CO_2 can be trapped as a supercritical fluid under a low permeability caprock. This process is known as hydrodynamic trapping (Bachu et al., 1994; Saripalli and McGrail., 2002; Klusman., 2003) and relies on the physical displacement of pore fluids. Second, CO_2 can dissolve into the fluids present in the formation, referred to as solubility trapping. Third, CO_2 can react directly or indirectly with the brine and minerals in the

geologic formation leading to the precipitation of secondary carbonate minerals referred to as mineral trapping. Fourth, methane molecules are adsorbed in reservoir rocks and clays; however, since the chemical bond between these rocks/clays and CO_2 is favorable, CO_2 will replace methane when it is injected into the reservoir. This mechanism is referred to as CO_2 adsorption.

The mechanism of Enhanced gas recovery and sequestration is gas displacement and pressurisation; as injected CO_2 moves through the pore space and surface area displacing CH_4 ahead of it. The high density of carbon dioxide can be exploited to favour displacement of methane with limited gas mixing by injecting carbon dioxide in low regions of a reservoir while producing from higher areas in the reservoir (Oldenburg et al., 2004). The process of Enhanced gas recovery and sequestration is depicted in Figure 3.7. It shows the separation and compression of CO_2 from industrial and petroleum refining sources, injection into a mature natural gas reservoir, re-pressurization and enhanced production of CH_4, and the beneficial use of the CH_4 as a fuel. (Oldenburg et al., 2004).

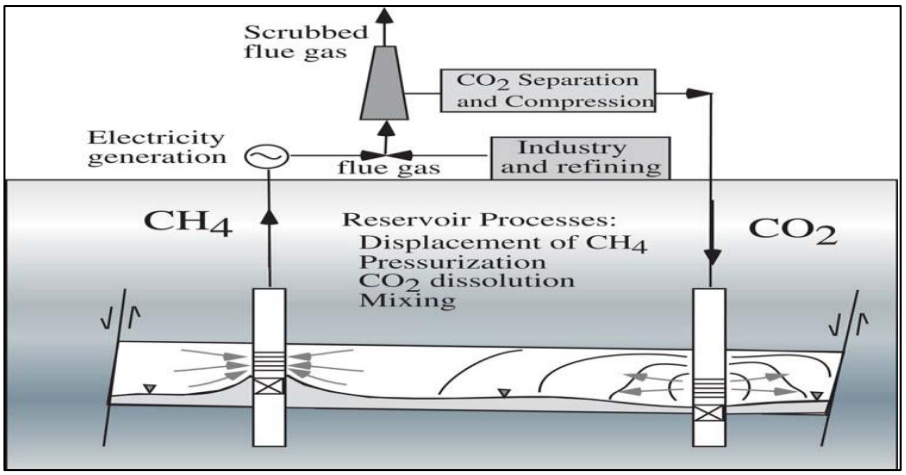

Figure 3.7: Schematic of EGR-CO_2 process (Oldenburg et al., 2014).

Van der Meer et al., (2009) advocate including the concept of total affected space, i.e. the entire space whose state or qualities change during the total storage time because of the storage operation in storage capacity calculations. Regarding the methane (CH_4) adsorption of sandstones gas reservoirs and its application in the Enhanced recovery and sequestration process, there are little to be found in the literature.

To date, there have only been few published papers on CH_4 and CO_2 adsorption in sandstones:

Fujii et al., (2010) measured CO_2 adsorption on Berea sandstones at 50°C and 100°C. They found Langmuir-like CO_2 of Berea sandstone to be 3.7 mmol/g and 2.8 mmol/g at 50°C and 100°C at 2900.75 psia or 20 MPa respectively.

Eliebid et al. (2017) measured CO_2 adsorption using Kentucky sandstone. They found CO_2 adsorption of Kentucky sandstone to be 8.92 mmol/g, 2.8 mmol/g and 10.06 mmol/g at 50°C, 100°C and 150°C and 725.189 psia or 5 MPa respectively.

3.4.3 Methane (CH_4) Adsorption of Clay-rich rocks

Early studies on clays adsorption focused on the adsorption study of polar organic compounds (Bissada and John., 1969; Berrada., 1992; Goss., 1994) or volatile organic compounds (Goss., 1996; Morrissey and Grismer., 1999; Donahue et al., 1999). Previously, methane and wet hydrocarbon gases were believed to be inherently non-adsorptive to mineral matter and clays (Crosdale et al., 1998; Stoessell and Byrne., 1982; Kosuge., 1994), although the adsorption of methane, ethane on crystalline silica (Choudhary and Mayadevi., 1996) and non-hydrocarbon gases including noble gases were already measured for clay systems (Aylmore., 1974; Cheng & Huang., 2004). Recently, using single gas measurements, higher adsorption of CO_2 compared to CH_4 have been reported under the same pressure and temperature conditions (Gensterblum, 2013).

Clay minerals may provide adsorption capacity in sandstone due to their high internal surface area (or micropore volume). Using powdered clay minerals & quartz minerals, Schettler et al. (1991) noted the significant adsorptive capacity of clay minerals when measured individually. Studies by Lu et al., 1995, Ross and Bustin, (2007) and recently Gasparik et al., (2012) and Ji et al., (2012) have shown significant methane adsorption capacities in clays and clay-rich rocks. Illite has significant methane storage capacity and in reservoirs with high clay composition act as the primary storage system (Lu et al., 1995; Gasparik et al., 2014). Analysis of composition and pore structure shows micro porosity in clay minerals, particularly illite and montmorillonite (Ross and Bustin, 2009). Most of the research on carbon dioxide (CO_2) and Methane adsorption

(Lu et al.,1995; Ross and Bustin., 2009; Gasparik et al., 2012; Ji et al., 2012; Schaef et al., 2014; Li and Wu., 2015;) were conducted on clay-rich shale or pure powdered clay.

Ji et al., (2012) used powdered clay (Montmorillonite, Kaolinite, Chlorite and interstratified illite/Smectite) at different temperatures of 35, 50, and 65˚C, respectively, and at a different pressure up to 2175.57psia (15MPa).

Table 3.2: Methane adsorption capacity of different clay-mineral dominated rocks.

	Montmorillonite	**I–S mixed layer**	**Illite**	**Kaolinite**	**Chlorite**
Langmuir maximum (mmol/g rock)	0.380	0.182	0.079	0.120	0.103
Langmuir constant (1/MPa)					
35.4˚C	0.451	0.269	0.211	0.179	0.165
50.4˚C	0.343	0.203	0.181	0.134	0.132
65.4˚ C	0.254	0.163	0.148	0.105	0.119

Note: Unit conversion factor: 1 mmol/g = 711.24 scf. /ton.

The results from this study are shown in Table 3.2 . They show an increasing sequence of the Langmuir maxima of CH_4 adsorption capacity following a sequence of montmorillonite/I–S mixed layer/kaolinite/chlorite/illite. In contrast, the Langmuir constant decreases following a sequence of montmorillonite/I–S mixed layer/illite/kaolinite/chlorite. Recently Zhang et al., (2013), have drawn a similar conclusion as well.

Liu et al., (2013) have found that the adsorption capacities of individual clay minerals decrease in the order: smectite >> mixed layer I/S > Kaolinite > Chlorite > illite (these results differ somehow from those presented by Ross and Bustin on pure clay standards, suggesting that texture of clay minerals and sample preparation techniques should be considered).

Schaef et al., (2014) conducted a study to investigate the interactions between dominant clay minerals and adsorbing gases (CH_4 and CO_2) and associated economic consequences. Where enhanced condensation of CO_2 followed by desorption on a clay surface is observed under supercritical conditions, a linear sorption profile emerges for

CH_4. Volumetric changes to montmorillonites occur during exposure to CO_2. Theory-based simulations identify interactions with interlayer cations as energetically favourable for CO_2 intercalation. In contrast, experimental evidence suggests CH_4 does not occupy the interlayer and has only the propensity for surface adsorption. Mixed CH_4: CO_2 gas systems, where CH_4 concentrations prevail, indicate preferential CO_2 adsorption as determined by in situ infrared spectroscopy and X-ray diffraction techniques.

Heller and Zoback, (2014) measured methane and carbon dioxide adsorption isotherms using pure clay minerals. Carbon dioxide isotherms were included to assess its potential for preferential adsorption in depleted gas reservoirs. They showed carbon dioxide has approximately 2–3 times the adsorptive capacity of methane in pure mineral constituents.

Li and Wu, (2015) clarified in more details on the gas adsorption contribution by individual clay minerals, showing that the sequence of gas adsorption contribution from high to low is montmorillonite/kaolinite/illite/chlorite.

Several investigators found positive correlations between clay content and adsorption capacity (Gasparik et al., 2012; Ji et al., 2012; Schettler and Parmely., 1991; Merkel et al., 2015). Compared with extensive studies of CO_2 adsorption in depleted reservoirs, less attention has been paid to CH_4 adsorption of clay minerals, although clay minerals are a critical component of sandstone. This lack of research may be because it is assumed that clay minerals have higher hydrophilicity and low porosity; consequently, it is expected that clay minerals would encounter difficulty in the adsorption of methane (CH_4). However, recent studies (Cheng and Huang., 2004; Lu et al., 1995; Ross and Bustin., 2009) have shown the ability of clay minerals for methane (CH_4) adsorption. Although the above-mentioned studies examined the CH_4 absorption capacity of clay minerals, unfortunately, the CH_4 adsorption mechanisms, including CH_4 adsorption sites and influencing factors, remain unclear (Liu et al., 2013). Abundant studies have focused on CO_2 adsorption of sandstones. However, results of adsorption capacity of CO_2 and CH_4 in clays, which are component of sandstones, have revealed high CO_2

adsorption capacity compared to CH_4 adsorption capacity (Cui et al., 2009; Lu et al., 1995; Liu et al., 2013; Heller and Zoback, 2014).

3.4.4 The effect of Water and Brine content on methane (CH_4) adsorption capability

Sandstone is the most widespread reservoir rock and have available pore spaces to reserve hydrocarbon (Alimoradi et al., 2011). These reservoirs consist of at least two different phases e.g. gas-water (Dandekar, 2006). The increasing price of natural gas in recent years has stimulated interest in methane-saturated formation waters of sandstone reservoirs as a potential source of energy. Most of the storage capacity identified in the subsurface consists of porous rocks saturated with brine or fresh water (Jordan & Doughty., 2009).

The result of depletion is that as hydrocarbon recovery declines in gas reservoirs, they become more like brine formations. However, hydrocarbon production rate commonly exceeds the rate at which brine can flow into a reservoir resulting in pressure depletion during production operations (Hovorka et al., 2009). Hydrocarbon reservoirs occur in the same types of rocks and have the same kinds of seals as their host brine formations; the CH_4 will move through and is trapped in substantially the same manner in both. As methane saturation decreases in depleted reservoirs, its rate of flow also decreases. In most depleted fields, water is mostly produced with a small percentage of hydrocarbon (Hovorka et al., 2009).

Different methods have been utilised to study the impact of water on methane adsorption in clays:

Liu et al. (2013) investigated the impact of adsorbed water and interlayer distance of montmorillonite, kaolinite and illite on CH_4 adsorption. Adsorbed water can occupy the adsorption sites, leaving little space for CH_4 adsorption. Results from their study indicates that Kaolinite and illite had lower contents of adsorbed water than Montmorillonite and more readily adsorbed CH_4. Montmorillonite adsorbed CH_4 molecules in its interlayer space because its interlayer distance is larger than the size of the CH_4 molecule. The entrance of CH_4 into the interlayer space of Montmorillonite

occurred at low pressures, and more CH_4 molecules entered the interlayer space at high pressures.

Jin & Foozabadi, (2014) quantified the effect of water on the methane adsorption of clays at the molecular scale and observed that for a sample with a pore size of the range 1nm – 4nm, methane sorption decreases significantly as the average water density increases. Water molecules interact actively and have a high affinity for clay surface leading to sorption capacity reduction.

Using relative humidity condition of 0.01 to 0.09 and water saturation of 5 to 50%, Li et al., (2015) showed that:

- Water saturation is significantly affected by pore size, and when the pore size is small, the water saturation is higher.
- Pores full of water have no capacity for gas adsorption.
- For partially saturated pores, the gas adsorption depends upon the interaction characteristic between the gas, solid and liquid interaction, which could lead to a reduction in adsorption by about 90%.

Researchers with interest in gas reservoirs have a general agreement that water has adverse effect on methane adsorption of reservoirs in general (Gasparik et al., 2013; Ross and Bustin., 2007; Tan et al., 2014; Yuan et al., 2014; Merkel et al., 2015). The ratio of adsorbed and free gas is strongly dependent on the water saturation of the sandstone, but quantitative impact analyses are not available in the literature. While the impact of water on methane adsorption using powdered clay minerals have been investigated (Ji et al., 2012; Heller and Zoback, 2011, 2014; Jin and Foozabadi, 2014; Liu et al., 2013), studies on the impact of water on the methane adsorption capacity of water or brine saturated sandstones are few. Notwithstanding, the effect of water on the adsorption behaviour of methane on the reservoir scale, hence also on enhanced gas recovery and sequestration, is still not sufficiently understood.

3.5 Summary

This section reviewed the Methane adsorption behaviour in sandstones, which is critical for using adsorption as a displacement process in depleted reservoirs for enhanced gas recovery and sequestration applications and the areas covered so far in the literature as are follows:

- Adsorption capacity of sandstones were mostly conducted with CO_2 under different (unconfined, isostatic) conditions.
- Most studies on depleted reservoirs were conducted using simulations with pressures higher than the abandonment pressures (i.e. greater than 1450.38 psia)
- The methane adsorption capacity of clay-rich shale and pure powdered clay have been more researched compared to sandstone.
- Gas storage capacity identified in most depleted reservoirs consists of porous rocks saturated with brine or fresh water.
- The result of depletion is that as hydrocarbon recovery declines in gas reservoirs, they become more like brine formations.
- Precise knowledge of CH_4-induced interactions between CH_4, water or saline and sandstone rock and of the impact on the chemical and physical properties of the reservoir system is critical to the design and operation of the EGR-CO_2 process.

CHAPTER 4

4 EXPERIMENT SET UP AND PROCEDURE

4.1 Introduction

This chapter introduces the experimental set up involved, procedures and description of detailed steps involved to ensure precise and accurate results. The research methodology focused on collecting and analysing experimental data acquired through a programme of experiments relating to the interaction of a range of different parameters and their influence on the adsorption of sandstones. The sandstone core samples used during this study are: 1) Bandera, and 2) Scioto. Details of the rock cores are presented in Subsection 4.2.1.

The chapter covers two phases of the work including:

- Phase 1: The Material characterisation was conducted by measuring the Void volume available for gas storage using a helium pycnometer (PORG 200). Many parameters affect the measurement of the helium void volume, but in this study, we concentrate on the pressure, contact time and water content. These mechanisms were investigated and analysed based on the results of experimental laboratory work.

- Phase 2: Quantitative measurement of sandstone adsorption was conducted using a self-assembled manometric set-up, some parameters, which affect methane sandstone adsorption such as the effect of equilibrium pressure, the abandonment pressure in depleted reservoirs, clay minerals; Brine and water content were investigated.

Details of the experimental scheme and steps are provided in Figure 4.1.The experimental set ups, procedures as well as precautionary measures and sources of error are detailed in each respective section.

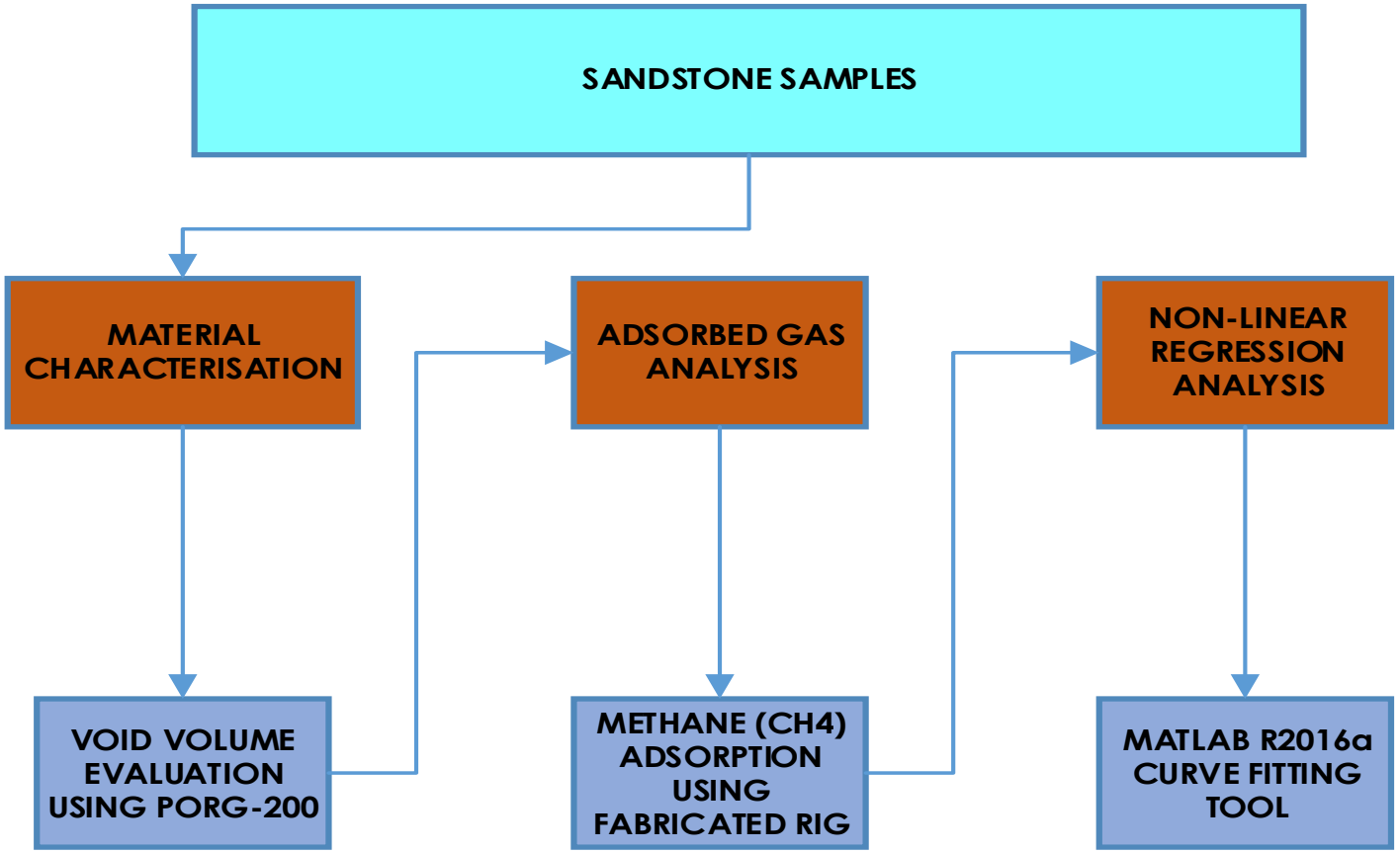

Figure 4.1: Schematic flow diagram of techniques.

4.2 Materials

4.2.1 Sandstone samples

Bandera and *Scioto* sandstone core samples of sizes 3 by 1.5 inches respectively (Figure **4.2**) were obtained from Kocurek Industries INC, Hard Rock Division, 8535 State Highway 36 S Caldwell, TX 77836). Table **4.1** presents the physical properties of the sandstone samples respectively:

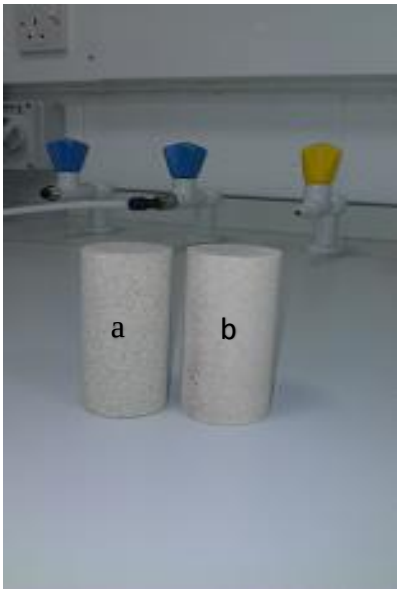

Figure 4.2: Image of 3 by 1.5-inch sandstone cored sample, (a) *Bandera* and (b) *Scioto*.

Table 4.1: Dimensions and Physical Properties of Core samples.

Core sample	Length(cm)	Diameter(cm)	*Porosity
Bandera Gray	7.6650	2.5199	21%
Scioto	7.6685	2.5179	11%

***This is the porosity determined by Kocure industries were samples were sourced.**

4.2.2 Laboratory gases

Helium stored in a BOC gas cylinder under a pressure of 2103.047 psia (14.50 MPa) and temperature 15°C was used to measure void volume. Meanwhile, the adsorption capacity measurement used Methane. The purity of all the gases was 99.996%. The gases were supplied by BOC in Surrey, UK.

4.3 Material Characterisation

4.3.1 XRD technique

XRD is a rapid analytical technique primarily used for phase identification of a crystalline material. The analysed material is finely ground, homogenised, and average bulk composition is determined. Table 4.2 presents the X-ray Diffraction (XRD) results by Kocurek Industries of the mineral constituents.

Table 4.2: XRD results by Kocurek Industries showing the mineralogy of samples.

Minerals	Bandera	Scioto
Quartz	57	70
Plagioclase	12	5
KFeldspar	Nil	2
Dolomite	16	Nil
Pyrite	Trace	Trace
Mica + illite	10	18
Kaolinite	3	Trace
Chlorite	1	4

4.4 SECTION 1: Void Volume evaluation

4.4.1 Experimental setup

The experimental apparatus was a PORG-200™, a manually operated helium pycnometer incorporating digital technology manufactured by Core Industries (11Princess Road, Suite H Lawrenceville, NJ 08648, a U.S.A). The component of the apparatus shown in Figure 4.3 consists of a helium inlet port: a 1/8" swagelok™ bulkhead fitting on the rear side of the device that allows connection of the PORG-200™ to a regulated helium source. Two chambers, the sample holder (with a removable gas-tight lid) hold the sample and the second chamber of fixed, known (via calibration) internal volume – referred to as the reference cell, was used as a reference volume for gas expansion. Stainless steel disk of varying known volumes were placed inside the sample holder. These disks were used for calibration procedures.

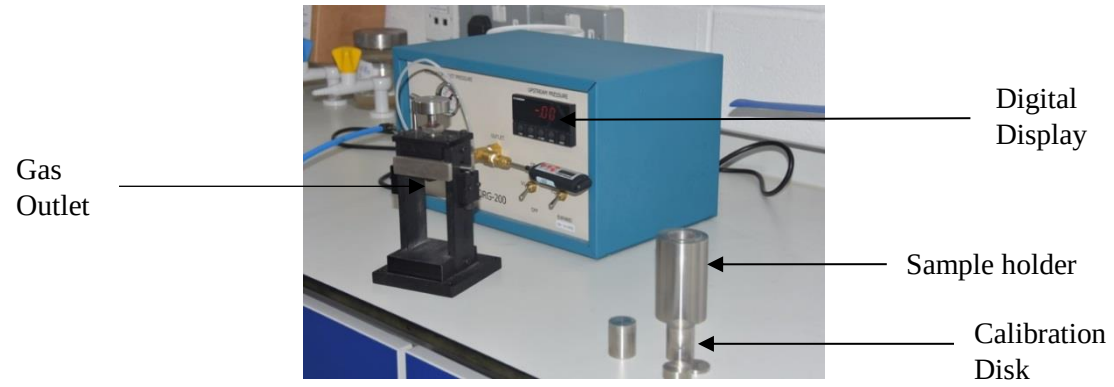

Figure 4.3: Experimental setup of Core Lab PORG™ 200.

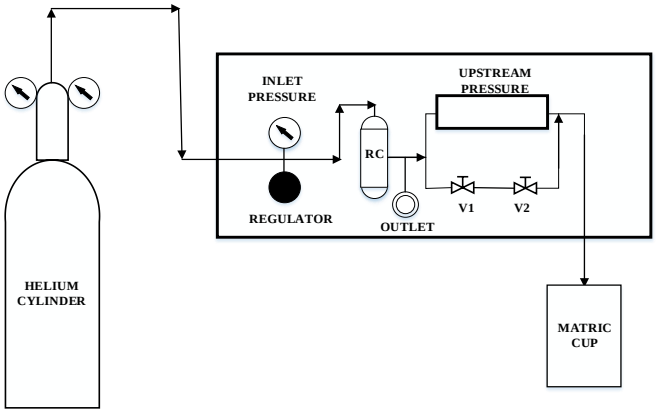

Figure 4.4: Schematic representation of PORG 200™

The device (Figure 4.4) additionally comprises of two valves, valve 1 (V1) controls the flow of helium from the regulator to the reference cell, and valve 2 (V2) is a two-position valve that directs helium from the reference cell to the sample cell or vents the cell after the measurement is complete. A Digital pressure display labelled upstream pressure reads reference pressure in psia, and a regulator allows fine-tuning of the input gas pressure to the desired reference pressure while a pressure gauge marked regulator inlet pressure displays the inlet helium pressure in psia. The outlet has a 1/8" Swagelok™ fitting that allows connection of the PORG-200™ to the sample holder for grain volume measurement. A digital temperature sensor measures the temperature of the helium.

4.4.2 Principle of operation of PORG 200™

The principle of operation of this device is based on the ideal gas Law. Grain volume is determined from the expansion of a known volume of helium into a calibrated sample holder. Using Ideal Gas Law (Eqn. 4.1) and a known volume of gas (Helium) expanded into a calibrated sample holder:

$$\frac{P_1V_1}{T_1} = \frac{P_2V_2}{T_2} \quad (4.1)$$

where:

p_1 = Initial Absolute Pressure

v_1 = Initial Volume

T_1 = Initial Absolute Temperature

p_2 = Expanded Absolute Pressure

v_2 = Expanded Volume

T_2 = Expanded Absolute Temperature

The reference volume was pressured to an initial pressure and expanded into a sample holder containing the sample to be analysed. A second pressure is read and used to compute the unknown volume. The following Eqn. 4.2 is often used to derive grain volume:

$$V_g = V_c - V_r\left(\frac{P_1-P_2}{P_2-P_a}\right) + V_{vd}\left(\frac{P_2}{P_2-P_a}\right) \quad (4.2)$$

Where:

V_g = Grain Volume

V_c = Sample Chamber Volume

V_r = Reference Chamber Volume

V_{vd} = Valve Displacement Volume

P_1 = Absolute Initial Reference Volume Pressure

P_2 = Absolute Expanded Pressure

Pa = Absolute Atmospheric Pressure Initially in Sample Chamber

4.4.3 Sample preparation

4.4.3.1 Bulk volume measurement

Bulk volume is the total volume of the sample including particle volume, inter-particle void volume, and internal pore volume. It can be calculated accurately from the dimensions of a core sample using a caliper (Figure 4.5) if it is an exact right cylinder and there are no surface irregularities.

Figure 4.5: Bulk Volume Measurement using Calliper method.

In this investigation, this was taken care of by making three measurements for both core samples and calculating the average (Table 4.3). The procedure used is outlined below:

a. The sample was dried in the oven for 24 hours at 60°C
b. Samples were then allowed to cool at for 3-4 hours
c. The dry mass of the samples was determined
d. The cored samples were rotated at 90° between each measurement
e. The Caliper was placed about 1/3 the length of the core sample each time the measurement was taken.
f. About three measurements were taken to determine the diameter of the sample
g. The calliper was kept perpendicular to the core during each measurement
h. Using a calliper to obtain several diameter measurements and several length measurements, the average diameter and average length were used to calculate the bulk volume (Eqn. 3.3) of the sample using the calliper method:

$$V_b = \pi r^2 L \qquad (4.3)$$

Where r is the radius of the cylinder, L is the length and π is a mathematical constant approximated as 3.14159.

Table 4.3: Bulk volume measurements of core samples.

	Scioto		**Bulk Volume**	**Bandera Gray**		**Bulk Volume**
3 by 1inch core sample						
	Radius(in)	**Length(in)**	$2.33in^3$ or $38.17cm^3$	**Radius(in)**	**Length(in)**	$2.33in^3$ or $38.22cm^3$
Average	0.4956	3.0191		0.4960	3.0178	
3 by 1.5-inch core sample						
Average	0.7540	3.0200	$5.39in^3$ ($88.3263cm^3$)	0.7337	2.9904	$5.06in^3$ ($82.91854cm^3$)

4.4.3.2 Water content determination

Water content was determined by drying the sandstone samples at 60˚C over a period of 48hrs in an oven – (173-001-1-Re oven (7979 Willow Chase Blvd. Houston, TX 77070, US). Sample mass before and after saturation was recorded (Figure 4.6a), followed by saturating the sample in water for 48 hrs (Figure 4.6b). For each determination, the water content (W_C) was calculated from the mass loss using Equation 3.4:

$$w_c = {}^{M_{wet} - M_{dry}}\Big/_{M_{dry}} \times 100 \qquad (3.4)$$

Where M_{dry} is the mass of the dry sample, M_{wet} is the mass of the wet sample.

Figure 4.6: a) Weight measurement and b) Water saturation procedures.

4.4.4 Experimental Procedure

The PORG-200™ was powered up thirty minutes before samples were to be run to allow the transducer to reach equilibrium. During this time, the gas supply pressure was set at 120 psia (0.83 MPa) for the helium supply. The matrix cup (sample holder) was then attached to the helium outlet on the front panel of the instrument. Valve V2 was then turned to the vent position, and Valve V1 was opened. The regulator was set at approximately 95 psia (0.66 MPa), and Valve V1 was then closed. Turning Valve V2 to expand led to a pressure drop, which stabilised immediately. The pressure was then observed for 10 to 20 minutes. If the pressure continues to fall, there is a leak in the system. The helium source was switched off, and Valve V1 was opened, setting V2 to expand (to the open matrix cup). The pressure reading on the digital readout was showing zero. After the leak test, the volume was calibrated using five (5) reference disks of known volume at 90Psia (0.62 MPa). The relationship between the calibrated disk volumes and the resultant pressure was ascertained experimentally. This direct approach considers any variability of the reference or Matrix Cup volumes due to changes in temperature or other factors.

The experimental procedure involved, placing the sample with a known bulk volume (V_b) into a sealed matric Cup (i.e. sample holder) (V_c). Gas was charged into a reference cell (V_r) at a predetermined reference pressure (P_1), which is higher than the pressure (P_2) into the sample holder. The reference cell gas was then expanded into a connected chamber of a known volume containing a core sample by opening a valve between the two cells. The pressure of the system is then allowed to equilibrate until a stable value is observed. The grain volume (Eqn. 4.5), which was used to calculate the measured void volume, can then calculated using:

$$V_g = V_c - V_r \left(\frac{P_1 - P_2}{P_2 - P_a}\right) + V_{vd} \left(\frac{P_2}{P_2 - P_a}\right) \quad (4.5)$$

Where:

V_g	=	Grain Volume
V_c	=	Sample holder Volume
V_r	=	Reference Chamber Volume
V_{vd}	=	Valve Displacement Volume
P_1	=	Absolute Initial Reference Volume Pressure
P_2	=	Absolute Expanded Pressure
Pa	=	Absolute Atmospheric Pressure Initially in Sample Chamber

The pore volume (V_p) can be calculated from the bulk volume and grain volume measurements using Eqn. 4.6:

$$V_p = V_b - V_g \quad (4.6)$$

However, the definition of void volume (V_v) in this study refers to the total free spaces in the system, which are the pore volume in sandstone core sample, and the dead volume between system and matrix cup (Eqn. 4.7). Therefore, the void volume can be determined from:

$$V_v = V_p + V_d \quad (4.7)$$

Where, Vv, V_b, V_g, V_p, V_d are the Void volume, Bulk volume, Grain Volume, Pore volume and Dead volume between the sample and the holder respectively. Considering that pressure does not impact void volume and that there is no adsorption of helium on the core samples (Eqn. 4.8), therefore:

$$P_{total} = P_1 + P_2 \quad \text{And } V_{ads,\ initial} = V_{ads,\ final} = 0 \quad (4.8)$$

Where, P_{total}, P_1, and P_2 are the total gas pressure, initial gas pressure and final gas Pressure respectively. Considering that, the void volume is constant overall pressure range and no adsorption on core samples at each pressure step (Eqn. 4.9), therefore:

$$Vv_{\text{initial void}(P,T)} = Vv_{\text{final void}(P,T)} \quad (4.9)$$

$Vv_{\text{initial void}(P,T)}$ and $Vv_{\text{final void}(P,T)}$ are the initial calculated void volume at initially expanded pressure step and final void volume at the final expanded pressure step respectively. Since the initial volume does not change, we consider the volume of water taken up in the pore space of the sandstone core samples. By subtracting the space taken up by water from the void volume (Eqn. 4.10) we have:

$$Vv_{total} = V_{\text{initial void}} - \sum \Delta V_{pore} \quad (4.10)$$

Where, Vvtotal is the total void volume, $V_{\text{initial void}}$ is the initial calculated void volume and ΔV_{pore} is volume of water in pore space of core sample.

4.4.4.1 Effect of Pressure measurements on void volume

To investigate the influence of a range of experimental pressure on the measured void volume, the sandstones initial weight (i.e. the sample weight and moisture content) in grammes(g) was determined using a KERN Precision Balance as shown in Figure 4.7a. Samples were then dried in an oven (Ofite limited instrument) (Figure 4.7b) for at least 48hrs at 60°c. This was to avoid altering the clay properties (Aljaman et al., 2015). The sample weight being monitored until a constant weight was achieved. Using the pycnometer, incremental experimental pressures of 15 psia (0.10MPa), 45 psia (0.31 MPa), 65 psia (0.49 MPa), 85 psia (0.59 MPa), 95psia (0.66 MPa), 105 psia (0.72 MPa) and 115 psia (0.79 MPa) were used to determine the void volume. Helium gas of an initial pressure of 15 psia (0.10 MPa) was expanded into the sample holder containing the sample, after allowing 30 minutes for the system to reach thermodynamic equilibrium as suggested by the vendors. The expanded pressure in the sample volume was then recorded; the same step was repeated until all pressure steps were carried out.

The temperature of the system was also registered for each experiment conducted.

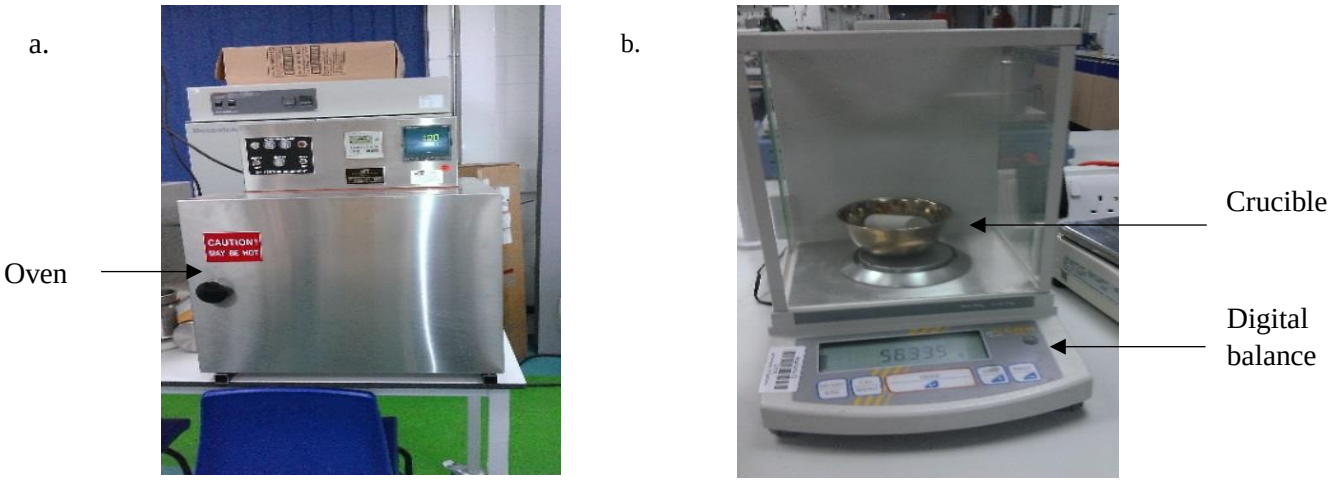

Figure 4.7: a) Electric Oven and b) Precision balance

4.4.4.2 Effect of Contact time measurement on void volume

Test to examine the influence of contact time on void volume values involved weighing the samples, and drying the samples in an ofite instrument – 173-001-1-Re oven (7979 Willow Chase Blvd. Houston, TX 77070, US. The temperature was kept at 60˚c for 48hrs. Once a constant weight was achieved, the samples were then placed into the sample holder of the helium pycnometer (PORG 200™). Helium expansions were carried out on the samples for each investigated pressure respectively. After each expansion, the system was allowed to reach thermodynamic equilibrium, and expanded pressure values were recorded at a 4-minute interval for about 4 hours (240mins) at a constant temperature of 23˚C.

4.4.4.3 Advantages of the PORG 200™ apparatus:

- Calibrated disk volumes and the resultant pressure is ascertained experimentally. This direct approach considers any variability of the reference or sample holder volumes due to changes in temperature or other factors.
- The void volume does not change with pressure; therefore, the void volume does not need to be recalculated at each step.
- The void volume is determined from grain volume. Therefore, error due to volume changes and reference cell to sample holder ratio are negligible.

- The determination of grain volume is not affected by the dead space between the sample and sample holder as the case with directly determining the void volume directly.

4.5 SECTION 2: Methane (CH_4) Adsorption capacity experiments

Since the inception of gas adsorption experiments until date, there have been some techniques used by various laboratories and researchers (Manometric, Volumetric, Gravimetric and chromatographic). The most widely used method in the laboratory to measure adsorption capacity is the manometric (Van Hemert et al., 2009; Battistutta et al., 2010; Ji et al., 2012; Khosrokhavar et al., 2014; Rani et al., 2015) and volumetric method (Sudibandriyo et al., 2003; Chareonsuppanimit et al., 2014; Guo et al., 2014). This technique is sometimes referred to as Sievert's method and can be designed as constant-volume (manometric) or constant pressure (volumetric) measurement (Liu et al., 1995). These methods are widely used because of their simplicity and ease of construction. Regarding modification and user designed equipment; researchers used several tactics:

a. Gasparik et al., (2013) modified their set up to enable sorption measurements at high temperatures, by separating the low-temperature zone (reference cell) and high-temperature zone (sample cell).
b. Li et al., (2015) developed a high-pressure gas adsorption–desorption instrument mounted on a constant-temperature oil bath,
c. Heller & Zoback., (2011) modified a conventional tri-axial machine to measure adsorption and gas permeability by incorporating a Quizix Series 1500 pump, using a method similar to volumetric adsorption principle.
d. Kang et al., 2011 used adsorption equipment in which an isothermal multistep gas- uptake process measures the storage capacity.

For this research, an adsorption rig was assembled by modifying a core flooding system by incorporating Swagelok fitting, tubing and digital measurement devices. The methane adsorption capacity of other rocks such as activated carbons, coals and shale (Lu et al., 1995) compared to sandstones might differ. Thus, an experimental design that is adequate for gas adsorption measurements on other microporous materials may not be

suitable for adsorption measurements on sandstone. Other researchers (Lu et al., 1993; Chareonsuppanimit et al., 2012) made a similar conclusion after making modifications to their experimental design.

4.5.1 Principle of operation

The principle of operation of the manometric adsorption equipment is based on the Ideal gas law (Eqn. 4.11) and is similar to void volume estimation using a helium pycnometer. The experimental set-up consists of two chambers, the reference cylinder (RC) and core holder (CH) separated by three valves (V1, V2, V3) as shown in Figure 4.8:

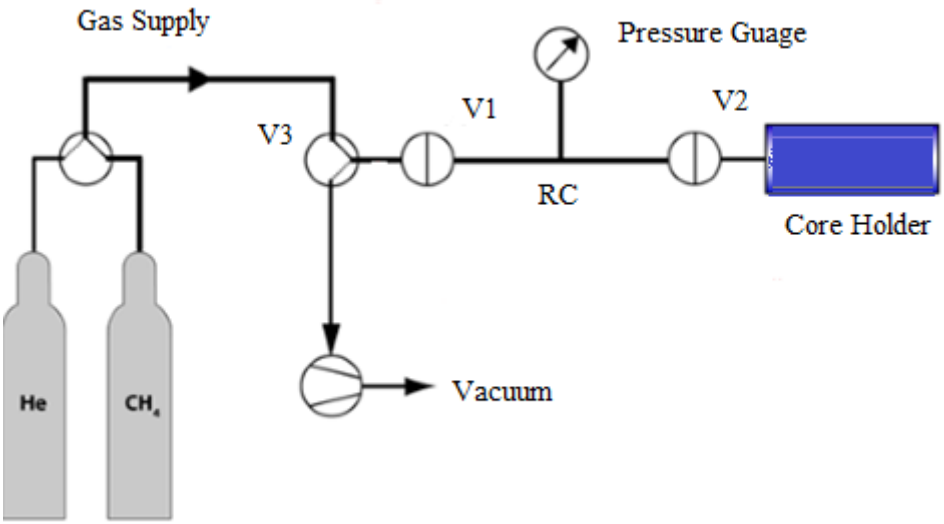

Figure 4.8: Schematic of self-built adsorption apparatus

The procedure involves pressuring the reference cylinder and then expanding the gas into a sample vessel of known volume and again measuring the pressure. The adsorbed amount n (moles) of gas is then calculated using the ideal gas law:

$$PV = nRT \qquad (4.11)$$

Where P is the pressure, V is the volume, n is the number of moles, R is the universal gas constant, and T is the temperature. This data is then used to calculate the void volume by applying Equation 4.12:

$$V_{void}=\frac{V_{ref}\left[\frac{P_{ref1}}{Z_{ref1}}-\frac{P_{ref2}}{Z_{ref2}}\right]}{\frac{P_{sam2}}{Z_{sam2}}-\frac{P_{sam1}}{Z_{sam1}}} \quad (4.12)$$

Where, V_v is the void volume, V_{ref} the volume of the reference cell, P_{ref1} is the initial reference cell pressure, P_{ref2} is the initial pressure in the reference cell, P_{sam1} and P_{sam2} is the initial pressure and pressure after expansion of helium in the sample cell, and Z are the respective compressibility factors of helium. The amount of gas adsorbed is determined by expanding methane from the reference cell at known initial pressure directly into the sample cell containing the sandstone core sample. The mass balance of gas within the reference cell and the void volume was then derived using the excess adsorbed volume equation (Eqn. 4.13). During the expansion of an adsorbing gas from the reference cell to the sample, the pressure will decrease due to both void volume filling as well as adsorption. Thus, the amount of gas adsorbed by the core sample at a certain pressure is the calculated as follows:

$$n^{excess}_{ads} = n_{inj} - n_{nonads} \quad (4.13)$$

Where n_{inj} is the number of moles originally in the reference cell (the number of moles expected to be in the system if no adsorption occurred), and n_{ads} is the number of molecules in the free phase at equilibrium (Eqn. 4.14), calculated as:

$$n_{nonads}=\frac{V_{void}}{RT}\left[\frac{P_{sam2}}{Z_{sam2}}\right] \quad (4.14)$$

The amount of gas injected from the reference cell to the sample cell can be determined using Eqn. 4.15:

$$n_{inj} = \frac{V_{ref}}{RT}\left[P_{ref1}/Z_{ref1} - P_{ref2}/Z_{ref2}\right] \quad (4.15)$$

Where V_{ref} and V_{sample} are the reference and sample cell volumes respectively, following a measurement at a single pressure, the valve separating the two chambers is closed, the

reference cell charged to a higher pressure and the process repeated until a full isotherm has been characterised. The procedure outlined above is for calculating what is termed excess adsorption (or sometimes Gibbs adsorption).

4.5.2 Experimental setup

The experimental setup is a customised manometric adsorption apparatus, it was designed and assembled to measure methane adsorption capacity at room temperature and specified pressure (Figure 4.9). It consists of a stainless-steel cylinder (core lab) and a Hassler-type core holder (Temco Inc.) used as the sample cell and reference cell respectively.

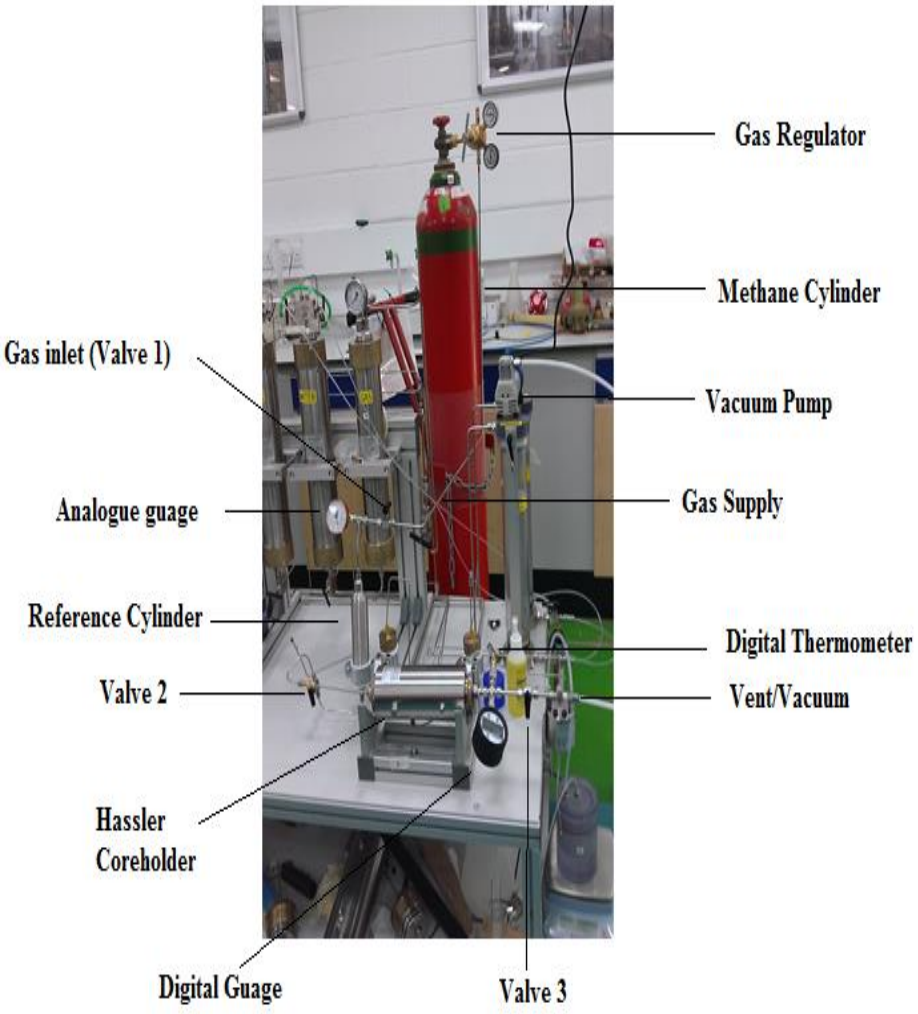

Figure 4.9: Self-assembled manometric adsorption apparatus.

Tempo ECH-series core holders, which are hassler-type core holders (Figure 4.10) are used as a sample cell. They are routinely used for gas and liquid permeability testing

and water flooding experiments. The core sample is held within a rubber sleeve by radial confining pressure, which simulates reservoir overburden pressures. Inlet and outlet distribution plugs allow fluids and gases to be injected through the core sample.

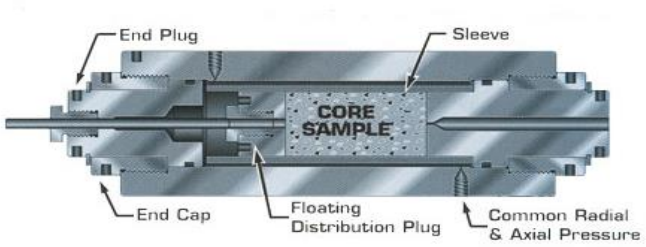

Figure 4.10: Temco core holder.

All apparatus components (valves, pressure gauges, temperature probe, a vacuum pump) were connected using Swagelok tees and crosses using 1/4" and 1/8" tubing with a combination of pipe with size 1/8" (316SS-Swagelok) and 1/4" with metal connections (Figure 4.11a and Figure 4.11b).

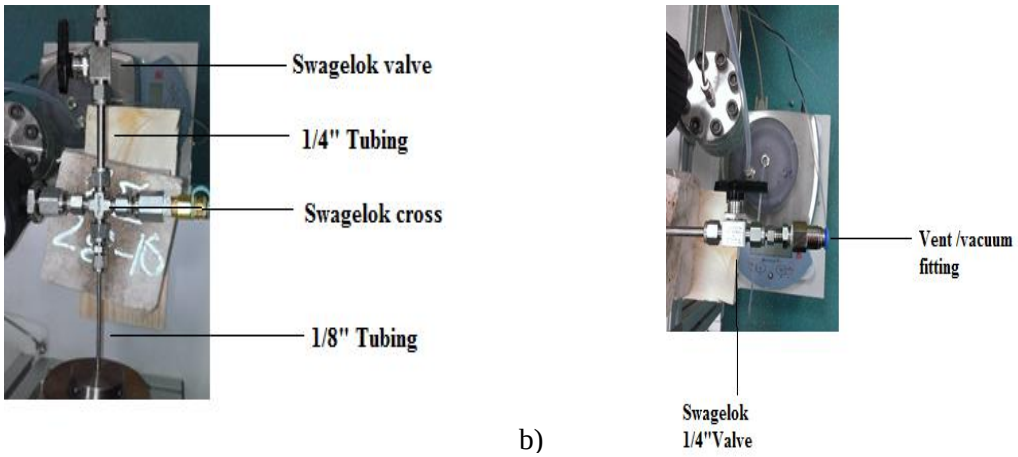

a) b)

Figure 4.11a, b: Swagelok Valves and Fittings.

Three Swagelok stainless steel valves are used as shut-off valves in front of the reference steel cylinder to control supply pressure, between the stainless-steel cylinder and core holder, and as a vent after the core holder. Due to their construction and operation mode, there is a zero-net change in dead volume upon switching the position of the valves. The pressure was monitored closely and efficiently using two pressure gauges, an analogue pressure gauge (Figure 4.12a) and a high precision, Omega digital gauge (Figure 4.12b) connected to the sample, and reference cell respectively is used to

measure pressure. The Omega DPG8001 Digital Series offers 0.25% full-scale terminal point accuracy in a rugged easy-to-use unit.

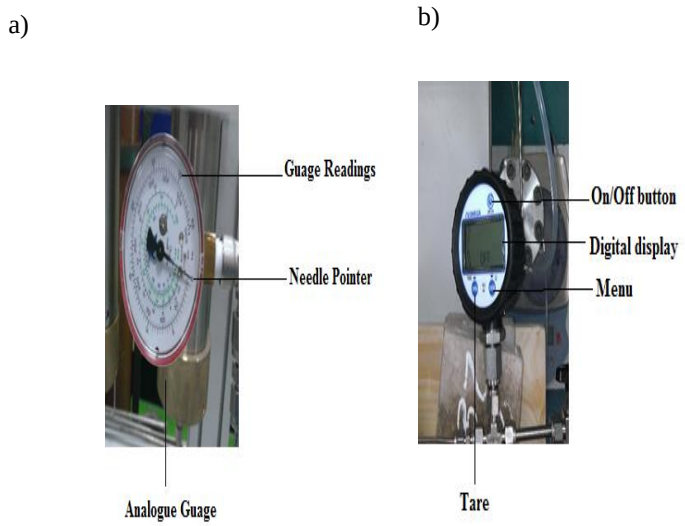

Figure 4.12a, b: Analogue and Omega DPG 8001 digital Pressure gauges.

Temperature readings were taken from a digital thermometer (Avax) installed externally and in proximity to the Hassler core holder with an estimated accuracy of ±1°C, with a measurement range of -50°C to +300°C (Figure 4.13).

Figure 4.13: Avax DT-1 digital thermometer.

A vacuum pump shown in Figure 4.14 was connected to the core holder set up to evacuate gases from the system. It was manufactured by Wenling Zhen-sheng machinery Co. Limited, Zhejiang Province, P.R China, with an ultimate vacuum of -11.60psia and motor speed of 3500r/m.

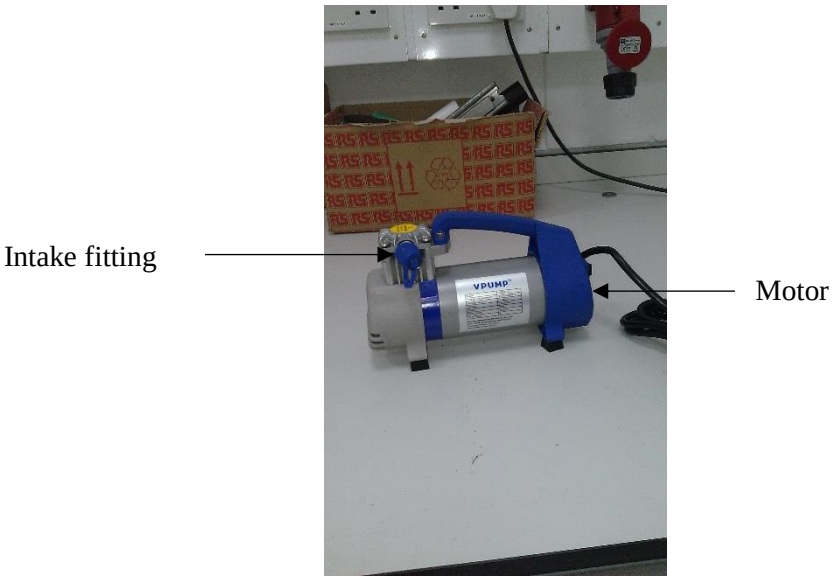

Figure 4.14: Vacuum Pump.

4.5.3 Sample preparation

4.5.3.1 Dry sample preparation

Before the experiment, the sandstone (Bandera and Scioto) core samples were placed in an oven for 24 hours at 60°c under vacuum conditions as shown in Figure 4.15. To apply vacuum pressure, the opening of the cell was connected to a vacuum pump inside the oven. To obtain optimal experimental condition during the dry adsorption determination; the moisture content was tried to be reduced to the least minimum. After the evacuation procedure, the sample cell was closed immediately.

Figure 4.15: Dry sample preparation using an oven.

4.5.3.2 Water saturation procedure

Samples were dried overnight in an oven at 60°C. This drying is necessary to remove any moisture taken up by the sample in contact with air humidity and as received moisture. Water saturated samples were prepared by saturating the sample with water at room temperature for 24, 48 and 72 hours. The resulting water uptake for each the investigated samples was measured using a high precision balance (Kern Model ABJ 320–4). The water content (w_c) was calculated using Eqn. 4.16:

$$w_c = {M_{wet} - M_{dry}} \Big/ {M_{wet}} \times 100 \qquad (4.16)$$

Here, M_{wet} and M_{dry} is the weight of water saturated and dry sample, respectively.

4.5.3.3 Brine saturation procedure

Brine was prepared by adding Sodium chloride (NaCl) salt into water; the salinity and concentration of salt in the fluid were determined to be 20% and 200,000ppm by using a refractometer. The samples were saturated for 24, 48, 72 hours, and the brine content calculation using the previous formula (Eqn. 4.17). The salts were purchased from Fisher Scientific and had a purity of 99.9%.

$$w_b = {}^{m_{wet} - m_{dry}}/_{m_{dry}} \; x\, 100 \qquad (4.17)$$

Where, M_{wet} and M_{dry} is the weight of Brine saturated and dry sample, respectively.

4.5.4 Experimental Procedure

4.5.4.1 Adsorption apparatus Leak test

The first step is to verify whether the system is leak free or not. For this purpose, the system was pressurised to 50, 100 and 120 psia (0.34, 0.67 and 0.83 MPa) at different intervals. The test was then divided into three stages. This phase involved connecting the reference cell to the Swagelok cross with digital pressure gauge, thermometer, and vent valve. Using gas detection fluid (screw fix) all gas pressurised connection and fittings were tested for leaks. The second stages involved inserting the pressurised set up into water in a closed sink, and any leakage from tubing, fittings or valves was then rectified. The third stage was carried out on the complete experimental setup. However, the core holder rubber sleeves were left exposed (Figure 4.16). The system was pressurised as before, then gas leak detection fluid was used to detect any visible leaks in the system, which were then rectified.

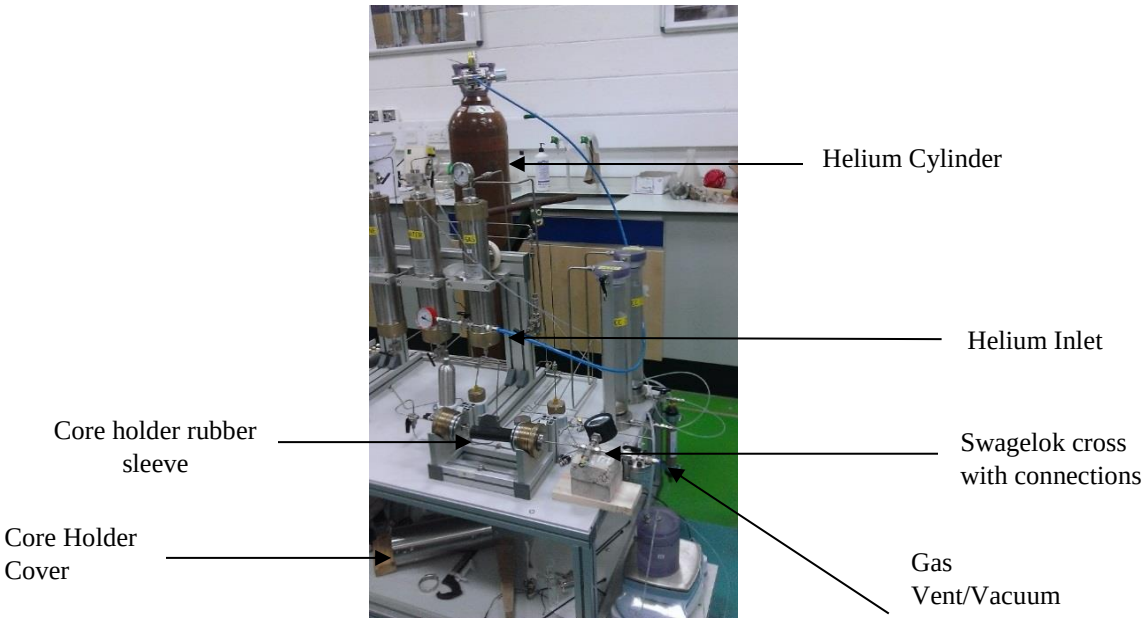

Figure 4.16: Stages of leak test using Helium.

The next step after the Helium leakage test was evacuation (Figure 4.17). For this purpose, the valve in between the reference and sample cells is closed, and the valve at the end of the sample cell is opened to decrease the Helium pressure. Afterwards, it was closed again, and the reference cell is evacuated by opening the valve in between the two cells leading to more pressure drop, the mid-point valves are closed once more and sample cell gas release procedure is done as described before.

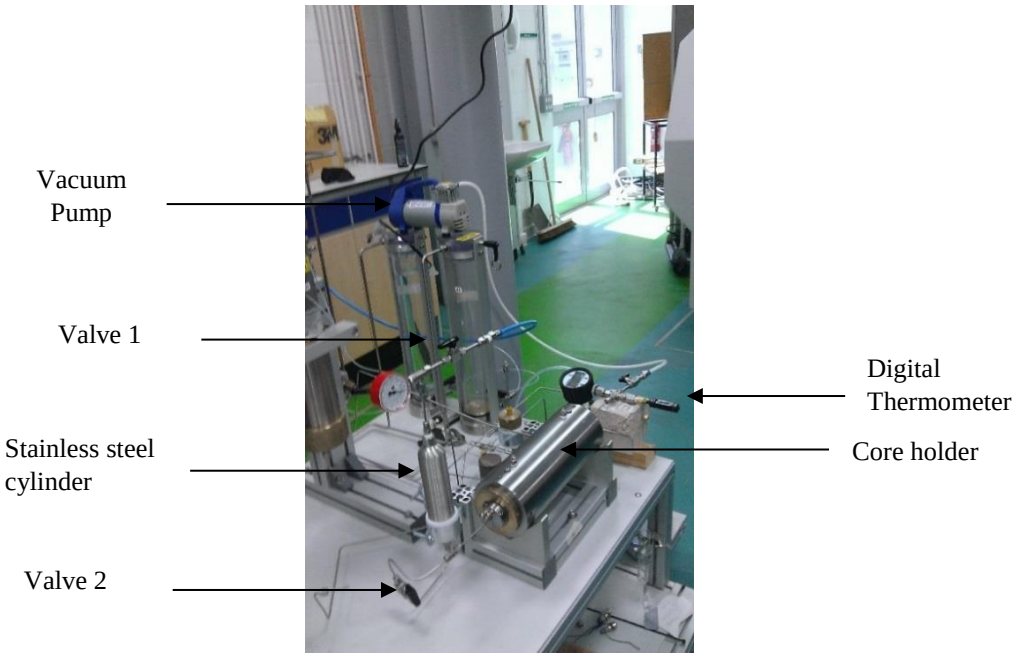

Figure 4.17: Helium Evacuation procedure.

Then the valve between the two compartments is opened, this causes deep evacuation of the helium gas used for the leak test. To remove air and remaining gas from the system, a vacuum pump is connected to the reference cell, and the valve connecting the two cells is shut off. To purge the sample cell stepwise, we use the following procedure in each step. Firstly, the reference cell is evacuated and stabilised for an hour until the absolute pressure of 0.39 ± 0.03 psia (0.0027± 0.03 MPa) is reached, then the vacuum pump is connected to the sample cell, the vacuum was applied for 3 minutes until all air was evacuated out of the system.

4.5.4.2 Void volume and equilibrium time of core samples

For void volume measurement, the reference cell was pressurised to about 115psia (0.79 MPa) after evacuation using helium. About 30minutes was allowed for the gas to reach thermodynamic equilibrium, the pressure (P_1) was recorded, and gas was expanded from the reference cell to the Hassler core holder by opening valve V-2 with the vent valveV-1 at the closed position. The gas is allowed to interact with the sandstone sample in the adsorption cell until thermodynamic equilibrium had been realised i.e. constancy of pressure and temperature, then the pressures in both the ref-cell (P_2) and adsorption cell (P_3) were recorded.

The contact time required for samples and gas to reach equilibration depends on the type of the gas and its temperature. This was determined by observing the pressure for about 3 hours. Therefore, a constant equilibrium time of 3 hours was determined for these components. After the void volume measurement, gas evacuation procedure was then repeated to prepare for methane (CH_4) adsorption capacity measurement.

4.5.4.3 Adsorption capacity measurements of core samples

The schematic of the self-assembled adsorption equipment is shown in Figure 4.18. Adsorption capacity measurements consisted of the addition of methane(CH_4) gas pressure to the reference cell by opening V-3 and V-5 with V-1 and V-2 at close position, after pressure and temperature stabilisation, the gas supplied was expanded to the adsorption cell containing the sandstone core sample by opening V-2 and closing V-3 and V-5. After this step, the system pressure is monitored until the adsorption equilibrium was reached, which is assumed to occur when the rate change of the pressure approaches zero under isothermal conditions, i.e., the pressure variation is

lower than 0.01450 psia (0.00001 MPa), which is the accuracy of the pressure transducers employed (0.05% of their full scale).

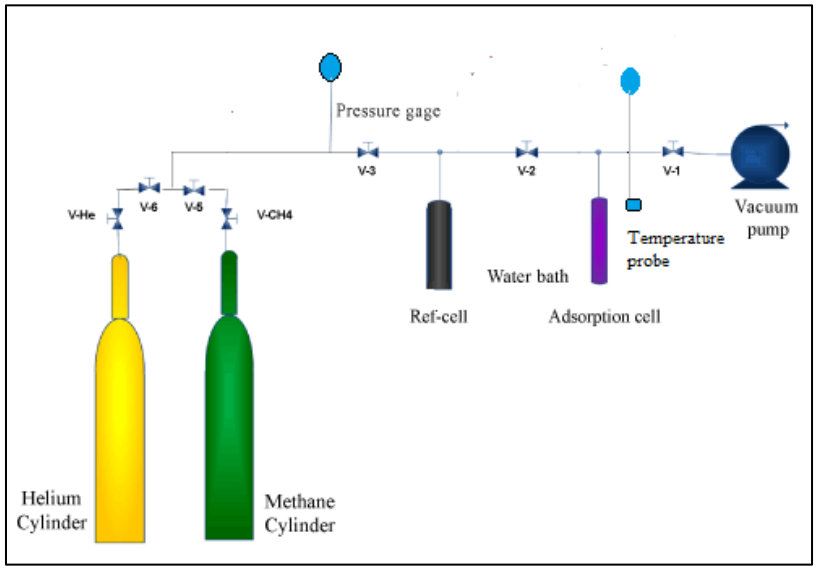

Figure 4.18: Schematic of the assembled manometric adsorption equipment

Then, the adsorption cell was once again isolated from the reference volume, by closing valve V-2, and the method is repeated until enough experimental points to generate the adsorption isotherm are obtained. When the maximum pressure is reached, a similar procedure is repeated, but this time by stepwise depressurization of the reference volumes and subsequent contact with the adsorption cell.

4.5.4.4 Manometric adsorption apparatus Optimisation

The first step in any adsorption experiment is to ensure that the results are as accurate as possible. To achieve this, the experimental set-up and design of the apparatus were re-optimized to reduce the expected experimental uncertainties from the adsorption measurements. A detailed analysis of factors (random errors) due to experimental uncertainties in the volume of gas adsorbed has been thoroughly researched (Mohammad et al., 2009; Chareonsuppanimit et al., 2012; Gasparik et al., 2014). The studies identified the major contributors to the experimental uncertainty to be the void volume, dead space and the precision or accuracy of measurement devices and operation errors. Therefore, in this research, the following steps have been taken to ensure accuracy:

a. Measuring the void volume in the sample cell using a core holder of the same size with the sandstone core sample;
b. Minimising the dead space within the apparatus (in lines, fittings, etc.).
c. Using measurement devices of high accuracy (i.e. digital pressure gauges and thermometer).
d. Sufficiently purging and evacuating the core holder with methane as gas impurities (e.g. air trapped in the sample) will affect the accuracy.
e. The operational design of the manometric adsorption apparatus was designed to allow independent control of the equilibration times.
f. Much care was taken when determining the void volume of the sample cell by conducting multiple pressure expansion during the helium pycnometry runs to minimize the error by averaging.
g. The equilibrium time was determined by observing the effect of contact time between methane gas and sandstone core samples, and choosing the most efficient time range for reaching equilibrium.
h. The drying cycle was monitored until there was no mass change, since small amount of moisture can affect the dry adsorption measurement.
i. High leak rates may result in a substantially overestimated sorption capacity and may still go unnoticed in the results. Leak test was conducted on the adsorption rig to ensure that its effect on the sorption measurement is avoided.

4.6 Summary

The methodology of this investigation followed a sequential approach to methane (CH_4) adsorption of sandstones using the following scheme:

- Bulk volume was determined using the calliper method by making three measurements for both core samples and calculating the average.
- Due to efficiency and accuracy, the application of a commercial helium pycnometer (Core Lab 200^{TM}) a manually operated helium pycnometer incorporating digital technology manufactured by Core Industries was solely adopted for void volume experiments instead of using the manometric setup currently utilized for adsorption measurements.
- The sandstones were characterised using Helium pycnometry to establish the effect of pressure, contact time and water at experimental pressures of 15 psia (0.10MPa), 45 psia (0.31 MPa), 65 psia (0.49 MPa), 85 psia (0.59 MPa), 95psia (0.66 MPa), 105 psia (0.72 MPa) and 115 psia (0.79 MPa) on the void volume.
- The experimental setup for adsorption capacity measurements was a customised manometric adsorption apparatus, which was designed and assembled to measure adsorption capacity at room temperature and specified experimental pressure.
- To ensure accurate results, the experimental set-up and design of the apparatus were re-optimized to reduce the expected experimental uncertainties from the adsorption measurements.

The results obtained from this section are presented and extensively discussed in the next Chapter. This consists of the presentation and discussion of results obtained from experimental runs for void volume evaluation and methane adsorption capacity of sandstones.

CHAPTER 5

5 RESULTS AND DISCUSSION

5.1 Introduction

This chapter discusses the results obtained from the experimental investigation conducted per the scheme set out in Figure 4.1. The primary objectives of this study were to explore:

a. What factors will influence the process of evaluating the void volume?
b. How reliable are the current method using helium to quantify the void volume as part of the adsorption quantification process in sandstone?
c. Which parameters control adsorbed gas storage of sandstone core at the simulated temperature and variable pressure?
d. What role does methane adsorption play in sandstones and in depleted reservoirs during the displacement process of EGR- CO_2 (Carbon Sequestration and Enhanced gas recovery and carbon dioxide sequestration?
e. How does the presence of water and brine affect methane (CH_4) adsorption of sandstones?

The experimental results provide insight into the Methane (CH_4) adsorption capacity of sandstones and the role of adsorption as a mechanism of depleted reservoirs as candidates for enhanced gas recovery and CO_2 sequestration. It also contributes to the understanding of the interaction between water/brine and methane (CH_4) gas in a competitive sorption environment for sandstones and their constituents. According to the original target of this investigation, the results are categorised into sections in which the experimental sequence followed:

- Section 1: Research conducted to define the sources of adsorption measurement uncertainty from measured helium void volume using sandstone core samples and to recommend the suitability of helium as an inert gas for void volume measurements. It determines how their propagation influences the results used for porous materials characterisation.

- Section 2: Results from the analyses of a series of CH_4 adsorption experiments using two sandstone core samples (*Bandera* and *Scioto*) conducted at 23°C and methane (CH_4) pressures up to 1250 psia (8.62 MPa) under dry conditions. Moreover, the result of CH_4 adsorbed on core samples at pressures up to 500psia under dry conditions are applied to analyse the impact of abandonment pressure of depletion reservoirs on the methane adsorption capacity of depleted gas reservoirs.

- Section 3: Methane adsorption capacity of sandstones saturated with water or brine to investigate the impact of pre-adsorbed water and brine at particular water content (33, 65, and 91%) on the adsorption capacity of core samples.

- Section 4: Result from adsorption measurements were validated using two methods (Repeatability and Best-fit model). The best-fitting model was determined using error functions. Then, the applicability of the proposed statistical tools was discussed based on a comparative study between them.

5.2 SECTION 1: Void Volume analysis using Helium pycnometry

5.2.1 Effect of averaging pressure on void volume measurements

Experimental uncertainties in quantifying the void volume as part of adsorption quantification are associated with averaging the experimental pressure (Mohammed et al., 2009; Gasparik et al., 2014). To investigate the effect of averaging pressure on void volume measurements, as a part of an overall study to quantify adsorbed methane (CH_4) storage in sandstone core samples, helium was used for the expansion test on two types of sandstone core samples, i.e. *Bandera* and *Scioto*. The sandstone core samples were chosen for their clay contents since clays have a high methane adsorption capability. These gas expansion tests were conducted in the laboratory using low pressure in the range of 15 – 115 psia (0.10 – 0.79 MPa) and at a room temperature of 23°C. Figure 5.1 shows the measured void volume calculated using helium expansion with increasing experimental pressures for the sandstone core samples studied. Figure 5.1(a) demonstrates the result of increasing experimental pressures on measured free gas storage capacity (void volume) for *Bandera* sample, while Figure 5.1(b) illustrates the result for *Scioto* sample. Figure 5.2(a) and Figure 5.2(b) show the standard deviation of void volume for *Scioto* and *Bandera* samples respectively. The standard deviation is a statistical measure that quantifies the amount of variation of a set of data values.

Figure 5.3(a) and Figure 5.3(b) shows the variation of the average void volume up to 5%. Table 5.1 and Table 5.2 presents the experimental result for measured void volume at variable pressure ranges (15 – 115 psia or 0.10 – 0.79 MPa) for the sandstone samples. The error due to averaging is calculated regarding deviations. The deviations in void volume data at each pressure step from the average void volume values were calculated for *Bandera* and *Scioto* sandstone. Figure 5.2 and Figure 5.3 indicate that there is a slight variation of about of less than 0.002 cm^3 and 0.001 cm^3 in average void volume for the *Bandera* and *Scioto* samples respectively with increasing pressure. Moreover, the pressure ranges investigated for both core samples (*Bandera, Scioto*) show similar results of a small variation with increasing pressure regarding the measured void volume value (Table 5.1 and Table 5.2). The averaging error values of the void volume are less than one, which is low.

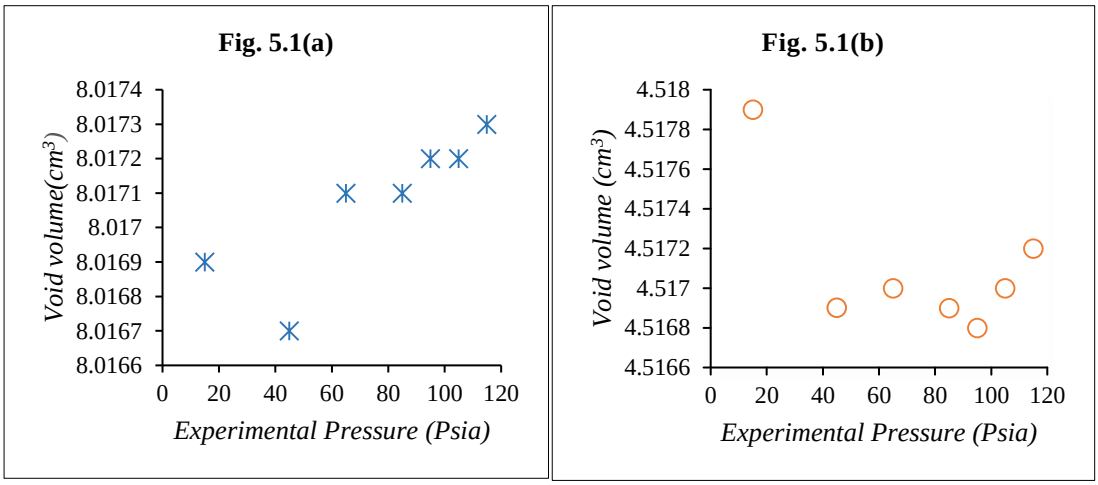

Figure 5.1: Effect of averaging pressure on void volume for Bandera and Scioto sandstones.

Table 5.1: Helium void volume at different studied pressures for *Bandera* sandstone.

Bulk Volume	Reference Pressure (psia)	Void Volume (V_v)(cm^3)
38.22 cm^3	15	8.0169
	45	8.0167
	65	8.0171
	85	8.0171
	95	8.0172
	105	8.0172
	115	8.0173

Table 5.2: Helium void volume at different studied pressures for *Scioto* sandstone.

Bulk volume	Reference Pressure (psia)	Void Volume (V_v)(cm^3)
38.17 cm^3	15	4.5179
	45	4.5169
	65	4.5170
	85	4.5169
	95	4.5168
	105	4.5170
	115	4.5172

The relationship between pressure and void volume for the two samples shown in Figure 5.1a and Figure 5.1b were not identical, the reason for this difference is that when analysing the plot showing the relationship between the pressure and void volume, the diffusion of the helium into the void volume determines the shape of the plot. The primary purpose of the plots is to answer two important questions:

a. Is the data deviation from averaging the void volume as a function of pressure close or far?

b. Do the plots resemble adsorption isotherms?

The answers to these question are in the negative for this research, therefore it can be concluded that the constancy of average void volume with pressure for sandstone core sample indicates that there was no Helium adsorbed in observable quantity, and as such there will be no decrease in the void volume as a result of helium adsorption for both samples investigated.

From Figure 5.1(a) and Figure 5.1(b), it is observed that in case of helium, the void volume is independent of pressure. The pressure independence of the helium void volume as seen in the present study is contrary to the finding of Ross and Bustin that suggests the void volume is pressure dependent (Ross and Bustin, 2007). However, it is supported by the study of Heller and Zoback, where void volume is found to be independent of pressure (Heller and Zoback, 2014) for shale. Moreover, (Gasparik et al, 2012, 2014) conducted a test to determine the void volume of organic shale using pressures of up to 2175.57 psia (15MPa), they also did not observe void volume measured value changing with pressure. Chareonsuppanimit et al., (2012) also reported a 0.5% deviation from the average void volume using helium.

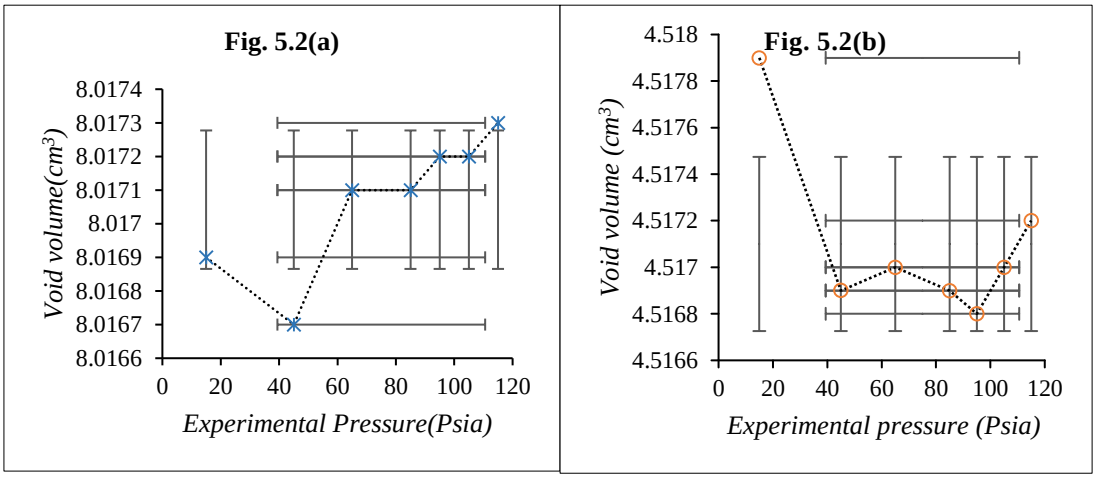

Figure 5.2: Standard deviation of void volume for Scioto and Bandera samples.

Figure 5.2a and b show horizontal and vertical error bars representing the standard deviation of the pressure measurements, while Figure 5.3a and Figure 5.3b are the deviation of data at 5%.

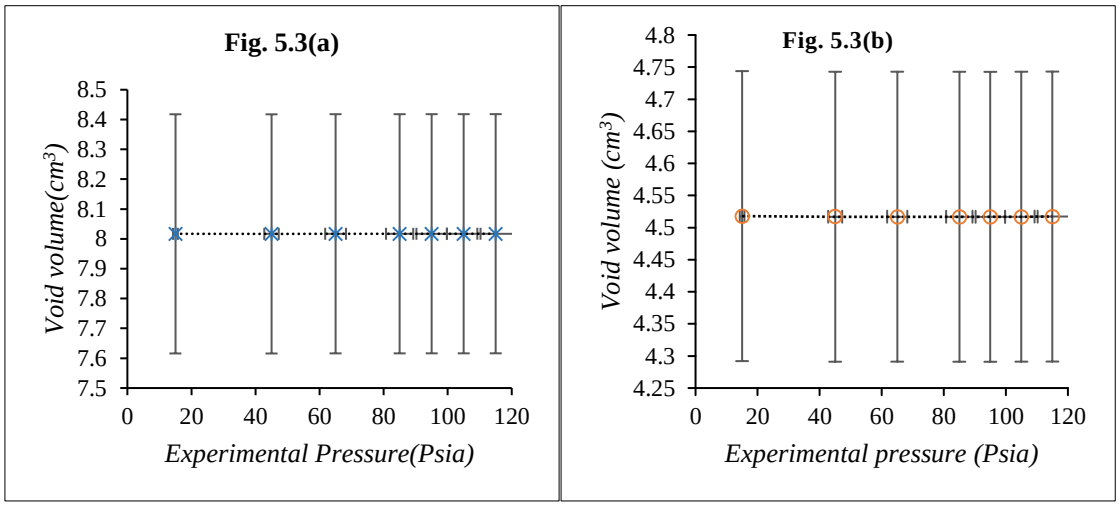

Figure 5.3: Variation of the average void volume up to 5% for Scioto and Bandera samples.

Figure 5.2(a), and Figure 5.2(b) indicate that the standard deviation of void volume data was averagely 8.017cm^3 for *Bandera* and 4.5171cm^3 for the *Scioto* sample respectively. Figure 5.3(a) and Figure 5.3(b) indicate that the difference between measured void volume is very close by observing the graph; the data show less than 1% deviation, which is negligible, and suggest that the measurements are very accurate. The constancy of pressure (Figure 5.3(a) and Figure 5.3(b) indicate that sandstone core samples will reach saturation independent of molecular diameter but by the rate at which gas transport by diffusion occurs and velocities of the helium particles.

For adsorbed gas, the pressure increases with respect to storage volume and leads to a decrease in the volume available for free gas storage in the void volume (Mohammed et al., 2009). From experimental data (Figure 5.3(a) and Figure 5.3(b) in this investigation, the constancy of average void volume with pressure for the sandstone core samples indicates that there was no increase in helium density at the surface of the investigated samples (i.e. Helium adsorption) in observable quantity. This result proves that there is no decrease in the void volume from adsorption for both samples investigated. This means helium is not adsorbed in both sandstone core samples at the investigated pressure (15 - 115 Psia or 0.10 – 0.79 MPa). If helium were adsorbed, then the plot of void volume as a function of pressure (Figure 5.1a, Figure 5.1b) would behave like an adsorption isotherm. Adsorption isotherms are used to determine the theoretical adsorption capacity of adsorbent and are defined by an exponential increase in pressure until a saturation point is reached where the isotherm plateaus. However, the

experimental data plot does not rise exponentially neither does it plateau at maximum saturation. Therefore, we can isolate helium adsorption by both samples studied. The experimental data indicate that at low pressure, the void volume in sandstone core samples corresponds to the total gas introduced into the system (helium gas), which is a result of void volume filling.

For sandstone core samples, as differential pressure increased and helium is transported by slow viscous flow into the cored samples of variable pore spaces and particles, there was no void volume data deviation at low pressure (15-115 psia or 0.10 – 0.79 MPa). This lack of increase of void volume data with pressure was also reported by Rani et al., 2015; Heller and Zoback., 2014; Gasparik et al., 2012, 2014,) for shale at high pressure (up to 2175.57 psia or 15 MPa). For powdered clays at high pressure, Ross and Bustin., (2009) has shown that a mechanism called "molecular sieving effect" was responsible for increased access of helium to finer pores and this is a likely cause of high void volume values in helium pycnometry. The molecular effect occurs because of helium molecular diameter, which is smaller than the particle size of most microporous solids (i.e. clays, shale, and coal).

This investigation was conducted at low pressure, using cored samples, with variable pore types and particle sizes. The constancy of pressure in the experimental result (Figure 5.1 (a) and Figure 5.1(b)) indicate that the *Bandera* and *Scioto* samples will reach saturation independent of molecular diameter but more on the rate at which gas transport by diffusion occurs and velocities of helium particles, all of which are pressure dependent.

5.2.2 Effect of water content on void volume measurements

Bandera and *Scioto* samples with pre-adsorbed water were used during this research to investigate the effect of water content on the experimentally measured void volume. Table 5.3 presents the calculated water content of each sample, and Table 5.4 shows the calculated void volume of water-saturated samples. Table 5.5 is a comparison of measured dry and wet sample void volume; Figure 5.4 presents measured water saturated void volume as a function of pressure for samples analysed.

Table 5.3: Water content of samples.

Core Sample	Wet Mass (g)	Dry Mass(g)	Water content (%)
Bandera Gray	89.41	84.65	5.62%
Scioto	88.17	83.59	5.48%

Table 5.4: Measured water saturated void volume for *Bandera* and *Scioto* sandstones.

Pressure(Psia)	Void Volume(cm^3)	
	Bandera	***Scioto***
15	7.0110	4.0080
45	7.0121	4.0126
65	7.0140	4.0120
85	7.0132	4.0117
95	7.0131	4.0115

Table 5.5: Comparison of measured Dry and Wet sandstones void volume.

Pressure(Psia)	***Bandera***		***Scioto***	
	Void Volume (cm^3)			
	Dry sample	Wet Sample	Dry Sample	Wet Sample
15	8.0169	7.0110	4.5179	4.0080
45	8.0167	7.0121	4.5169	4.0126
65	8.0171	7.0140	4.5170	4.0120
85	8.0171	7.0132	4.5169	4.0117
95	8.0172	7.0131	4.5168	4.0115

Fig 5.4a

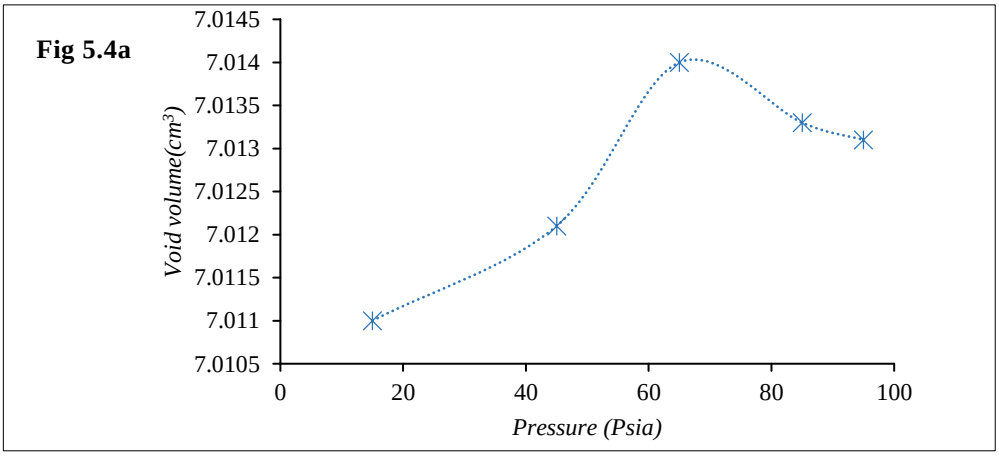

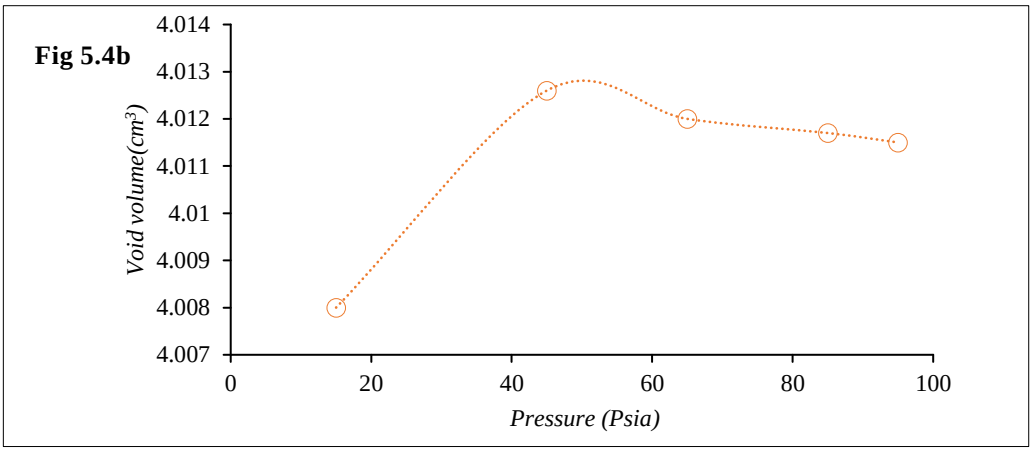

Figure 5.4: Effect of averaging pressure on void volume for water saturated sandstones.

Figure 5.4(a) and Figure 5.4(b) indicates that the void volume values scattered about a mean of 7.0127cm^3 and 4.0011cm^3 for the *Bandera* and *Scioto* samples saturated with water respectively. Table 5.5 presents a comparison of the measured void volume for dry and *Bandera* and *Scioto* samples saturated with water.

From Table 5.5, the void volume of dry samples is compared to that of samples saturated with water. The results indicate that the gas access to the void volume is restricted by the presence of water. The measured average void volume of dry samples compared to water saturated sandstones show that water content of 5.62 wt. % and 5.48wt. % for *Bandera* and *Scioto* respectively can reduce the dry samples average void volume by as much as 12.53% and 11.20% for investigated *Bandera* and *Scioto* samples.

The reduction of void volume for samples saturated with water in Table 5.5 proves that water blocked the pore spaces available to helium gas, as compared to dry samples where the gas has complete access to the total void volume. Pore spaces in the sandstone samples are hydrophilic due to the presence of clay minerals, which have a natural affinity for water compared to helium. Moreover, the connectivity of these hydrophilic pore networks in the sandstones will cause preferential uptake of water compared to helium and will be one of the leading cause of void volume reduction in sandstones with water content. Variations in pore size that are closely related to permeability will determine to a large degree the relative amounts of the storage capacity of helium and water in pore space.

Water or brine content in sandstones will affect their natural material properties such as the gas porosity and permeability and in turn the void volume measurement. These are geometric properties of the rock and are both the result of it's lithological (composition) character. These properties determine the amount of gas that can be stored in the sandstones and the type of methods that should be used in the sample characterization and analysis. The cause of the decrease in the void volume of sandstone samples with water can be attributed to water blockage of pore space and throat.

5.2.3 Effect of contact time on void volume measurements

Contact time between helium gas and the solid adsorbent is a critical factor in void volume determination because it determines the accuracy of measured void volume (Ross and Bustin, 2007) and in turn, affects the estimated capacity of free gas storage of sandstones at reservoir scale. This investigation was conducted to quantify the impact of longer contact time between helium and sandstones core samples on void volume.This effect is quantified by carrying out a comparative analysis of pressure (15 to 95 psia or 0.10 – 0.79 MPa) as a function of contact time. About 30 minutes were allowed for thermal equilibration, followed by close observation of expanded pressure (P_2), taken every 4 min for about 240 minutes (four hours) period. Thus the void volume was measured with respect to time.

For *Bandera* sample, Figure 5.5 shows the impact of contact time on the average void volume value at incremental pressures. Figure 5.5(a), Figure 5.5(b), Figure 5.5(c), Figure 5.5(d) and Figure 5.5(e) demonstrates the influence of contact time on measured void volume from 0 - 240 minutes at 15, 45, 65, 85 and 95 psi respectively. Figure 5.7 presents a comparison of void volume as a function of contact time at differential pressures.

For *Scioto* sample, Figure 5.6 shows the effect of contact time on average void volume value. Figure 5.6(a), Figure 5.6(b), Figure 5.6(c), Figure 5.6(d) and Figure 5.6(e) show the influence of contact time on average measured void volume at 0 to 240 minutes for 15, 45, 65 and 95 psia respectively. For comparison purposes, measured average void volume as a function of contact time is presented in Figure 5.8.

The dependence of helium diffusion on increasing time was observed from calculated helium void volume for different contact times (Figure 5.5 and Figure 5.6). The result shows that there was an increase in the void volume values for contact times of 100, 150 and 250 minutes (Figure 5.6 - Figure 5.8). The results suggest that for shorter calibration times there is less time available for helium to diffuse into the sample, which produces a smaller void volume. The experimental data indicate that pore access at increasing contact time is critical for accurate void volume calculations.

Figure 5.7 and Figure 5.8 shows that total saturation was attained at an average duration of 180 minutes and 184 minutes for *Bandera* and *Scioto* respectively. Furthermore, as pressure increased with a corresponding increase in contact time between helium and sandstone core samples, the total equilibrium or saturation was achieved at about 240 minutes (4hrs). The movement of helium into pore space and particles with different sizes in core samples is a slow viscous flow described by Darcy's Law. The movement of gas depends upon the fact that gas flow in core samples is directly related to the difference in pressure between the points of the sample cell and the distance between the points, and are related to contact time. The relationship between the pressure, distance and contact time is the cause of faster saturation or equilibrium time at an incremental pressure (Figure 5.5a, Figure 5.5b, Figure 5.5c, Figure 5.5d and Figure 5.6a, Figure 5.6b, Figure 5.6c, Figure 5.6d). This result implies that at a higher pressure, the helium particles have higher velocities and would travel the distance of sample cell faster than its previous lower pressure.

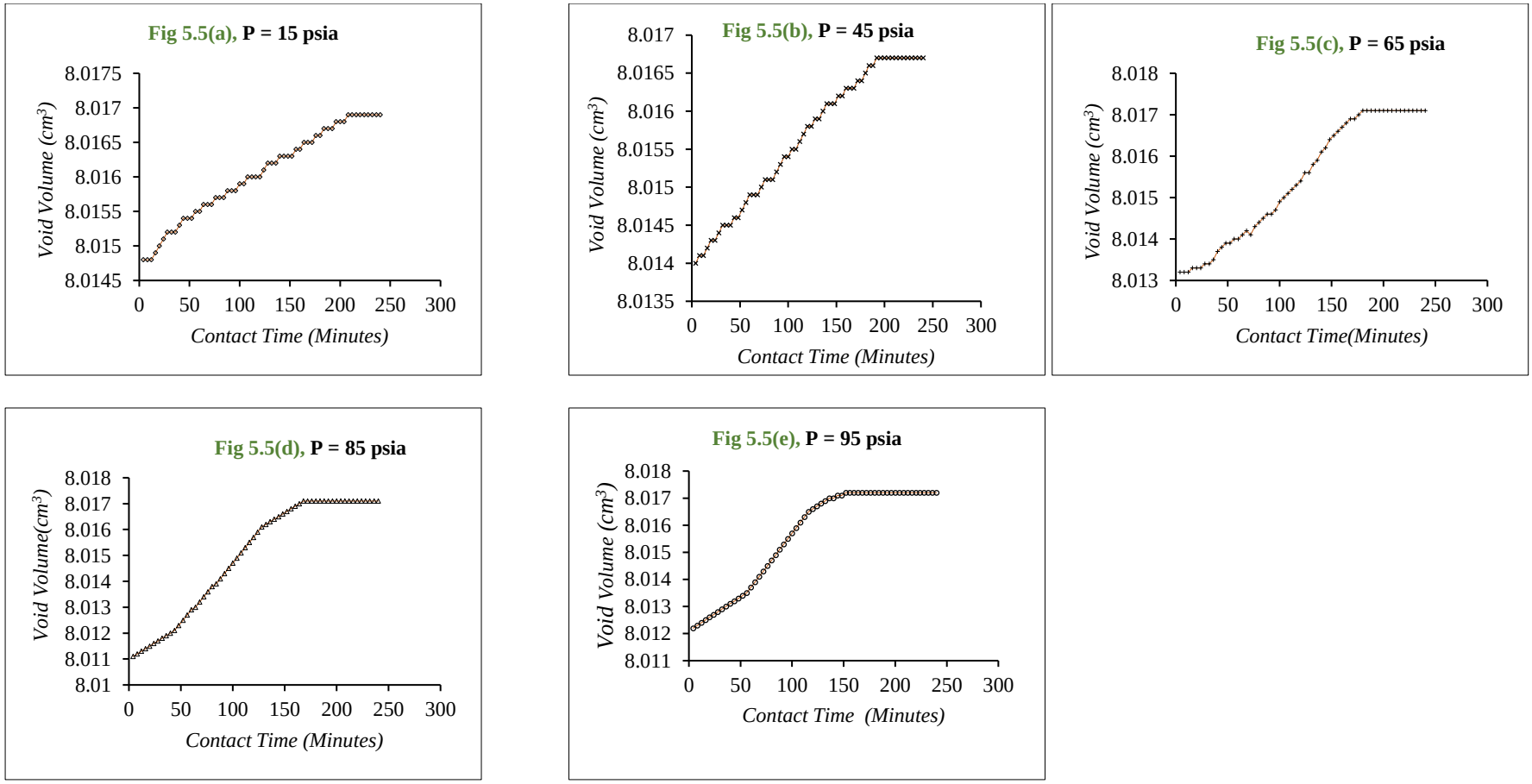

Figure 5.5: Effect of contact time on void volume for *Bandera* sandstone.

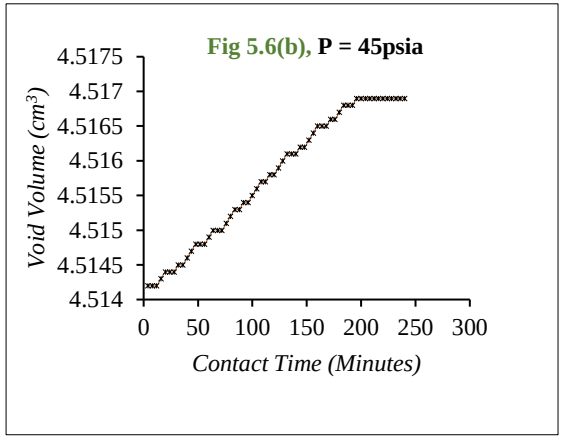

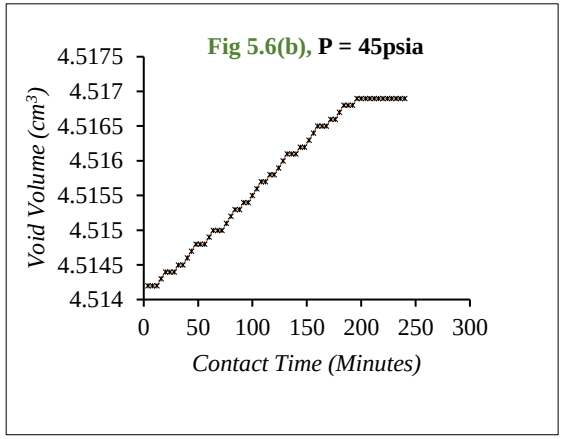

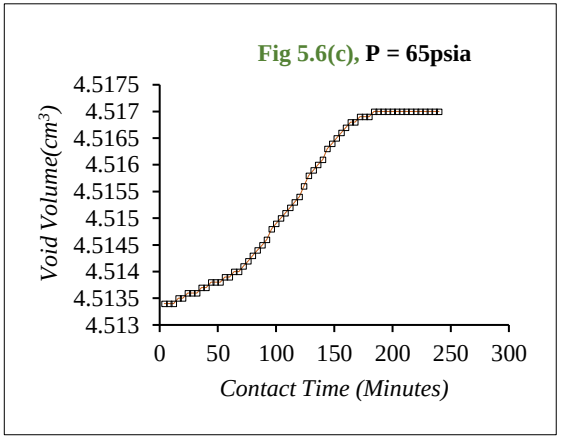

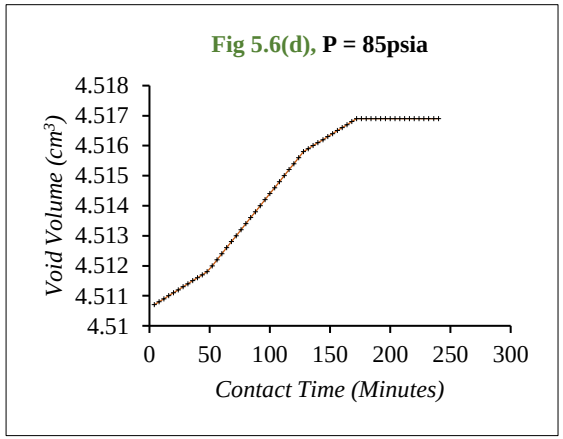

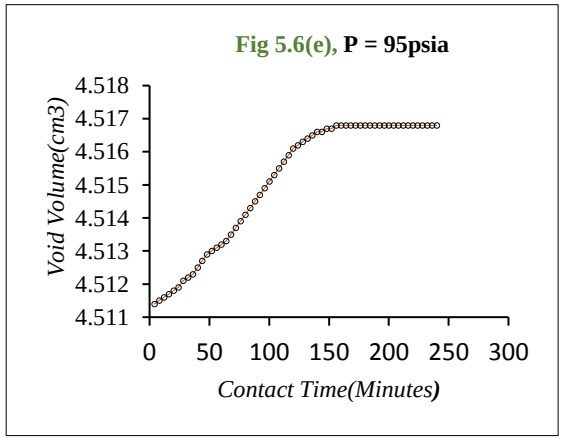

Figure 5.6: Effect of contact time on void volume for Scioto.

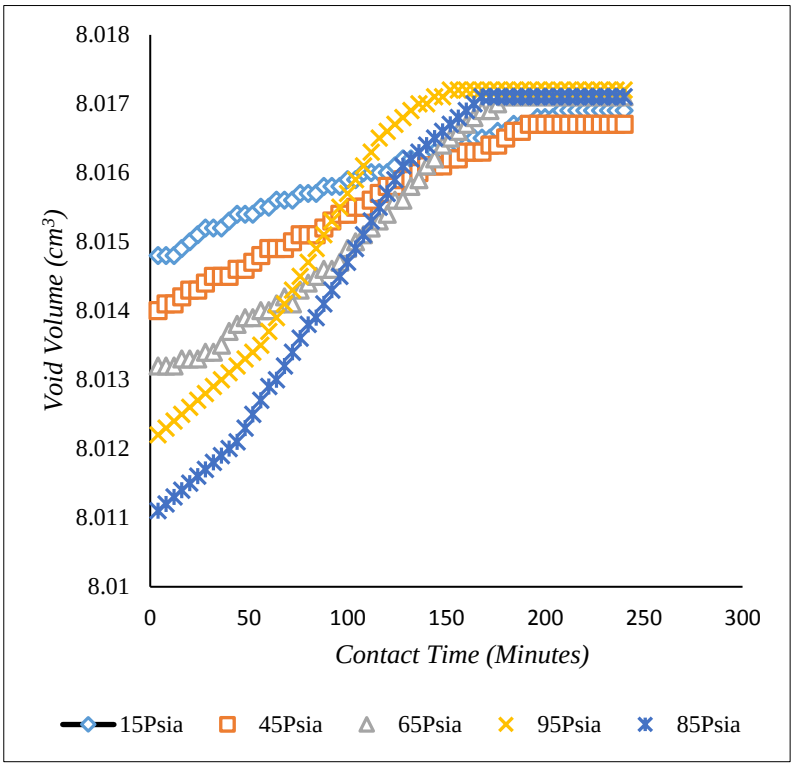

Figure 5.7: Comparison of Contact time at studied pressure ranges on void volume for Bandera.

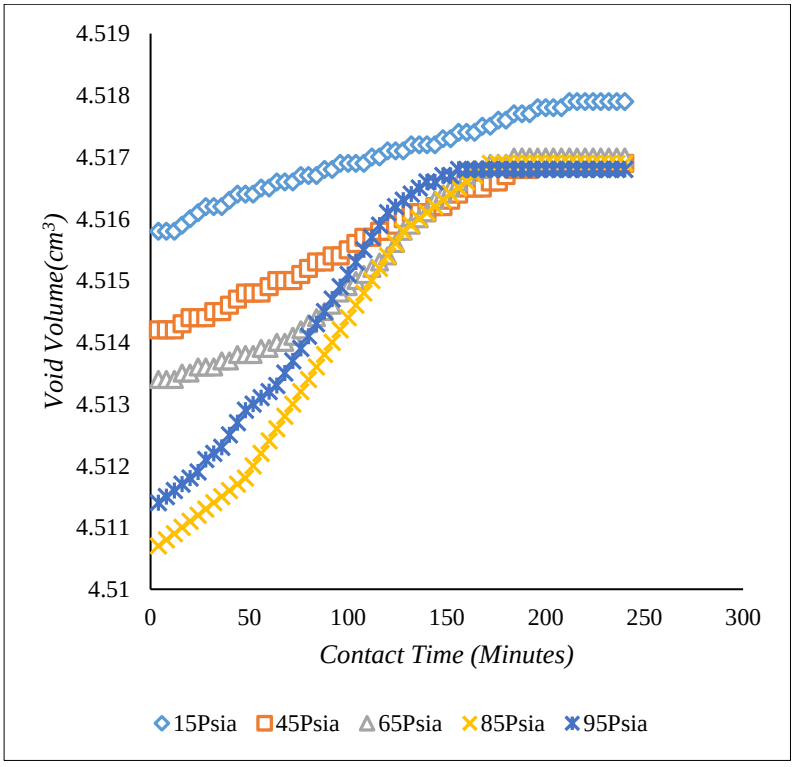

Figure 5.8: Comparison of Contact time at studied pressure ranges on void volume for Scioto.

Figure 5.7 and Figure 5.8, indicates that the overall interconnectivity of flow pathways, the permeability, the pore size distribution and particle size in the sandstone samples are the dominant factors that determine the gas saturation with contact time. For example, Pore size scale is a major factor and has been shown to influence gas transport in gas reservoirs (Feast et al., 2015). The pore sizes of the investigated core samples are in the range of 2nm –100 nm (micro to mesopores). Therefore, the distance between gas molecules and pore size is large. In such conditions, the gas molecules will travel faster compared to microporous materials with smaller pore sizes. Helium will move in a random manner through the pores of differential sizes and connectivity, followed by slow filling of all accessible empty spaces in the sample as a function of time, until complete saturation is reached (Figure 5.7 and Figure 5.8).

The permeability will determine the ease at which helium gas will travel through the sample length. For example, Gasparik et al., 2013 showed that due to the very low permeability of shale, the equilibration times for core samples could be as high as > 10 hours. However, for sandstone core samples, the equilibrium time was about 240 minutes (4hours); this is to be expected since the permeability of sandstone is higher compared to shale. It is therefore suggested that for accurate void volume measurement, an average waiting time of 180 to 184 minutes and complete equilibrium time of 240 minutes should be allowed for helium expansion until full saturation is reached as indicated in Figure 5.7 and Figure 5.8.

The void volume distribution was also non-uniform at all contact time as a function of pressure for both samples (Figure 5.5 and Figure 5.6(a-d)) i.e. scattering of measured void volume data about a mean, this seems to be an issue of methodology (Gasparik et al., 2014). The reason for data noise is that void volume calculation is carried out using different approaches such as pressure ratio (Bustin et al., 2009), differential and cumulative (Gasparik et al., 2014), the equation of state (Heller and Zoback. 2014) and in this study, using grain volume calculation. These methods are all reliable and precision guaranteed; the only difference is that some might reduce the noise associated with significant data as proved by Gasparik et al., (2014). It is largely a matter of preference and experimental setup.

5.3 SECTION 2: Evaluation of CH_4 adsorption capacity of sandstones using a manometric method

5.3.1 Experimental Equilibrium methane (CH_4) adsorption capacity (The adsorption capacity of sandstones (Bandera and Scioto) using methane)

Adsorption is a process by which atoms, ions, or molecules of a gas or liquid adhere to a surface. This process creates a film of the adsorbate on the surface of the adsorbent. For the measurement of the amount of adsorbed gas, the adsorption isotherms are determined in the laboratory using core samples. In this work, a series of methane (CH_4) adsorption capacity experiments were conducted on two sandstone core samples at pressures up to 1250 psia (8.62 MPa) and a constant temperature of 23°C. Appendix A-1 shows the experimentally measured data, Figure 5.9a, and Figure 5.9b shows the corresponding Equilibrium adsorption capacity plot for *Bandera* and the *Scioto* samples respectively. The experiments were conducted up to a pressure of 1250 psia (8.62 MPa) in twenty (20) steps until the sandstone samples became fully saturated by reaching equilibrium.

a)

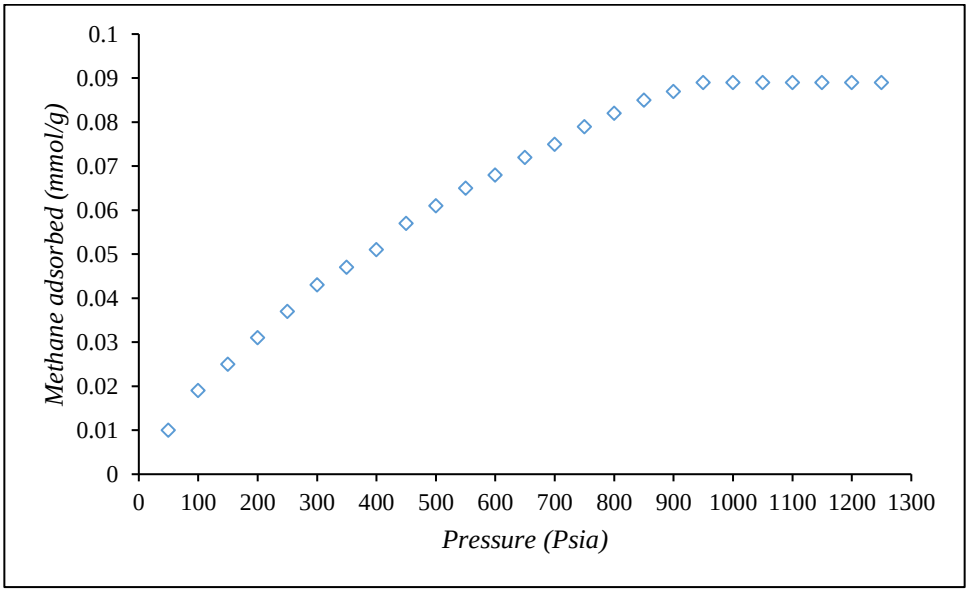

b)

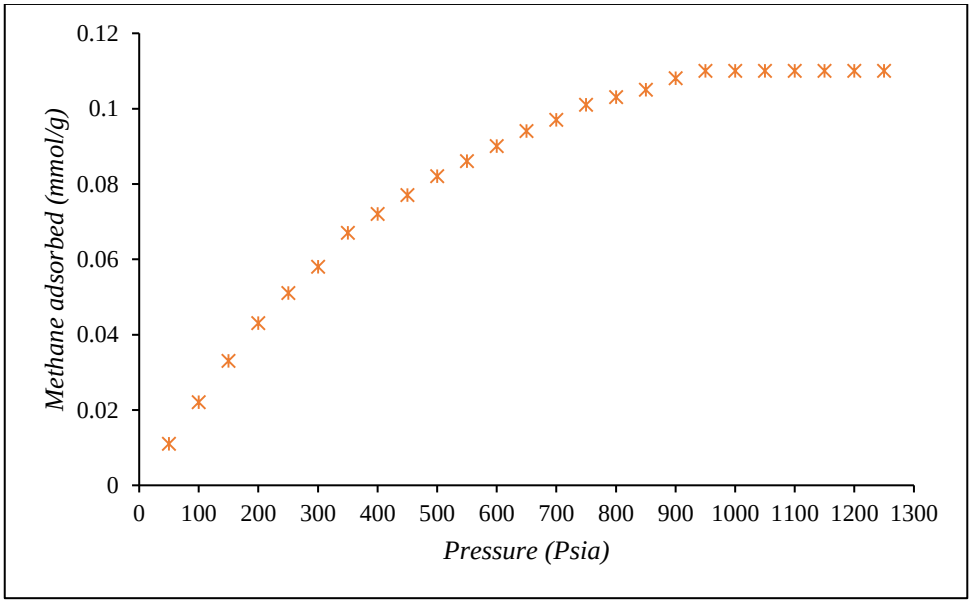

Figure 5.9: Equilibrium Methane Adsorption isotherm of a) Bandera and b) Scioto sandstones.

The experimental adsorption values for *Bandera* and *Scioto* sandstone samples plotted in Figure 5.9a, b show that the amount of gas uptake increases with an increase in the pressure, but when the adsorbent monolayer becomes saturated, for example at a pressure of 950 psia (6.55 MPa) the plateau of the system was observed. The results were obtained at each pressure increment at a constant experimental temperature (23^0C), and at the saturation, the system reached equilibrium before readings were recorded.

These indicated that the surface interactions on the *Bandera* and *Scioto* with CH_4 are dependent of the equilibrium and saturation pressure, however other factors such as the distribution of pore sizes in the material, the effective molecular size of the adsorbing gas, and the combined attraction energy of the surface material and the adsorbing gas play a role in determining the shape of the isotherm. The potential forces from the adjacent walls of the pores increase the interaction energy between the sandstone (*Bandera* and or *Scioto*) surface and CH_4 molecules, which causes an increase in adsorption and cause complete filling of pores at low pressures. The isotherms obtained for methane adsorption of sandstones investigated in this research belong to type 1 of the IUPAC classification. For materials that demonstrate a type I isotherm for a particular gas, the equilibrium energy state for the gas-surface system would be a single

or monolayer of adsorbed gas molecules. Hence, after filling nearly all pores, at higher pressures, the peaks of the adsorption capacity becomes stable. The results indicate that pore sizes and surface area are important for adsorption capacities of the sandstones.

The methane (CH_4) adsorption capacity varied for the different sandstone types, which for the present studies *Bandera* and *Scioto* are considered. The *Scioto* sandstone has the largest CH_4 adsorption capacity of the tested samples with a maximum amount of adsorbed CH_4 of 0.110 mmol/g while the *Bandera* sandstone had significantly less CH_4 sorption capacity with a maximum amount of adsorbed CH_4 of 0.089 mmol/g.

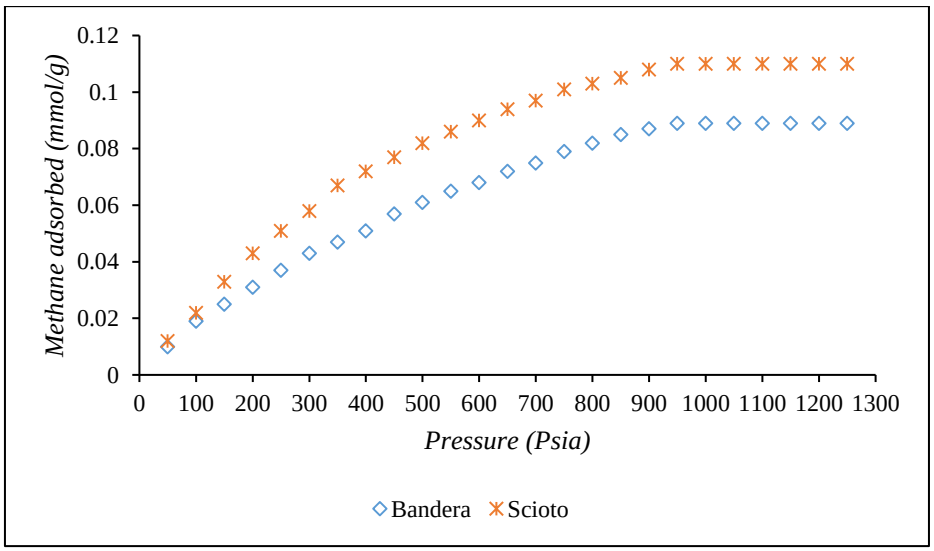

Figure 5.10: Comparison of Methane (CH_4) adsorption capacities of Bandera and Scioto samples.

Figure 5.10 presents a comparison of methane (CH_4) adsorption capacities of *Bandera* and *Scioto* sample. As indicated in the figure, the *Scioto* sample has a higher adsorption capacity compared to *Bandara* sample. This may be attributed to their mineralogical content of the two samples.

Figure 5.11 shows the scanning electron microscope (SEM) images of pore types in the *Bandera* and *Scioto* sandstones and Table 5.6 shows the X-ray diffraction (XRD) results of sandstone cores.

The mineralogical differences of these samples indicate that composition was one factor responsible for variance in methane adsorption capacity between the samples analysed. Moreover, previous investigations using shale have shown the negligible methane (CH_4) adsorption capacity of other components (i.e. quartz and dolomite). For example, Lu et

al., concludes that "the principal mineral constituents of Devonian shale are clay (mainly illite), carbonates and quartz, and since carbonates and quartz do not adsorb methane, illite may be a factor for adsorbed gas storage" (Lu et al., 1994).

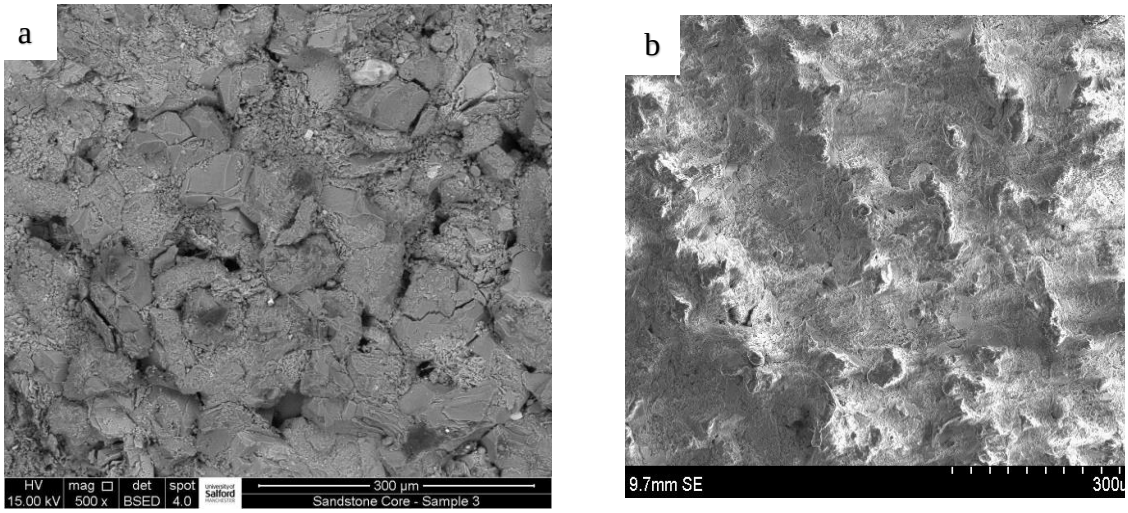

Figure 5.11: SEM images of pore types in (a) Bandera and (b) Scioto samples

Table 5.6: XRD results of sandstone cores

Minerals	Bandera	Scioto
Quartz	57	70
Plagioclase	12	5
KFeldspar	Nil	2
Dolomite	16	Nil
Pyrite	Trace	Trace
Mica + illite	10	18
Kaolinite	3	Trace
Chlorite	1	4

X-ray diffraction (XRD) results (Table 5.6) confirmed the mineralogy of the sandstone samples. For example, the *Bandera* sample is composed of illite (10%), Kaolinite (3%) and Chlorite (1%), while the *Scioto* has a kaolinite content of 18% and chlorite of 4%. The *Scioto* sample had the highest total amount of clays present (22%) compared to *Bandera* (14%) and had the highest adsorption capacity. The previous analyses imply that high content of clay minerals in the *Scioto* sample relative to the *Bandera* provides extra surface area for adsorption of methane (CH_4). As a result, it can be concluded that there exists a correlation between methane (CH_4) adsorption capacity and surface area of clay present in the samples.

The pores in the sandstones sample are mainly the inorganic pores and inter-particle pores as seen from the SEM images in Figure 5.11. The abundance of micro and mesopores in the size range of 10s of nanometres in chlorite and illite interstratified clay, high internal surface area with pores of 1–2 nm radius between crystal layers and variable micropore volume in sandstone samples (mainly kaolinite, illite and chlorite) utilised for this investigation provide extra adsorption sites for methane (CH_4) resulting in an overall increase in adsorption capacity.

The clay minerals in the sandstone investigated are composed of different particle sizes. The particle size determines the extent of adsorption in powdered clays as shown by Ji et al., (2013). Furthermore, Gasparik et al., (2013), showed that when preparing powder samples that are widely used for adsorption measurement, an increased internal surface area is provided by confined pores spaces which lead to an increase in adsorption capacity of powdered samples compared to core samples that are utilised in this work. However, these entirely depend on the method employed in the investigation.

The two sandstone samples, i.e. *Bandera* and *Scioto* are comprised of clay minerals with differences in type and structure, which plays a critical role in their methane (CH_4) adsorption capacity. For example, Kaolinite clay has a 1:1 type clay structure comprising a water–Al layer and a Si–O layer (Palomino and Santamarina, 2005); Kaolinite does not have shrinking or swelling abilities and comprises of an inactive layer and internal surface area (Ji et al., 2015). Illite has a structure similar to montmorillonite with relatively little expandability (Ross and Bustin, 2009; Cheng and Huang, 2004). In illite, the replacement of Si atoms by Al^- atoms in the tetrahedral layer causes a negative charge imbalance that is compensated by K^+ between the clay layers (Ji et al., 2012). Illite has a small internal surface area and average adsorption capacity. Chlorite has a similar crystal layer structure to illite, but an additional octahedral layer containing Mg or another cation (Milliken et al., 2012) replaces the K^+ layer.

Sandstone reservoir consists of different minerals, and the dominant are Sand-quartz, feldspar and clay minerals. The clay minerals vary based on the sandstone depositional environment; the clay types include; kaolinite, illite, montmorillonite and chlorite. The clays contribute to their gas adsorption capacity because of their large surface areas which give them significant gas adsorption capacity (Ji et al., 2012; Heller and Zoback. 2015; Zhang et al., 2014). The adsorption capacity of pure clays was reported by

previous work (Ji et al., 2012; Heller and Zoback. 2015; Zhang et al., 2014), which indicates that the adsorption capacities of individual clay minerals decrease in the order: smectite >> mixed layer I/S > Kaolinite > Chlorite > illite. These results differ somehow from those presented by Ross and Bustin. (2007), who used pure clay standards, suggesting that texture of clay minerals and sample preparation techniques should be considered.

The experimentally measured values of methane (CH_4) adsorption capacity of sandstones are listed in Appendix A-2 and plotted in Figure 5.10. The pressure ranges used for adsorption capacity experiments represent those occurring in depleted reservoirs at abandonment as reported by MacRoberts, 1962; Okwananke et al., 2011; and Mathias et al., 2014. Moreover, methane adsorption capacity at equilibrium is used in this section to investigate the difference between the natural adsorption capacities of adsorbed CH_4 at equilibrium pressure versus abandonment pressure.

The adsorption isotherm of the core samples (sandstone) at equilibrium shows that the potential adsorption surfaces become filled up by methane molecules until they become fully gas saturated, and the plot becomes linear indicating that the microporous solid has reached gas saturation representing type 1 isotherm. These statements appear to be true for sandstone samples in Figure 5.9a,b and powdered pure clay samples (Ji et al., 2012, Gasparik et al., 2014) at a pressure up to 1000 psia (6.89 MPa) and 2175.57 psia (15 MPa) respectively. However, for sandstone core samples at abandonment pressures, the experimental adsorption capacity at pressures up to 500 psia (3.45 MPa) for both *Scioto* and *Bandera* sandstones indicate that there are more adsorption site available as equilibrium was not reached. Therefore, CO_2 injection at a higher pressure will build up the system pressure, and due to the higher adsorption capacity of CO_2, CH_4 gas would be replaced in the system there by recovering more of CH_4 in the reservoir.

The experimental result for maximum adsorption capacities of methane (CH_4) at equilibrium pressure for the *Bandera* and *Scioto* sandstones were 0.089 mmol/g and 0.110 mmol/g respectively. However, the adsorption capacity of CH_4 at abandonment pressure (500psia) is 0.061 mmol/g and 0.082 mmol/g respectively. In the literature, all studies were conducted at 50 and 100°C. Fujii et al., (2010) estimated CO_2 adsorption on *Berea* sandstones at 50°C and 100°C. They found Langmuir-like CO_2 of *Berea* sandstone to be 3.7 mmol/g and 2.8 mmol/g at 50°C and 100°C at 2900.75 psia (20

MPa) respectively. Eliebid et al. (2017) measured CO_2 adsorption using *Kentucky* sandstone. They found carbon dioxide (CO_2) adsorption of Kentucky sandstone to be 8.92 mmol/g, 2.8 mmol/g and 10.06 mmol/g at 50°C, 100°C and 150°C and 725.189 psia (5 MPa) respectively. The results for methane (CH_4) adsorption capacity of *Scioto* and *Bandera* at equilibrium and abandonment pressure are lower than those for CO_2 found in the literature. These results indicate that for the sandstone sample, CO_2 has an adsorption capacity approximately 2–5 times greater than that of CH_4.

5.4 SECTION 3: Water and brine saturation dependence on CH_4 sorption capacity of sandstones

5.4.1 Effect of Water content on Methane adsorption capacity

The analysis of the methane adsorption capacity of dry sandstone samples in sections 5.3.1 indicates that physical and experimental parameters such as the pressure, clay structure and mineralogy determines the gas adsorption capacity of the sandstones core samples. However, most sandstone reservoirs consist of at least two different phases e.g. gas-water (Dandekar, 2006; Jordan and Doughty, 2009; Sloss et al., 2015). Trace amounts of water (usually in ppm range) in high-purity gases contribute in errors from adsorption experiments (Gasparik et al., 2014).

Adsorption isotherms are best measured on dry samples as wet samples give less reliable results (Gasparik et al., 2014). The uncertainties associated with the reservoir storage capacity calculation include the presence of formation water and the reactions of methane (CH_4) with the rock and saline water. The effect of the presence of adsorbed water, which occurs from the sandstone-water interaction cannot be avoided owing to the hydrophilic nature of the rocks (clays), therefore the determination of the adsorption isotherm is required for both states. In this investigation sandstone samples (*Bandera*, *Scioto*) with pre-adsorbed water were measured to determine their methane (CH_4) adsorption capacity at different water content, by which the effect of water on methane adsorption was analysed.

Appendix A-3 presents the experimentally measured methane (CH_4) adsorption capacity of water saturated *Bandera* and *Scioto* samples respectively, and Table 5.7 presents the estimated percentage decrease in adsorption capacity due to the presence of water. Figure 5.12 and Figure 5.13 show the plot of experimentally measured adsorption

capacity of both samples at different water content (33, 65 and 91%) for *Bandera* and Scioto core samples respectively.

Table 5.7: Calculated percentage decrease in adsorption capacity to water content.

	Scioto			Bandera		
	Decrease in adsorption capacity (%)					
	Water content (%)					
Pressure (psia)	**33%**	**65%**	**91%**	**33%**	**65%**	**91%**
50	58.33	75	91.67	30	50	50
100	45.45	68.18	72.73	31.58	52.63	52.63
150	48.48	60.61	66.67	24	40	40
200	46.51	58.14	62.79	19.35	32.26	32.26
250	50.98	54.90	62.74	21.62	35.13	35.13
300	48.27	51.72	58.62	20.93	30.23	30.23
350	47.76	50.75	56.72	21.28	31.91	31.91
400	41.67	47.22	52.78	9.80	19.61	19.61
Total Decrease (%)	**47.21**	**54.47**	**60.89**	**10.26**	**24.36**	**38.03**

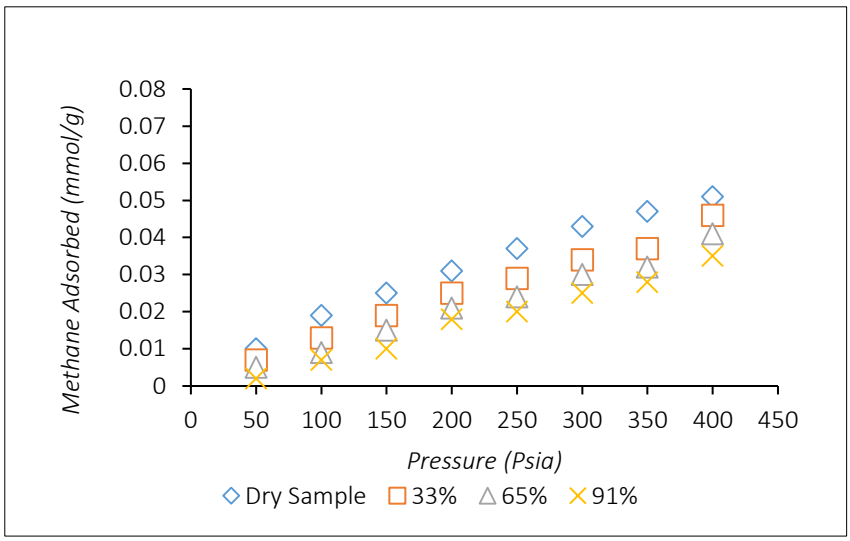

Figure 5.12: Experimental Methane (CH_4) sorption capacity of water saturated samples for Bandera at varying water content.

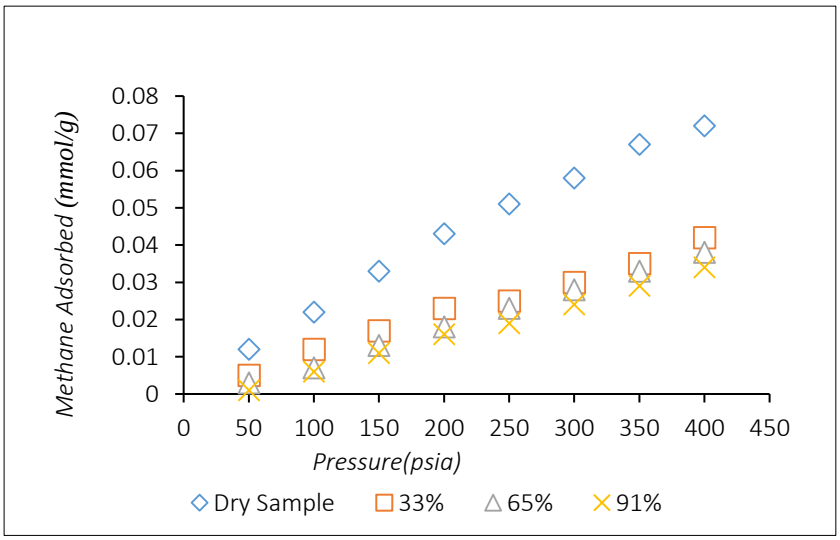

Figure 5.13: Experimental Methane (CH_4) sorption capacity of water saturated samples for Scioto at varying water content.

Table 5.7 indicate that the amount of gas adsorbed on water saturated samples decreased at an overall rate of 47.21%, 54.47% and 60.89 for *Scioto* and 10.26%, 24.36%, and 38.03% for *Bandera* with increasing water content. These values were much lower than the adsorption capacity of dry samples at the same variable pressure. However, to quantify the effect of water content on sandstones, a plot of a comparison between experimental adsorption capacity of dry and water-wet samples is presented (Figure 5.12 and Figure 5.13). For water content of 33%, although the shape of the adsorption isotherms remains almost similar, the adsorption isotherms experiments show a

substantial decrease in CH_4 adsorption amounts compared to the dry sample. The experimental data further showed a decline in the adsorbed amounts of methane upon increasing the water content from 65 to 91%.

The experimental results in Figure 5.12 and Figure 5.13 indicate that the interaction of water with sandstones is controlled by two adsorption types, a) physical adsorption and b) chemisorption onto clay surfaces, which results in a substantial water adsorption capacity due to extra electric charges formed on their surface by isomorphous substitution. Which occurs when an element substitutes another element in a mineral without a significant change in the crystal structure. In addition, water tends to form solid-like clusters via hydrogen bonds. For small amounts of adsorbed water, although the shape of the experimentally measured adsorption capacity plots remains similar, the adsorption capacity decreased in the investigated *Bandera* and *Scioto* core samples as seen in Table 5.7. It was observed that the adsorbed amount of methane decreases with increasing water content (33, 65 and 91%) at variable pressure (0 – 400Psia or 0 – 2.76 MPa) as shown in Figure 5.12 and Figure 5.13.

Competition for adsorption sites between water and methane (CH_4) is another cause of the observed decline in the methane adsorption capacity of sandstones. Water has a strong affinity to clay, moreover, since water and methane molecules will be adsorbed on the same sandstone surface, there will be competition between Methane (CH_4) gas molecules and water for pore space and surface area. Clay pores spaces and the surface will be blocked by water clusters due to their hydrophilic nature (high water adsorption), and this will lead to pore and surface area blockage. The cause of water blockage is due to hydrophilic nature of clays, which results because their structure is made of hydrous aluminium silicate platelets, with spaces between the alumina and silica layers occupied by exchangeable cations such as Mg^{2+}, Ca^{2+}, Na^{+}, $K^{+,}$ and Li^{+}.

The cause of this phenomenon can be explained by differentiating between the mechanism of hydrophobicity and hydrophilicity. The boundary between hydrophobicity and hydrophilicity occurs when the difference between the polar attraction and repulsion between clay particles immersed in water is equal to the cohesive polar attraction between the water molecules. Under these conditions, the interfacial free energy of interaction between particles immersed in water (ignoring electrostatic interactions) is exactly zero. When the interfacial free energy is positive,

the interaction in the material with water becomes dominant, and the surface of the material is hydrophilic; however, if the interfacial free energy is negative, the polar cohesive attraction between the water molecules dominates, and the material is hydrophobic (Van Oss and Giese., 1995).

A critical moisture holding capacity was reported in the literature (Day et al., 2008; Joubert et al., 1973, 1974; Levy et al., 1997) typically observed at 75 – 99% relative humidity. This phenomenon has been observed in studies (Merkel et al., 2015, Gasparik et al., 2014) of adsorption capacities conducted at different moisture contents and relative humidity using shales and coal samples. This is a point where a linear decrease up to certain "critical moisture" content is observed above which there was no change in adsorption capacity with a further increase in moisture (Day et al., 2008; Joubert et al., 1973, 1974; Levy et al., 1997). However, in this study, the samples were not saturated up to 75% or 99% water content; therefore, we could not observe the latter fact.

The particle sizes of water and methane are relatively small at molecular level and can easily penetrate clay layers. Moreover, it is expected that competition for adsorption sites between water and methane entering the clay layer will be dependent upon the structure of clay, hydrophilicity, and type of clay in the individual samples (*Bandera, Scioto*). These differences are due to the variation in the amount and distribution of the water within the different sandstone samples. Hydrophilic sorption sites are concentrated within the micro and mesoporosity as a positive trend occurs between the moisture content and the micro and mesoporous surface area. The pore size distribution, in turn, is controlled by mineralogy, pore space, internal surface area and particle size.

5.4.2 Effect of Brine on Methane(CH_4) Adsorption capacity

Following the previous investigation in section 5.4.1, Dry and samples saturated with water were used to analyse the adsorption capacity of sandstones. Using these two samples, the adsorption capacity yielded different results. To verify the effect of brine on investigated samples, further research was conducted using low salinity (20%) Brine made using NaCl (sodium chloride).

Appendix A-4 presents experimental values of the adsorption capacity of *Bandera* and *Scioto* sample at 33%, 65%, and 91% brine content respectively. Figure 5.14 and Figure 5.15 shows a plot of the experimentally measured methane (CH_4) sorption capacity of

Bandera and *Scioto* sandstones saturated with brine respectively at varying brine content. Table 5.8 shows the percentage decrease in adsorption capacity due to brine content.

Experimental results in Table 5.8 indicates that for both samples saturated with brine, the presence of brine caused an overall reduction in the methane adsorption capacity of 30.17%,43.57%, 43.57% and 69.83 for *Scioto* sandstone saturated with brine and 28.90%, 42.58% and 52.85% for *Bandera* sandstone saturated with brine compared to dry samples. This decrease was also observed in sandstone samples saturated with water in Section 5.4.1. Furthermore, it was noted that at 20% brine salinity, there was an additional loss of methane adsorption capacity compared to raw water saturated samples (47.21%, 54.47%, 60.89% for *Scioto* and 10.26%, 24.36%, 38.03% for *Bandera*). The additional loss of adsorption suggests that the initial amount of adsorbed water desorbs with methane pressure or due to the removal of small quantities of residual moisture after the exposure to low-pressure gas and subsequent evacuation. Analysis of experimental data indicates that blockage of both sample pore space and surface area by low salinity brine led to a decrease of methane (CH_4) adsorption capacity.

The microstructure of the sandstones exhibits a large surface area from clays, significant pore size viability and a pore system associated with clay and other constituents such as quartz, dolomite, Plagioclase, Feldspar. A general hypothesis is that when in contact with water or brine, the large surface area, pore size viability, multiple pore systems and differential particle sizes of sandstone will be in contact with interfacial forces (electrical double layer and solvation) that bound them to the low salinity brine at varying degrees. The clay surfaces, which will become water-wet, develop high capillary forces that bound the brine with a strength that is inversely proportional to the pore radius.

Table 5.8: Percentage (%) decrease of methane (CH_4) adsorption due to brine content.

	Scioto			**Bandera**		
	% Reduction in adsorption capacity					
	Brine content at 20% salinity					
Pressure (Psia)	**33%**	**65%**	**91%**	**33%**	**65%**	**91%**
50	66.67	83.33	91.67	50	70	90
100	59.09	68.18	86.36	36.84	63.16	78.95
150	57.57	63.63	81.81	40	52	68
200	55.81	60.46	74.42	35.48	51.61	58.06
250	52.94	56.86	70.59	27.03	37.84	51.35
300	50	53.45	67.24	27.91	41.86	46.51
350	49.25	52.24	64.18	27.66	38.30	46.81
400	45.83	48.61	59.72	15.69	27.45	37.25
Total Decrease (%)	**30.17**	**43.57**	**69.83**	**28.90**	**42.58**	**52.85**

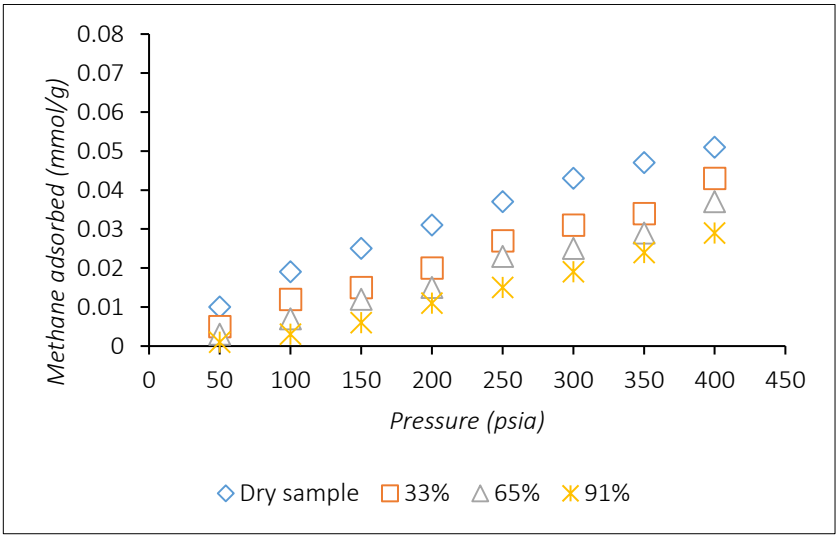

Figure 5.14: Experimental Methane (CH_4) adsorption capacity of Brine saturated Bandera at variable Brine content.

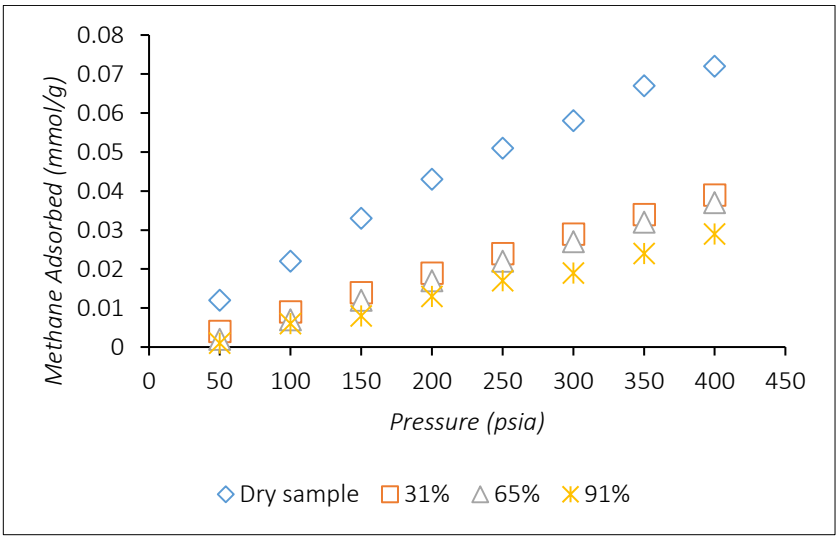

Figure 5.15: Experimental Methane (CH_4) sorption capacity of Brine saturated Scioto at variable Brine content.

In addition, structurally bound hydroxyls are present and are part of the clay structure. As a result, there is a continuum range of capillary and surface forces keeping water attached to the pore surfaces, and these forces then are stronger than the weak van der Waal forces in physical adsorption of methane to clay. For methane to be adsorbed at high capacity, these forces must be overcome.

Secondly, the experimental result suggests that 20% sodium chloride (NaCl) low salinity brine will alter the *Bandera* sandstone wettability toward strongly water-wet

conditions, while the surface charge of *Scioto* sandstone will be affected by low-salinity water, and the zeta potential of illite and chlorite clays will be significantly decreased.

5.4.3 Summary

Using Helium Pycnometry as a measurement tool for void volume of two sandstone samples (Bandera, Scioto); data was presented which documents the effect of pressure, time and water content on void volume measurements. The following summary has been drawn from this chapter:

- The pressure ranges investigated showed close results regarding the measured void volume value with measurement scattered about an average of 8.017cm^3 for *Bandera*, and 4.5171cm^3 for the *Scioto* samples.
- Void volume data showed that there was little data deviation of 0.002 cm^3 and 0.001 cm^3 in void volume with pressure for the *Bandera* and *Scioto* samples.
- Equilibrium was attained after a 240mintes (four hour) interval indicating that longer times yield better void volume data; this is because as contact time increased, helium was able to access pores of tiny sizes.
- The investigation indicates that water content of 5.62 wt. % and 5.48wt. % for both samples respectively, can reduce the dry capacity by as much as 12.53% and 11.2%.
- Water blocks some of the pores accessible to helium and leads to a decrease in void volume. When quantifying storage in sandstone at reservoir scale, which is water-wet, it is necessary to make corrections by accounting for pore blocked by water.

The CH_4 adsorption capacity of dry sandstones was measured using a purposely-built adsorption apparatus under pressure (0–1000 psia) and 0 – 500 psia and a constant temperature (23°C).The results showed that:

- Sandstones reached equilibrium adsorption capacity at 950 - 1250 psia (6.55 to 8.62 MPa) while at abandonment pressure (0 - 500 psia or 0 – 3.45 MPa), the adsorption isotherm remained convex indicating available adsorption sites.
- Based on types, some clays in sandstones have higher adsorption capacity than others.

- Methane (CH_4) adsorption capacity of sandstones at abandonment and equilibrium pressure were lower than that of carbon dioxide (CO_2).
- The results indicate that the adsorption capacity of CO_2 of sandstone is approximately 2–5 times greater than that of CH_4.

Using sandstones saturated with water, and 20% salinity brine content (33%, 65%, and 91%). The experimental findings from this research reveal that:

- Sandstone samples saturated with water showed an overall decrease of 47.21, 54.47 and 60.89% for *Scioto* and 10.26, 24.36, and 38.03% for *Bandera* with increasing water content (33, 65 and 91%) and were much lower than that adsorption capacity of dry samples at the same variable pressure.
- The presence of brine caused an overall decrease in the methane adsorption capacity by 30.17, 43.57, 43.57 and 69.83% for *Scioto* and 28.90, 42.58 and 52.85% for *Bandera* compared to dry samples. Furthermore, it was observed that for 20% brine salinity saturated samples, there was an additional loss of methane adsorption capacity compared sandstones saturated with water (47.21, 54.47, 60.89% for *Scioto* and 10.26, 24.36, 38.03% for *Bandera*).
- Two adsorption types control the interaction of water with sandstone core samples: (a) physisorption onto polar surfaces and (b) chemisorption onto clay surfaces, which results in a substantial water adsorption capacity due to extra electric charges formed on their surface by isomorphous substitution.
- At 20% sodium chloride (NaCl) rich low salinity brine will alter the *Bandera* sandstone wettability toward strongly water-wet conditions, while the surface charge of *Scioto* sandstone will be strongly affected by low-salinity water and the zeta potential of illite and chlorite clays will be significantly decreased.

5.5 SECTION 4: Accuracy of experimental data

To verify the accuracy of the current available adsorption model, the first and crucial step is to set comparison criteria for each model. Two general criteria are used here. First, the repeatability denotes the consistency of repeated measurements for a given sample, on the same setup at the same conditions and by the same operator (Gasparik et al., 2014). It is crucial to prove the reliability of the adsorption experiments (Merey et al., 2016). Secondly, the goodness-of-fit of the model to test data will be evaluated. This is a straightforward approach to show whether the proposed model can describe the experimental measurements. An accurate model should closely match the data using the minimal but the most significant assumptions. If the proposed model meets the all the above two standards, the model should be treated as valid.

5.5.1 Repeatability & verification of Adsorption measurements

The repeatability of the adsorption data for the two sandstone samples (i.e. *Scioto* and *Bandera* sandstone) was checked by conducting repeat experiments. Similar experimental conditions (T = 23°C and up to a pressure of 400 psia (2.76 MPa) in eight pressure steps) was maintained for water and brine saturated sandstones, while the dry samples were conducted at equilibrium (i.e. 1000 psia or 6.89 MPa and 23°C). Figure 5.16 presents the test data for the repeatability of methane (CH_4) adsorption capacity of sandstones using dry, and sandstones core samples saturated with water and brine. Table 5.9 shows the measured repeatability values for methane adsorption of dry sandstone samples at equilibrium while Table 5.10 lists the pressure, adsorption capacity and the expected experimental uncertainty for each datum compared to those found in the literature.

a)

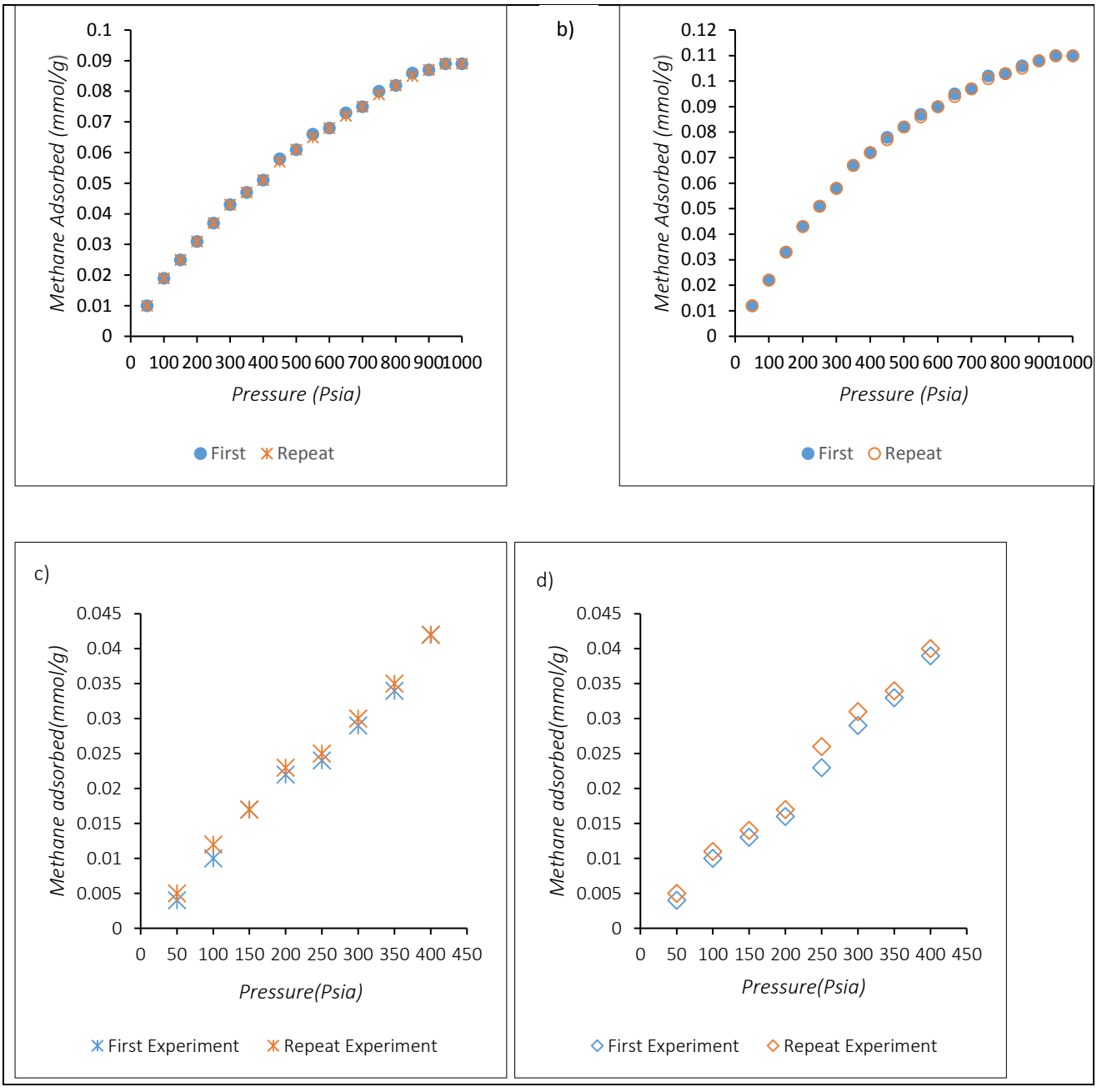

Figure 5.16: Comparison of repeatability and accuracy of CH_4 adsorption experimental data using; a) Dry Bandera sandstone; b) Dry Scioto sandstone and; c) water saturated Scioto and; d) Brine saturated Scioto.

Two replicate runs were conducted to investigate the reproducibility of the isotherm measurements (Figure 5.16 a – d). The average data deviation was 0.33 and 0.42 for dry Scioto and Bandera samples respectively, while the deviations were 3.85 and 3.59 for samples saturated with water and brine respectively between the first and repeat experiments. Excellent repeatability of experimental data for both sandstone samples

(*Scioto* and *Bandera*) was observed. As can be seen, the adsorption isotherms for dry sample agree closely. However, the higher data deviation for the samples saturated with water and brine is because the interaction of water and methane is a function of a number of processes occurring simultaneously (i.e. physical and chemical adsorption, pore space blockage). Moreover, wet samples give less reliable results (Gasparik et al., 2013, 2014; Sloss et al., 2015).

The results of the adsorption experiments indicate that the self-assembled equipment used for this research is sufficient for simultaneously measuring adsorption. The data deviations from all the experimental runs were accurate and within the range reported in the literature, for example, Chareonsuppanimit et al., (2012) data was 9.0. The differences of repeated results were all within 3.0 for Lu et al., (1994), while that of Rani et al., (2015) was 6.4.

Table 5.9: Repeatability data of Dry sandstone samples.

Dry Experiments				
Pressure (Psia)	Scioto		Bandera	
	First	Repeat	First	Repeat
50	0.012	0.012	0.010	0.010
100	0.022	0.022	0.019	0.019
150	0.033	0.033	0.025	0.025
200	0.043	0.043	0.031	0.031
250	0.051	0.051	0.037	0.037
300	0.058	0.058	0.043	0.043
350	0.067	0.067	0.047	0.047
400	0.072	0.072	0.051	0.051
450	0.078	0.077	0.058	0.057
500	0.082	0.082	0.061	0.061
550	0.087	0.086	0.066	0.065
600	0.09	0.090	0.068	0.068
650	0.095	0.094	0.073	0.072
700	0.097	0.097	0.075	0.075
750	0.102	0.101	0.08	0.079
800	0.103	0.103	0.082	0.082
850	0.106	0.105	0.086	0.085
900	0.108	0.108	0.087	0.087
950	0.11	0.110	0.089	0.089
1000	0.11	0.110	0.089	0.089

Table 5.10: Experimental data of water/Brine samples and comparison of repeatability data to literature.

	Water saturated Experiments		**Brine saturated Experiments @ 20% salinity**		**Comparison of reliability Data to Literature**			
	Scioto (33%)		*Scioto (33%)*					
Pressure (psia)	First	Repeat	First	Repeat	Authors	Method	Type	Data Deviation
50	0.004	0.005	0.004	0.005	Experiments from this research	Manometric	Dry	0.33
100	0.010	0.012	0.010	0.011	Experiments from this research	Manometric	Dry	0.42
150	0.017	0.017	0.013	0.014	Experiments from this research	Manometric	water	3.85
200	0.022	0.023	0.016	0.017	Experiments from this research	Manometric	Brine	3.59
250	0.024	0.025	0.023	0.026	Lu et al., 1995	Manometric	Dry	3
300	0.029	0.030	0.029	0.031	Chareonsuppanimit et al., 2012.	Manometric	Dry	9
350	0.034	0.035	0.033	0.034	Rani et al., 2015	Manometric	Dry	6.4
400	0.042	0.042	0.039	0.040				

5.5.2 Best Fit model output

In this section, firstly, the best-fitting model was determined using error functions. Then, the applicability of the proposed statistical tools was discussed, based on a comparative study between them. Three theoretical isotherm models, namely: Langmuir, Freundlich, and Redlich were employed to fit two sets of experimental methane(CH_4) adsorption capacity results, which were from adsorption experiments in Sub section 5.3.1, using two sandstone core samples (*Bandera, Scioto*). The non-linear regression fitting was carried out using MATLAB R2016A software. The non-linear regression procedure provides better fits and can be performed for different models with the same set of adjustable variables, allowing for more direct comparison of distinct model fits. The application of the non-linear model is direct and does not require mathematical manipulations as in the case of linear regression.

Experimental data was inputted into the MATLAB software along with the analytical models for adsorption presented in section 2.4 , followed by curve fitting using non-linear regression and error functions. Three criterion, SSE (sum of squares due to error), RMSE (root mean squared error), r^2 (Coefficient of multiple determination) and Residual Plots were used to determine the goodness of fit for the two sandstone types. The non-linear regression fittings are presented in Figure 5.17a, Figure 5.17 b, Figure 5.18a, Figure 5.18b and Figure 5.19a, Figure 5.19b. Table 5.11 shows the values of corresponding isotherm parameters, their multiple correlation coefficients (r^2) and the sum of squares due to error (SSE) for each parameter.

The coefficient of multiple determination (r^2) for the fit should range between 0.9 and 1.00 to show a good fit for the model. Fitting results (Figure 5.17, Figure 5.18, Figure 5.19 and Table 5.11) show that for *Bandera* sample, the Redlich Paterson isotherm and Langmuir have the same r^2 value of $r^2 = 0.9992$, while the Freundlich isotherm model has a value of that $r^2 = 0.9935$. For the *Scioto* sample, the r^2 values of the three isotherm models are 0.9996, 0.9978 and 0.9798 for the Redlich Paterson, Langmuir and Freundlich, respectively. The coefficients of multiple determination (r^2) for fitting the Langmuir, Redlich-Paterson and Freundlich isotherm models were all of high value as shown in Table 5.11. The coefficient of multiple determination (r^2) for all isotherm fit ranged between values of 0.9935 to 0.9798 showing an overall good fit by all isotherm models. These fitting results indicate that based on the r^2 analysis the Redlich-Paterson

and Langmuir isotherm model will generate a satisfactory fit to the experimental data compared to the Freundlich, isotherm model.

a)

b)

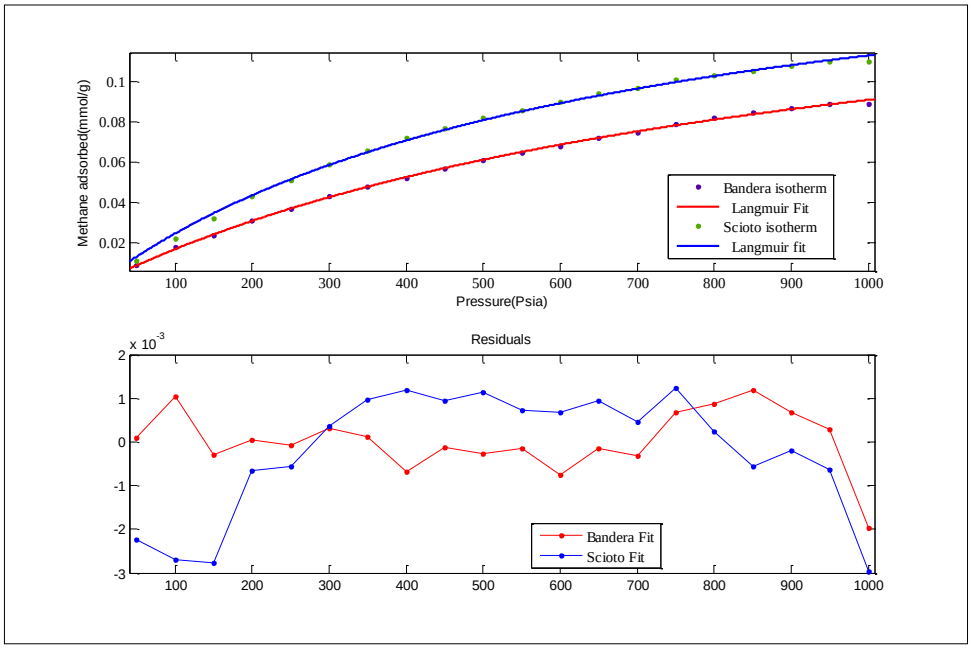

Figure 5.17: a) Non-linear fitting of experimental data and b) Residuals of Langmuir isotherm model to core samples (Bandera, Scioto).

a)

b)

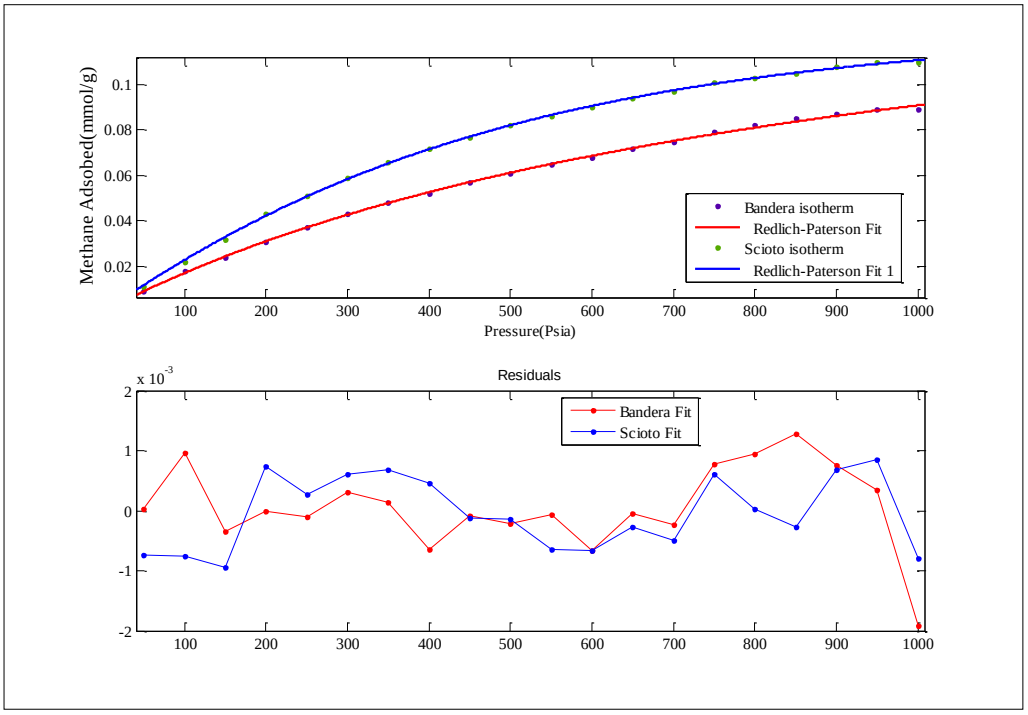

Figure 5.18: a) Non-linear fitting of Experimental data and b) Residuals of Redlich Paterson isotherm model to core samples (Bandera, Scioto).

a)

b)

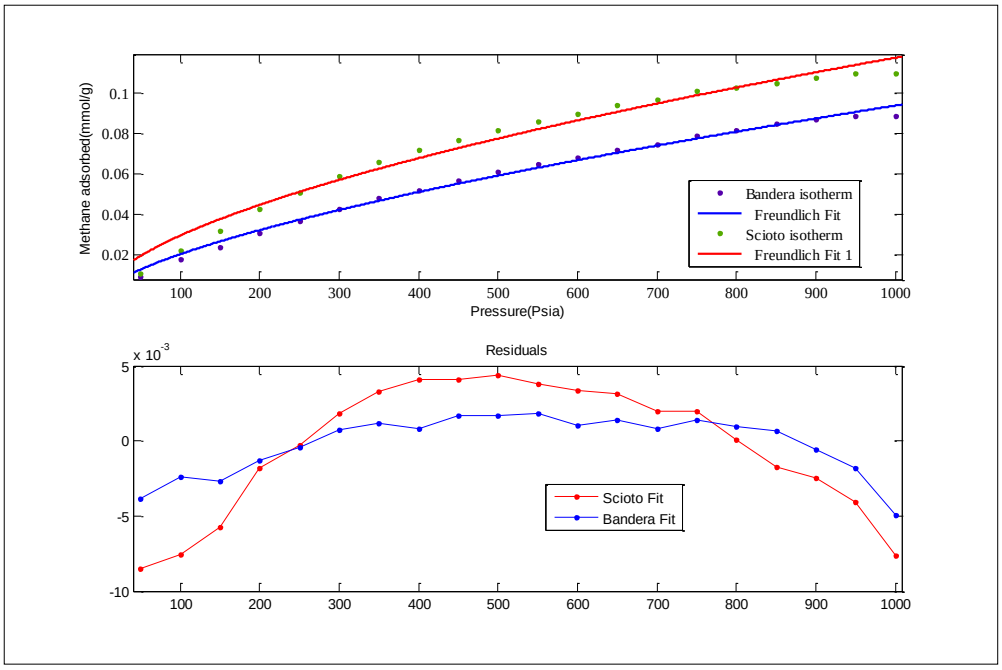

Figure 5.19: a) Non-linear fitting of experimental data and b) Residuals of Freundlich isotherm model to core samples (Bandera, Scioto).

Table 5.11: Estimated values of statistical indicators and model parameters.

Isotherm model / Error Function	Bandera	Scioto
Freundlich K_F n	 0.0173 0.6632	 0.0187 0.5993
Goodness of Fit	SSE: 7.665e-4 r^2: 0.9935 RMSE: 0.002064	SSE: 3.609e-4 $r^{2:}$ 0.9798 RMSE: 0.004478
Langmuir VL PL	 0.095 0.1064	 0.116 0.1520
Goodness of Fit	SSE: 9.605e-6 r^2: 0.9992 RMSE: 0.0007305	SSE: 3.854e-5 r^2: 0.9978 RMSE: 0.001463
Redlich Patterson K_R a_R g	 0.092 0.9848 0.830	 0.113 1.343 0.9186
Goodness of Fit	SSE: 9.65e-6 r^2: 0.9992 RMSE: 0.0007534	SSE: 7.138e-6 r^2: 0.9996 RMSE: 0.000648

The sum of squares due to error (SSE) for the fit should be closer to zero (0) to indicate a good fit for the model. From, Table 5.11, the values of the sum of squares due to error (SSE) from fitting result showed that the Freundlich isotherm model had values further from zero (0) in both *Scioto* (7.665e-04) and *Bandera* (3.609e-04) samples respectively. The SSE values of the Redlich Paterson and Langmuir models were 9.65e-6, 7.138e-6 and 9.605e-6, 0.004478 for the *Bandera* and *Scioto* samples respectively. Just as with SSE, a root mean squared error (RMSE) value closer to 0 indicates a fit that is more useful for prediction. The small values of RMSE show the better model fitting and similarity of the model with the experimental data respectively. The value of the RMSE of the fitting result (Table 5.11) from the best fit to the least was 0.0007534 and 0.000648 for Redlich-Paterson, 0.0007305 and 0.001463 for Langmuir and 0.002064 and 0.004478 for the Freundlich model for the *Bandera* and *Scioto* Samples respectively.

The theoretical values of maximum adsorption capacity determined using the Redlich Paterson isotherm were 0.092mmol/g and 0.113mmol/g for *Bandera* and *Scioto* respectively. These values are near the experimental maximum adsorbed amounts of 0.089mmol/g and 0.110mmol/g (Appendix A-1) for the *Bandera* and *Scioto* samples, which indicates that the Redlich-Paterson model can accurately be used to determine sandstone adsorption capacity. However, the fitting result shows that values of theoretical adsorption capacity for the Langmuir model were 0.095mmol/g and 0.116mmol/g and are close to the Values from the Redlich-Paterson. The Values from the Freundlich model were 0.0173mmol/g and 0.0187mmol/g; these results are greater than the Maximum adsorption capacity of sandstones from experimental result in Sub section 5.3.1.

The experimental data fitting with Freundlich isotherm is shown in Figure 5.19 with normal coordinate. Relatively large deviations are observed between the experimental data and the non-linear fitting values for the Freundlich isotherm. One of the possible reasons for the disagreement of experimental data with Freundlich isotherm is that, Freundlich isotherm is based on the adsorption phenomena, in which an indefinite multi-layer formation is formed after completion of the monolayer and that was not the case for the sandstone/methane adsorption system. To include the homogeneity of the adsorbent surface, Langmuir isotherm and Redlich-Paterson was also used to fit the

experimental data. The data fitting with Redlich-Paterson and Langmuir isotherm is shown in Figure 5.17 and Figure 5.18.

The agreement of experimental result with Redlich Paterson isotherm is better than that of Langmuir isotherm. The Langmuir isotherm fits the experimental data for each sandstone sample (i.e. *Bandera and Scioto*), however, the Redlich-Paterson isotherm fit was more within the experimental temperature and pressure range of this research. This implies that adsorption is monolayer since at low pressure; the Redlich-Paterson describes the Langmuir isotherm while at high pressure it becomes the Freundlich isotherm. The adsorption of methane by the two sandstone samples was found to be well represented by both Langmuir and Redlich-Peterson isotherm. Therefore, by comparison, the order of the isotherm best fits from r^2, SSE and RMSE error function for two sandstone samples (i.e. *Bandera* and *Scioto*) in this chapter is Redlich-Paterson >Langmuir> Freundlich.

The best-fitting isotherm is determined using three well-known functions to calculate the error deviation between experimental and predicted equilibrium adsorption data, after non-linear analysis. Hence, per Table 5.11, the Redlich–Peterson model is the most suitable model to describe the methane adsorption phenomenon satisfactorily. Indeed, the highest r^2 value and the lowest RMSE and SSE values were found when modelling the equilibrium data using the Redlich–Peterson.

5.5.3 Summary

Using repeatability/ verification and best-fit model output in validating the experimental trials investigated in this work, the following summary have been derived from the results:

- The coefficient of multiple determination (r^2) for all isotherms were all in the range of 0.9935 to 0.9798. This indicates an overall good fit by all isotherm models showing that all isotherm model will generate a satisfactory fit to the experimental data.
- The sum of squares due to error (SSE) for the fit should be closer to zero (0) to indicate a good fit for the model. The SSE values of the Redlich Paterson and Langmuir models were 9.65e-6, 7.138e-6 and 9.605e-6, 0.004478 for the *Bandera* and *Scioto* samples respectively which indicate a good fit. However, the Freundlich isotherm model had values further from zero (0) in both Scioto (7.665e-04) and Bandera (3.609e-04) samples respectively.
- Just as with SSE, a root mean squared error (RMSE) value closer to 0 indicates a fit that is more useful for prediction. The small values of RMSE show the better model fitting and similarity of the model with the experimental data respectively. The value of the RMSE of the fitting result from the best fit to the least was 0.0007534 and 0.000648 for Redlich-Paterson, 0.0007305 and 0.001463 for Langmuir and 0.002064 and 0.004478 for the Freundlich model for the *Bandera* and *Scioto* Samples respectively.
- The average data deviation was 0.33% and 0.42% for dry *Scioto* and *Bandera* samples respectively, while the deviations were 3.85% and 3.59% for water and brine saturated samples respectively between the first and repeat experiments.
- The higher data deviation for the water and brine saturated samples was more; this was because of the procedure used in saturating the core samples.
- The theoretical values of maximum adsorption capacity determined using the Redlich Paterson isotherm were 0.092mmol/g and 0.113mmol/g for *Bandera* and *Scioto* respectively. These values are near the experimental maximum adsorbed amounts of 0.089mmol/g and 0.110mmol/g.

CHAPTER 6

6 CONCLUSIONS AND RECOMMENDATIONS

6.1 Conclusions

6.1.1 Effect of averaging pressure, water and contact time

The standard methods (gravimetric, manometric/volumetric) used for adsorption capacity measurements depend on the use helium as an inert gas to determine the void volume of microporous solids (manometric/volumetric). The use of helium as an inert gas to measure the free gas volume or void volume is not unique, and several works have reported that a non-negligible adsorption of helium takes place at ambient temperatures on activated carbons and zeolites (Malbrunot et al., 1997; Sircar., 2001; Gumma and Talu., 2003). The void volume, i.e. the amount or volume of space, in which free or non-adsorbed gas is stored and is present in the sample cell (SC) during the experimental adsorption set-up, was estimated using a helium pycnometer (PORG™ 200). Many parameters affect the measurement of the helium void volume; however, this research concentrated on the effect of pressure, equilibrium time and water content. Moreover, it is also important to take account of the sample form (crushed, core) and type (pure clay, clay shale, sandstone) used for these tests since each material has different properties. These parameters were investigated and analysed using two sandstone core samples (Scioto and Bandera) based on the results of experimental laboratory work. The conclusion from section 1 of chapter 5 is:

- The constancy of average void volume with pressure for sandstones core samples indicates that there were no adsorption of helium in observable quantity, and as such, there was no decrease in the void volume from adsorption for both samples investigated.
- At low pressure, core samples with variable pore types and particle sizes, the constancy of pressure indicate that sandstone core samples will reach saturation independent of molecular diameter but more on the rate at which gas transport by diffusion occurs and velocities of helium particles, all of which are pressure dependent.

- The gas access to the total pore spaces or void volume is restricted by the presence of water. Water content of 5.62 wt. % and 5.48wt. % for *Bandera* and *Scioto* respectively can reduce the dry samples average void volume by as much as 12.53% and 11.20% for investigated *Bandera* and *Scioto* samples. This decrease in free gas storage by water saturated sandstone samples is due to water blockage of pore space and throat.
- The transport of helium into pore space and particles of different size in core samples is described by slow viscous flow described by Darcy flow. This type of flow depends on the fact that gas flow in cored samples is directly related to the difference in pressure between the points of the sample cell and the distance between the points, which are related to contact time, and therefore were the cause of faster saturation or equilibrium time at incremental pressure. The latter implies that at higher pressure, the helium particles have higher velocities and would travel the distance of sample cell faster than its preceding lower pressure. The overall interconnectivity of flow pathways in the cored sampled between the points, the permeability, the pore size distribution and particle size will be the dominant factors that will determine overall gas saturation with contact time. The permeability will ascertain the ease at which helium gas will travel through the sample length.

6.1.2 Methane (CH_4) adsorption of sandstones and the impact of water and brine.

Adsorption processes in methane rich gas reservoirs are of growing importance in both science and engineering. This is reflected – for example – in a growing number of research papers (Passey et al., 2010; Shi et al., 2010; Sondergeld et al., 2010; Ji et al., 2012; Kalantari-Dahaghi., 2010; Gensterblum., 2010, 2013; Heller and Zoback., 2014; Rexer et al., 2014; Gasparik et al., 2012, 2013, 2014; Rani et al., 2016) investigating methane adsorption capacity using either crushed or core reservoir rock samples. As gas adsorption equilibria data up to now cannot be calculated accurately by theoretical or analytical simulation based models, it is necessary to measure them, i.e. to determine them by reliably and precisely performed experiments (Keller and staudt, 2005). Depleted sandstones gas reservoirs are globally abundant, and the development of these resources can increase CH_4 production while permanently isolating green gases emissions such as CO_2. The purpose of this thesis is to understand methane adsorption

in sandstone and the role it plays in depleted sandstone gas reservoirs. This objective is achieved by exploring the impact of CH_4 adsorption on enhanced gas recovery and sequestration (EGR-CO_2). Using sandstone core samples in dry, with water and 20% salinity brine content (33%, 65%, and 91%); the methane (CH_4) adsorption capacity was measured using a purposely-built adsorption apparatus. Earlier studies indicate that in reservoirs, with adsorption capabilities, the ratio of CO_2 storage was higher for every molecule of CH_4 produced. However, the technical feasibility of enhanced gas recovery and sequestration (EGR-CO_2) needs to be investigated in more detail (Khosrokhavar et al., 2014).

In Chapter 3, a custom-built adsorption apparatus was used to measure the methane (CH_4) adsorption capacity of dry sandstone samples up to equilibrium pressures (0 – 1250Psia or 0 – 8.62 MPa) with the following conclusions:

- The result for maximum adsorption capacities of methane at depleted reservoir pressure were 0.61 and 0.82mmol/g. This indicates that the adsorption rate of CH_4 depends strongly on pressure.
- For the *Bandera* sandstone, the maximum adsorbed volume at 1250 psia or 8.62 MPa was 0.089 mmol/g. For the *Scioto* sample, the maximum adsorbed volume at the maximum adsorbed volume at 1250 psia or 8.62 MPa is 0.110 mmol/g. The amount of methane uptake increases with an increase in the pressure for experimental equilibrium adsorption data, but when the adsorbent monolayer is saturated the amount of adsorption approaches to a limit gradually.
- For sandstone core samples at abandonment pressure of depleted reservoirs, the experimental adsorption capacity at very low pressures up to 500psia or 3.45 MPa shows that the isotherm does not have a flat part indicating that a full saturation state has not been reached. The result for maximum adsorption capacities of methane at depleted reservoir pressure were 0.61 and 0.82mmol/g. This indicates that the adsorption rate of CH_4 depends strongly on pressure. The time required for adsorption was approximately 30h at abandonment pressure and 54h at equilibrium adsorption capacity.
- Methane (CH_4) is readily adsorbed onto sandstone in depleted reservoirs.

- The values of the methane adsorption capacity for each sandstone indicate how likely it is for the CO_2 to adsorb and remain in place in the depleted reservoirs being targeted.
- Mineralogical differences, structure, particle and pore size of clays in sandstone samples caused variance in methane adsorption capacity between samples. Clay minerals in sandstone core samples are composed of different particle sizes, For example, the abundance of micro- and mesopores in the size range of 10s of nanometres in chlorite and illite interstratified clay. The high internal surface area with pores of 1–2 nm radius between crystal layers and variable micropore volume in sandstone samples (mainly kaolinite, illite and chlorite) utilised in this investigation will provide an overall increase in adsorption capacity.
- The difference in the composition of clay minerals in the sandstones samples influences the CH_4 adsorption. An analysis of the mineralogical differences between these samples indicated that composition was one factor responsible for variance in methane adsorption capacity between cored samples. Moreover, the *Scioto* sample had the highest total amount of clays present (22%) compared to *Bandera* (14%) and had the highest adsorption capacity. This implies that high content of clay minerals in the *Scioto* sample relative to the *Bandera* provide extra surface area for adsorption of methane(CH_4) therefore contributing to the overall sorption capacity of the samples.

6.1.3 Data verification using reproducibility and best-Fit method.

- Two replicate runs were conducted to investigate the reproducibility of the isotherm measurements at 1000 psia (6.89 MPa) and 400 psia (2.75 MPa). An average data deviation of 0.33%, 0.42% for dry *Scioto* and *Bandera* samples were calculated while a value of 3.85% and 3.59% was calculated for water and brine saturated samples respectively between the first and repeat experiments. Excellent repeatability of experimental data for both sandstone samples (*Scioto* and *Bandera*) was observed.
- In any single component isotherm study, determining the best-fitting model is a key analysis to mathematically describe the sorption system and, therefore, to explore the related theoretical assumptions. Hence, error calculation functions

have been widely used to estimate the error deviations between experimental and theoretically predicted equilibrium adsorption values. In this research, equilibrium adsorption of methane by sandstones has been carried out. The related results have been modelled using Freundlich, Langmuir and Redlich–Peterson equations, via nonlinear regression analysis. The best-fitting model was evaluated using three different error functions. The examination of all these error estimation methods showed that the Redlich-Peterson model provides the best fit for the experimental equilibrium data (i.e. highest r^2 and lowest SSE and RMSE values). The applicability of three statistical tools to determine best-fitting isotherm model was investigated for non-linear analysis. The related results showed that the r^2, SSE and RMSE seem to be adequate to point out the best-fitting isotherm model after a non-linear regression approach.

- Theoretical fitting of experimental adsorption capacity showed that both Langmuir isotherm model and the Redlich Paterson isotherm model could generate a satisfactory fit to the experimental data, while Freundlich isotherm model will not. The theoretical values of maximum adsorption capacity determined using Redlich-Paterson isotherm were 0.00092mmol/g and 0.00113mmol/g for *Bandera* and *Scioto* respectively. The values are near the experimental adsorbed amounts of 0.089mmol/g and 0.110mmol/g which corresponding closely to the adsorption isotherm plateau, indicating that the Redlich-Paterson model accurately determines the methane adsorption capacity of sandstone. Therefore, by comparison, the order of the isotherm best fits from r^2, SSE and RMSE value for *Bandera* and *Scioto* samples in this study is Redlich-Paterson >Langmuir> Freundlich isotherm.

6.2 Recommendations

The research objectives of this study focused on a comprehensive investigation of both sample-free gas storage capacities from void volume measurement and methane (CH_4) adsorption capacity of sandstones, allowing the key research questions to be investigated within the scope of this study. However, based on the knowledge and feedback gained from the present study; the following are recommended:

- An inter-laboratory research should be conducted using a large number of sandstones samples to compare with other available methods for measuring void volume.
- Methane (CH_4) Adsorption experiments should be continued with more sandstones with different clay mineralogical composition, variable experimental conditions (pressure, temperature) as well as various components of gases present in sandstone reservoirs.
- Clay contents, pore sizes, particle sizes of these samples should be known. This experiments will be helpful to understand the effects of temperature, clay materials, composition and structure on the adsorption dynamics of clays in sandstones. Moreover, this is critical for improving the calculations used in initial gas-in-place calculations for sandstone gas reservoirs.
- The accuracy of experimental setup should be increased for most accurate adsorption isotherms by increasing the sensitivity of pressure transducers, thermocouples, constant water temperature bath and pump.
- Only a few measurements were performed on water, and brine saturated sandstones; more measurements should be carried out for a range of different water content and brine salinity.
- Adsorption measurements using water and brine samples should be treated as is being done for gas adsorption by considering that water exists as two phases, i.e. free and adsorbed phase.
- It would also be interesting to compare the impact of water by using relative humidity method and water saturation method (this research) to compare their accuracy.

- A joint research should be conducted using two or more custom-built adsorption apparatuses such as the one custom built for this research (Chapter 3, section 3.4.2) to determine the accuracy of these modifications on adsorption capability.
- Full characterisation of depleted sandstone gas reservoirs might be achieved through the integration of standard nuclear, electrical and acoustic logs with geochemical laboratory and log measurements to solve for all the important minerals present at the sandstone gas formation.
- A complete research on adsorption in sandstones should be conducted by combining experimental, imaging and numerical simulation techniques.
- An investigation related to the chemistry of adsorption in depleted sandstones reservoirs should be carried out to analyse reaction, chemisorption and sorption kinetics, this is important since these have been observed during this investigation as fundamental issues affecting the methane adsorption of sandstones.

7 REFERENCES

Aasen, K., Vigeland, B., Norby, T., Larring, Y., Mejdell, T., (2004). Development of a hydrogen membrane-based reformer based CO_2 emission free gas fired power plant. Proceedings of the seventh International Conference on Greenhouse Gas Control Technologies,Vancouver,Canada.Availableat:http://uregina.ca/ghgt7/PDF/papers/nonpeer/529.pdf.

Afanasyev, A. A., (2013). Multiphase compositional modelling of CO_2 injection under subcritical conditions: the impact of dissolution and phase transitions between liquid and gaseous CO2 on reservoir temperature. Intl J. Greenh. Gas Control 19, 731–742.

Aimard, N., Lescanne, M., Mouronval, G., Prebende, C., (2007). The CO_2 pilot at Lacq: An integrated oxycombustion CO_2 capture and geological storage project in the South West of France. International Petroleum Technology Conference 2007 (Society of Petroleum Engineers, Richardson, TX), pp 1717–1724.

Akimoto, K., Kotsubo, H., Asami, T., Li, X., Uno, M., Tomoda, T., (2004). Evaluation of carbon dioxide sequestration in Japan with a mathematical model. Energy 2004; 29:1537–49.

Akpa, O.M, and Unuabonah, E.I., (2006). Small sample corrected Akaike information criterion: an appropriate statistical tool for ranking of adsorption isotherm models, Desalination, vol. 272, pp. 20-26, 2006.

Al-Asheh, S., Banat, F., Al-Omari, R., and Duvanjak, Z., (2003). Predictions of binary sorption isotherms for the sorption of heavy metals by pine bark using single isotherm data, Chemosphere, vol.41, pp. 659-665.

Al-Hasami, A., Ren, S., Tohidi, B. (2005). CO_2 injection for enhanced gas recovery and geo-storage: reservoir simulation and economics. In: SPE Europec/EAGE Annual Conference. Society of Petroleum Engineers Inc., Madrid, Spain. http://dx.doi.org/10.2118/94129-MS.

Alimoradi, A., Moradzadeh, A., and Bakhtiari, M. R., (2011). Methods of water saturation estimation: Historical perspective, 2(March), 45–53.

Allen, S., Gan, Q., Matthews, R., and Johnson, P.A., (2003). Comparison of optimised isotherm models for basic dye adsorption by kudzu", Bioresource Technol., vol. 88, pp. 143-152.

Aljamaan, H., (2015). Multi-Component Physical Sorption Investigation of Gas Shales. Presented at the SPE International Student Paper Contest at the SPE Annual Technical Conference and Exhibition Held in Houston, Texas, USA, 28–30 September 2015. SPE-178736. doi:10.2118/178736-STU.

Aljamaan, H., Alnoaimi, K., & Kovscek, A. R., (2013). In-Depth Experimental Investigation of Shale Physical and Transport Properties. Unconventional Resources Technology Conference, Denver, Colorado, 12-14 August 2013, 1120–1129. doi:10.1190/urtec2013-114.

ANSI/ASME., (1985). Measurement Uncertainty, Supplement to ASME Instruments and Apparatus Performance Test Codes, the American Society of Mechanical Engineers, New York.

Ampomah, W., Balch, R. S., Grigg, R. B., Dai, Z., and Pan, F., (2015). Compositional Simulation of CO_2 Storage Capacity in Depleted Oil Reservoirs. Carbon Management Technology Conference, 1–20. doi:10.7122/439476-MS.

Ampomah, W., Balch, R. S., and Grigg, R. B., (2015). Analysis of Upscaling Algorithms in Heterogeneous Reservoirs with Different Recovery Processes. SPE Production and Operations Symposium March 1-5 2015, Oklahoma USA. doi:10.2118/173588-MS.

Andre, L., Azaroual, M., and Menjoz, A., (2010). Numerical simulations of the thermal impact of supercritical CO_2 injection on chemical reactivity in a carbonate saline reservoir. Transp. Porous Med. 82, 247–274.

Anovitz, L. M., and Cole, D. R., (2015). Characterization and Analysis of Porosity and Pore Structures. Reviews in Mineralogy and Geochemistry, 80, 61–164. doi :10.2138/rmg. 2015.80.04.

Atkinson, B.K., (1979). A fracture mechanics study of subcritical tensile cracking of quartz in wet environments. Pure and Applied Geophysics 117, 1011–1024.

Atkins, P.W., (2006). Physical Chemistry, 8th edition. Oxford University Press, Oxford, New York, p.917.

Audus, H., (2001). Leading options for the capture of CO_2 at power stations. In: Williams D, Durie B, McMullan P, Paulson C, Smith A (Eds) Proceedings of the 5th International Conference on Greenhouse Gas Control Technologies. CSIRO, Collingwood, Australia, pp 91–96.

Avasthi, S. M., Ghotekar, A., and Stein, M., (2010). CO_2 Sequestration in a Depleted Gas Field - A Material Balance Study (SPE-131384). 72nd EAGE Conference & Exhibition Incorporating SPE Europec 2010, (June 2010), 14 – 17.

Aylmore, L.A.G., (1974). Gas sorption in clay mineral systems. Clays and Clay Minerals, Vol. 22, 175–183.

Bachu, S., (2000). Sequestration of Carbon Dioxide in Geological Media: Criteria and Approach for Site Selection in Response to Climate Change. Energy Conversion and Management. 41(9), pp. 953 - 970.

Bachu, S., (2002). Sequestration of CO_2 in geological media in response to climate change: roadmap for site selection using the transform of geological space into the CO_2-phase space. Energy Conservation and Management 43, 87–102.

Bachu, S., D. Bonijoly, J. Bradshaw, R. Burruss, S. Holloway, N.P. Christensen and O.M. Maathiassen, (2007). CO_2 storage capacity estimation: Methodology and gaps. International Journal of Greenhouse Gas Control, vol. 1, no. 4, p. 430-443.

Bachu, S., (2015). Review of CO_2 storage efficiency in deep saline aquifers, International Journal of Greenhouse Gas Control, doi: 10.1016/j.ijggc.2015.01.007.

Bachu, S., Gunter, WD., Perkins, EH., (1994). Aquifer disposal of CO_2: Hydrodynamic and mineral trapping. Energy Conversion and Management 35, 269–279.

Bachu, S., Haug, K., (2005). Carbon Dioxide Capture for Storage in Deep Geologic Formations, ds SM Benson, C Oldenburg, M Hoverstein, and S Imbus (Elsevier, Amsterdam), pp 867–876.

Bachu, S., and Shaw, J., (2003). Evaluation of the CO_2 sequestration capacity in Alberta's oil and gas reservoirs at depletion and the effect of underlying aquifers. J. Can. Petrol. Technol., 42(9), 51–61.

Badalyan, A., and Pendleton, P., (2008). Analysis of uncertainties in manometric gas-adsorption measurements. II. Uncertainty in S-analyses and pore volumes. Journal of Colloid and Interface Science, 326(1), 1–7. doi:10.1016/j.jcis.2008.07.001.

Baines, S.J., and Worden, R.H., ed. (2004), Geological Storage of Carbon Dioxide, Geological Society Special Publication No. 233. The Geological Society of London.

Battistutta, E., van Hemert, P., Lutynski, M., Bruining, H., and Wolf, K. H., (2010). Swelling and sorption experiments on methane, nitrogen and carbon dioxide on dry Selar Cornish coal. International Journal of Coal Geology, 84(1), 39–48. doi:10.1016/j.coal.2010.08.002.

Benson, S., Cook, PJ, (2005). Carbon Dioxide Capture and Storage, eds B Metz et al. (Cambridge University Press, Cambridge, UK).

Bergman, PD., Winter, EM, (1995). Disposal of carbon dioxide in aquifers in the US. Energy Convers Manage; 36:523–6.

Bergman, PD., Winter, EM, Chen, ZY, (1997). Disposal of power plant CO_2 in depleted oil and gas reservoirs in Texas. Energy Convers Manage; 38: S211–6.

Berrada, A., (1992). Thermodynamic study of adsorption of polar molecules in petroleum reservoir rocks; the origin of wettability. Doctoral dissertation of Universite de Montpellier II, France.

Bolourinejad, P., Shoeibi Omrani, P., and Herber, R., (2014). Effect of reactive surface area of minerals on mineralization and carbon dioxide trapping in a depleted gas reservoir. International Journal of Greenhouse Gas Control, 21, 11–22. doi:10.1016/j.ijggc.2013.11.020.

Busch, A., Alles, S., Gensterblum, Y., Prinz, D., Dewhurst, D. N., Raven, M. D., Krooss, B. M., (2008). Carbon dioxide storage potential of shales. International Journal of Greenhouse Gas Control, 2(3), 297–308. doi:10.1016/j.ijggc.2008.03.003.

Busch, A., Gensterblum, Y. and B.M., K., (2003). Methane and CO_2 sorption and desorption measurements on dry Argonne Premium Coals: Pure components and mixtures. International Journal of Coal Geology, 55: 205-224.

Busch, A., Gensterblum, Y., Krooss, B.M. and Siemons, N., (2006). Investigation of high-pressure selective adsorption/desorption behaviour of CO_2 and CH_4 on coals: An experimental study. International Journal of Coal Geology, 66(1-2): 53-68.

Blok, K., Williams, RH, Katofsky, RE., Hendriks, CA, (1997). Hydrogen production from natural gas sequestration of recovered CO_2 in depleted gas wells and enhanced natural gas recovery. Energy Convers Manage; 22:161–8.

Bissada, K.K., John, W.D., (1969). Montmorillonite-organic complexes, gas chromatographic determination of energies of interactions. Clays and Clay Minerals 17, 197–204.

Bolourinejad, P., Shoeibi Omrani, P., and Herber, R., (2014). Effect of reactive surface area of minerals on mineralization and carbon dioxide trapping in a depleted gas reservoir. International Journal of Greenhouse Gas Control, 21, 11–22.doi: 10.1016/j.ijggc.2013.11.020.

Brunauer, S., Deming, LS, Deming, WS, Teller, E., (1940). On a theory of van der Waals adsorption of gases. J Am Chem Soc 1940; 62:1723–32.

Brunauer, S., Emmett, P. H., Teller, E., (1938). Adsorption of gases in multimolecular layers. J. Am. Chem. Soc. 1938, 60 (2), 309−319.

Bolourinejad, P., (2015). Effects of impurities on subsurface CO_2 storage in gas fields in the northeast Netherlands [Groningen]: University of Groningen.

Blok, K., Williams, R., Katofsky, R., Hendriks, C.A., (1997). Hydrogen production from natural gas, sequestration of recovered CO2 in depleted gas wells and enhanced natural gas recovery. Energy 22, 161–168.

Billemont, P., Coasne, B., and De Weireld, G., (2013). Adsorption of carbon dioxide, methane, and their mixtures in porous carbons: effect of surface chemistry, water adsorption, and pore disorder. Langmuir, 29(10), 3328–3338. doi:10.1021/la3048938.

Chadwick, RA., Williams, GA., Williams, JDO, Noy DJ. (2012). Measuring pressure performance of a large saline aquifer during industrial scale CO_2 injection: The Utsira Sand, Norwegian North Sea. International Journal of Greenhouse Gas Control 2012; 10:374-88.

Chalmers, G. R., Bustin, M. R. (2010). The Effects and Distribution of Moisture in Gas Shale Reservoir Systems. Poster Presented at AAPG Annual Convention and Exhibition, New Orleans, Louisiana, April 11-14, 2010, 1.

Chalmers, G.R.L., Bustin, R.M., (2007). The organic matter distribution and methane capacity of the Lower Cretaceous strata of North-eastern British Columbia, Canada. International Journal of Coal Geology 70 (3), 223–239.

Chalmers, G.R.L., Bustin, R.M., (2008). Lower Cretaceous gas shales in north eastern British Columbia, part 1: geological controls on methane sorption capacity. Bulletin of Canadian Petroleum Geology 56 (1), 1–21.

Chalmers, G.R.L., Bustin, R.M., (2008). Lower Cretaceous gas shales in north eastern British Columbia, Part II: evaluation of regional potential gas resources. Bull. Can. Petrol. Geol. 56 (1), 22–61.

Chang, Y.-B., Coats, B. K., and Nolen, J. S., (1998). A Compositional Model for CO_2 Floods Including CO_2 Solubility in Water. SPE Journal. doi:10.2118/35164-PA.

Chareonsuppanimit, P., Mohammad, S. A., Robinson, R. L., & Gasem, K. A. M., (2012). High-pressure adsorption of gases on shales: Measurements and modelling. International Journal of Coal Geology, 95, 34–46. doi: 10.1016/j.coal.2012.02.005

Chester, F.M., Chester, J.S., Kronenberg, A.K., Hajash, A., (2007). Subcritical creep compaction of quartz sand at diagenetic conditions: effects of water and grain size. Journal of Geophysical Research 112, B06203.

Cheng, A. L., and Huang, W. L., (2004). Selective adsorption of hydrocarbon gases on clays and organic matter. Organic Geochemistry, 35(4), 413–423. doi:10.1016/j.orggeochem. 2004.01.007.

Choudhary, V.R., Mayadevi, S., (1996). Adsorption of methane, ethane, ethylene, and carbon dioxide on silicalite-I. Zeolites 17, 501–507.

Croizé, D., Bjørlykke, K., Jahren, J., Renard, F., (2010). Experimental mechanical and chemical compaction of carbonate sand. Journal of Geophysical Research 115, B11204.

Crosdale, P.J., (1998). Experimental evidence supporting pore filling models for gas storage by coal. Abstracts—Geological Society of Australia 49, 102.

Crosdale, P.J., (1999). Mixed Methane/carbon Dioxide sorption by coal: New evidence in support of pore-filling models. Int. CBM Symposium, Univ. of Alabama, Tuscaloosa: 359-366.

Crosdale, P.J., Beamish, B.B., Valix, M., (1998). Coalbed methane sorption related to coal composition. International Journal of Coal Geology 35, 147–158.

Crosdale, P. J., Moore, T. A., and Mares, T. E., (2008). Influence of moisture content and temperature on methane adsorption isotherm analysis for coals from a low-rank, biogenically-sourced gas reservoir. International Journal of Coal Geology, 76(1-2), 166–174. doi:10.1016/j.coal.2008.04.004.

Cui, X., Bustin, A., Bustin, R.M., (2009). Measurements of gas permeability and diffusivity of tight reservoir rocks: different approaches and their applications. Geofluids 9 (3), 208–223.

Curtis, M. E., Ambrose, R. J., and Sondergeld, C. H., (2010). Structural Characterization of Gas Shales on the Micro- and Nano-Scales. Canadian Unconventional Resources and International Petroleum Conference, (October), 137693. doi:10.2118/137693-MS.

Curtis, J.B., (2002). Fractured shale-gas systems. AAPG Bull. 86 (11), 1921–1938. Gregg, S., Sing, K., 1967. Adsorption, Surface Area, and Porosity. Academic Press, Inc., Ltd., London.

Czernichowski-Lauriol, I., Sanjuan, B., Rochelle, C., Bateman, K., Pearce, JM., Blackwell, P., (1996). Inorganic geochemistry. In: Holloway S, editor. Final report of the Joule II project No. CT92-0031: the underground disposal of carbon dioxide. Keyworth, Nottingham, UK: British Geological Survey; 1996. p. 183–276.

Daarnhouwer, M., (2013). Assessing the potential of depleted gas reservoirs for Geothermal Energy. Delft University of Technology, The Netherland.

Dai, Z., R. Middleton, H., Viswanathan, J., Fessenden-Rahn, J., Bauman, R., Pawar, S. Lee., and B. McPherson, (2014), An integrated framework for optimizing CO_2 sequestration and enhanced oil recovery, Environ. Sci. Technol. Lett., 1, 49-54.

Dandekar, A. Y., (2006). Petroleum reservoir rock and fluid properties (1st Ed.). Boca Raton, FL: CRC/Taylor & Francis.

Davidson, C. L., Dahowski, R. T., Dooley, J. J., and McGrail, B. P., (2014). Modelling the deployment of CO2 storage in U.S. Gas-bearing shales. Energy Procedia, 63, 7272–7279. doi: 10.1016/j.egypro.2014.11.763.

Day, S., Sakurovs, R., Weir, S., (2008). Supercritical gas sorption on moist coals. Int. J. Coal Geol. 74, 203–214.

Dewers, T.A., Hajash, A., (1995). Rate laws for water-assisted compaction and stress-induced water–rock interaction in sandstones. Journal of Geophysical Research100, 13093–13112.

Doctor, RH, Molburg, JC, Thimmapuram, P., (2001) .Transporting carbon dioxide recovered from fossil-energy cycles. In: Williams D, Durie B, McMullan P, Paulson C, Smith A (Eds)Proceedings of the 5th International Conference on Greenhouse Gas Control Technologies. CSIRO, Collingwood, Australia, pp 567–571.

Do, Duong D., (1998). Adsorption Analysis: Equilibria and Kinetics. Vol. 2, Series on Chemical Engineering. London: Imperial College Press.

Donahue, R.B., Barbour, S.L., Headley, J.V., (1999). Diffusion and adsorption of benzene in Regina Clay. Canadian Geotechnical Journal 36, 430–442.

Draper, N.R, and Smith, H., (1981). "Applied Regression Analysis". 2nd ed., Wiley: New York, 1981.

Dreisbach, F., Staudt, R. and Keller, J.U., (1999). High pressure adsorption data of methane, nitrogen, carbon dioxide and their binary and ternary mixtures on activated carbon. Adsorption, 5: 215-227.

Du, X., Wu, E., (2006). Physiosorption of hydrogen in A, X and ZSM-5 types Zeolites at moderately high pressures. Chin J Chem. Phy. 2006; 19:457–62.

Ehlig-Economides, C., and Economides, M. J., (2010). Sequestering carbon dioxide in a closed underground volume. Journal of Petroleum Science and Engineering, 70(1-2), 123–130. doi:10.1016/j. petrol.2009.11.002.

EI-Khaiary, M.I., and Malash, G.F., (2010). Common data analysis errors in batch adsorption studies", Hydrometallurgy, vol. 105, pp. 314-320, 2010.

EI-Khaiary, M.I., Malash, G.F., and Ho, Y., (2007). On the use of linearized pseudo-second-order kinetic equations for modelling adsorption systems, Desalination, vol. 257, pp. 93-101, 2007.

Eshkalak, M. O., Al-Shalabi, E. W., Sanaei, A., Aybar, U., and Sepehrnoori, K., (2014). Simulation study on the CO_2-driven enhanced gas recovery with sequestration versus the re-fracturing treatment of horizontal wells in the U.S. unconventional shale reservoirs. Journal of Natural Gas Science and Engineering, 21(November), 1015–1024. doi: 10.1016/j.jngse.2014.10.013.

Eshkalak, M. O., Aybar, U., and Eshkalak, M. O., (2015). Carbon Dioxide Storage and Sequestration in Unconventional Shale Reservoirs. Journal of Geoscience and Environment Protection, 03(01), 7–15. doi:10.4236/gep.2015.31002.

EIA, (2006). U.S. Underground Natural Gas Storage Developments: 1998:2005. Energy Information Administration, Office of Oil and Gas, October 2006, 16pp.

Fang, Z., and Khaksar, A., (2013). Role of geomechanics in assessing the feasibility of CO_2 sequestration in depleted hydrocarbon sandstone reservoirs. Rock Mechanics and Rock Engineering, 46(3), 479–497. doi:10.1007/s00603-013-0381-z.

Feast, G., Wu, K., Walton, J., Cheng, Z., and Chen, B., (2015). Modelling and Simulation of Natural Gas Production from Unconventional Shale Reservoirs. International Journal of Clean Coal and Energy, 4(4), 23–32. doi:10.4236/ijcce.2015.42003.

Ferronato, M., Gambolati, G., Janna, C., and Teatini, P., (2010). Geomechanical issues of anthropogenic CO_2 sequestration in exploited gas fields. Energy Conversion and Management, 51(10), 1918–1928. doi:10.1016/j.enconman.2010.02.024.

Fischer, C., Schmidt, C., Bauer, A., Gaupp, R. and Heide, K., (2009). Mineralogical and geochemical alteration of low-grade metamorphic black slates due to oxidative weathering. Chemie der Erde-Geochemistry, 69(2): 127-142.

Fischer, S., Liebscher, A., Wandrey, M., The CO_2 SINK Group. (2010). CO_2–brine–rock interaction — first results of long-term exposure experiments at in situ P–T conditions of the Ketzin CO_2 reservoir. Chemie der Erde 70, 155–164.

Fitzgeralda, J.E., Pana, Z., Sudibandriyoa, M., Robinson, R.L., Jr. A., Gasema, K.A.M., Reevesb, S., (2005). Adsorption of methane, nitrogen, carbon dioxide and their mixtures on wet Tiffany coal. Fuel, 84(18): 2351-2363.

Fletta, M., Brantjesa, J., Randal, G., Jason, M., Terrell, T., and Mark, T., (2009). Subsurface development of CO_2 disposal for the Gorgon Project. Energy Procedia 1:3031–3038.

Foo, K.Y., Hameed B.H., (2010). Insights into the modelling of adsorption isotherm systems. Chemical Engineering Journal 156, 2-10.

Forrester, S. D., and Giles, C. H., (1972). For a historical account of the earliest quantitative studies of adsorption and of isotherm determinations: Chem. Ind. (London) 831, 1314 (1971); 318(1972).

Freundlich. H.M.F., (1906). Over the adsorption in solution, Zeitschrift fur Physikalische Chemie 57A (1906) 385.

Gale, J. F. W., and Holder, J., (2008). Natural fractures in the Barnett Shale: constraints on spatial organization and tensile strength with implications for hydraulic fracture treatment in shale-gas reservoirs. The 42nd U.S. Rock Mechanics Symposium (USRMS). doi:ARMA 08-96.

Gasparik, M., Bertier, P., Gensterblum, Y., Ghanizadeh, A., Krooss, B. M., & Littke, R. (2014). Geological controls on the methane storage capacity in organic-rich shales. International Journal of Coal Geology, 123, 34–51. doi: 10.1016/j.coal.2013.06.010.

Gasparik, M., Ghanizadeh, A., Bertier, P., Gensterblum, Y., Bouw, S., & Krooss, B. M. (2012). High-pressure methane sorption isotherms of black shales from the Netherlands. Energy and Fuels, 26(8), 4995–5004. doi:10.1021/ef300405g.

Gasparik, M., Bertier, P., Gensterblum, Y., Ghanizadeh, A., Krooss, B.M., Littke, R., (2013). Geological controls on the methane storage capacity in organic-rich shales, Int. J. Coal Geol., http://dx.doi.org/10.1016/j.coal.2013.06.010.

Gasparik, M., Ghanizadeh, A., Gensterblum, Y., Krooss, B.M., (2013). Multi-temperature method for high-pressure sorption measurements on moist shales. Rev. Sci. Instrum. 84, 85–116.

Gasparik, M., Rexer, T. F. T., Aplin, A. C., Billemont, P., De Weireld, G., Gensterblum, Y., Zhang, T., (2014). First international inter-laboratory comparison of high-pressure CH_4, CO_2 and C_2H_6 sorption isotherms on carbonaceous shales. International Journal of Coal Geology, 132, 131–146. doi: 10.1016/j.coal.2014.07.010.

Gaus, I., Azaroual, M., Czernichowski-Lauriol, I., (2005). Reactive transport modelling of the impact of CO_2 injection on the clayey cap rock at Sleipner (North Sea). Chemical Geology 217, 319–337.

Gaus, I., (2010). Role and impact of CO_2–rock interactions during CO_2 storage in sedimentary rocks. International Journal of Greenhouse Gas Control 4, 73–89.

Gensterblum, Y., van Hemert, P., Billemont, P., Battistutta, E., Busch, A., Krooss, B. M., De Weireld, G., Wolf, K.-H.A.A., (2010). European inter-laboratory comparison of high pressure CO_2 sorption isotherms. II: natural coals. Int. J. Coal Geol. 2010, 84, 115–124.

Gensterblum, Y., (2013). CBM and CO_2 -ECBM related sorption processes in coal (Ph.D. Thesis). RWTH Aachen University, Germany.

Gensterblum, Y., Merkel, A., Busch, A., and Krooss, B. M., (2013). High-pressure CH_4 and CO_2 sorption isotherms as a function of coal maturity and the influence of moisture. International Journal of Coal Geology, 118, 45–57. doi:10.1016/j.coal.2013.07.024.

Gibbs, J.W., (1928). The Collected Works of J. W. Gibbs, Vol 1 (Longmans, Green and Co, New York) p 55-354.

Glorioso, J. C., and Rattia, A., (2012). Unconventional Reservoirs: Basic Petrophysical Concepts for Shale Gas. SPE 153004, (March), 1–38. doi:10.2118/153004-MS.

G, Mckay., and J.F. Porter., (1997). A Comparison of Langmuir based models for predicting multicomponent metal ion equilibrium sorption isotherms on peat, Trans. IChem. E., vol. 75B, pp. 171-180, 1997.

Goater, A.L., Bijeljic, B., Blunt, M.J., (2013). Dipping open aquifers – the effect of top surface topography and heterogeneity on CO_2 storage efficiency. Int. J. Greenh. Gas Contr. 17, 318–331.

Godec, M., Koperna, G., Petrusak, R., Oudinot, A., (2013). Assessment of Factors Influencing CO_2 Storage Capacity and Injectivity in Eastern U.S. Gas Shales. Energy Procedia vol.37, Pg.6644-6655.

Godec, M., Koperna, G., Petrusak, R., and Oudinot, A., (2014). Enhanced gas recovery and CO_2 storage in gas shales: A summary review of its status and potential. Energy Procedia, 63, 5849–5857. doi:10.1016/j.egypro.2014.11.618.

Goodman, A. L., Busch, A., Duffy, G. J., Fitzgerald, J. E., Gasem, K. A. M., Gensterblum, Y., White, C. M., (2004). An inter-laboratory comparison of CO2 isotherms measured on argonne premium coal samples. Energy and Fuels, 18(4), 1175–1182. doi:10.1021/ef034104h.

Goss, K.U., (1994). Adsorption of organic vapours on polar mineral surfaces and on a bulk water surface; development of an empirical predictive model. Environmental Science & Technology 28, 640–645.

Gregg, S. J., and Sing, K. S. W., (1967). Adsorption, surface area and porosity, 1st Edition, Academic Press, London, 371 p.

Grigg, RB, (2005). Carbon Dioxide Capture for Storage in Deep Geologic Formations, eds. SM Benson, C Oldenburg, M Hoverstein, and S Imbus (Elsevier, Amsterdam).

Gubik, A., Baffoe, J., and Schulze-Riegert, R., (2013). Determination of turnover and cushion gas volume of a prospected gas storage reservoir under uncertainty. Oil Gas European Magazine, 39(2), 72–78.

Gumma, S., and Talu, O., (2003). Gibbs dividing surface and helium adsorption. Adsorption, 9(1), 17–28. doi:10.1023/A:1023859112985.

Gunter, WD., Bachu, S., Law, DHS, Marwaha, V., Drysdale, DL, McDonald, DE, (1996). Technical and economic feasibility of CO_2 disposal in aquifers within the Alberta sedimentary basin, Canada. Energy Convers Manage 1996; 37:1135–46.

Gunter, W.D., Perkins, E.H., McCann, T.J., (1993). Aquifer disposal of CO_2-rich greenhouse gases: reaction design for added capacity. Energy Conversion and Management 34, 941–948.

Gunter, W.D., Perkins, E.H., Hutcheon, I., (2000). Aquifer disposal of acid gases: modelling of water–rock reactions for trapping of acid wastes. Appl. Geochem. 15, 1085–1095.

Gunter, W.D., Wiwchar, B., Perkins, E.H., (1997). Aquifer disposal of CO_2-rich greenhouse gases: extension of the time scale of experiment for CO_2-sequestering reactions by geochemical modelling. Mineralogy and Petrology 59, 121–140.

Guo, H., Jia, W., Peng, P., Lei, Y., Luo, X., Cheng, M., Jiang, C., (2014). The composition and its impact on the methane sorption of lacustrine shales from the Upper Triassic Yanchang Formation, Ordos Basin, China. Marine and Petroleum Geology, 57, 509–520. doi:10.1016/j.marpetgeo.2014.05.010.

Guo, W., Xiong, W., Gao, S., Hu, Z., Liu, H., and Yu, R., (2014). Impact of temperature on the isothermal adsorption/desorption of shale gas. Petroleum Exploration and Development, 40(4), 514–519. doi:10.1016/S18763804(13)60066- X.

Han, W. S., Kim, K. Y., Park, E., Mcpherson, B. J., Lee, S.Y., and Park, M.H., (2012). Modelling of spatiotemporal thermal response to CO_2 injection in saline formations: interpretation for monitoring. Transp. Porous Med. 93, 381–399.

Hangx, S., van der Linden, A., Marcelis, F., and Bauer, A., (2013). The effect of CO_2 on the mechanical properties of the Captain Sandstone: Geological storage of CO_2 at the Goldeneye field (UK). International Journal of Greenhouse Gas Control, 19, 609–619. doi:10.1016/j.ijggc.2012.12.016.

Hawkes, C.D., Mcleallan, P.J., and Bachu, S., (2004). Geomechanical Factors Affecting Geological Storage of CO_2 in Depleted Oil and Gas Reservoirs. Presented at the Petroleum Society's 5th Canadian International Petroleum Conference (55th Annual Technical Meeting), Calgary, Alberta, Canada, June 8 – 10, 2004, Paper 2004.

Hawkes, C., Mclellan, P., and Bachu, S. (2005). Geomechanical Factors Affecting Geological Storage of CO_2 in Depleted Oil and Gas Reservoirs. Journal of Canadian Petroleum Technology, 44(10), 52–61. doi:10.2118/05-10-05.

Herrera, L., Do, D. D., Nicholson, D. A, (2010). Monte Carlo integration method to determine accessible volume, accessible surface area and its fractal dimension. J. Colloid Interf. Sci. 2010, 348(2), 529–36.

Herrera, L., Fan, C., Do, D. D., Nicholson, D., (2011). A revisit to the Gibbs dividing surfaces and helium adsorption. Adsorption 2011, 17(6), 955–965.

Heller, R., and Zoback, M., (2011). Adsorption, Swelling and Viscous Creep of Synthetic Clay Samples. ARMA Meeting 2011. Retrieved from http://www.onepetro. Org / mslib /servlet /onepetropreview? id =ARMA-11-469.

Heller, R., and Zoback, M., (2014). Adsorption of methane and carbon dioxide on gas shale and pure mineral samples. Journal of Unconventional Oil and Gas Resources, 8(C), 14–24. doi: 10.1016/j.juogr.2014.06.001.

Hellevang, H., Pham, V.T.H., Aagaard, P., (2013). Kinetic modelling of CO_2–water–rock interactions. Int. J. Greenh. Gas Contr. 15, 3–15.

Hendriks, CA, Blok, K., (1993). Underground storage of carbon dioxide. Energy Convers Manage; 34:949–57.

Hesse, M.A., Orr, F.M., Tchelepi, H.A., (2008). Gravity currents with residual trapping. Journal of Fluid Mechanics 611, 35–60, http://dx.doi.org/ 10.1017/S002211200800219X.

Hester, R.E., and Harrison, R.M., ed (2010). Carbon Capture Sequestration and Storage, Issues in Environmental Science and Technology Vol. 29, RSC Publishing.

Hettema, MHH, Schutjens, PMTM, Verboom, BJM, Gussinklo, H.J., (2000). Production-induced compaction of a sandstone reservoir: the strong influence of stress path. SPE Reservoir Evaluation & Engineering 2000; 3(4):342-7.

Hildenbrand, A., Krooss, B.M., Busch, A., Gaschnitz, R., (2006). Evolution of methane sorption capacity of coal seams as a function of burial history—a case study from the Campine Basin, NE Belgium, Int. J. Coal Geol. 66 (2006) 179–203.

Hitchon, B., Gunter, WD., Gentzis, T., Bailey, RT., (1999). Sedimentary basins and greenhouse gases: a serendipitous association. Energy Convers Manage1999; 40:825–43.

Ho, Y., and Wang, C.C., (2004). Pseudo-isotherms for the sorption of cadmium ion onto tree fern, Process Biochem., vol. 39, pp. 759-763, 2004.

Ho, Y.S., (2004). Selection of optimum sorption isotherm, Carbon, vol. 42, pp. 2113-2130, 2004.

Ho, Y.S., (2006). Isotherms for the sorption of lead onto peat: comparison of linear and non-linear methods, Polish J. Environ. Stud. 15 (1) (2006) 81–86.

Ho, Y.S., Chiu, W.T., Wang, C.C., (2005). Regression analysis for the sorption isotherms of basic dyes on sugarcane dust, Bio resource. Technol. 96. 1285–1291.

Ho, Y.S., Huang, C.T., and Huang, H.W., (2002). Equilibrium sorption isotherm for metal ions on tree fern, Process Biochem., vol. 37, pp. 1421-1430, 2002.

Ho, Y.S., Porter, J.F., and McKay, G., (2002). Equilibrium Isotherm Studies for the Sorption of Divalent Metal Ions onto Peat: Copper, Nickel and Lead Single Component Systems. Water, Air, and Soil Pollution, 141(1-4), 1-33.

Holloway, S., (1997). An overview of the underground disposal of carbon dioxide. Energy Convers. Manag. 38, 193 – 198.

Holloway, S., (2005). Underground sequestration of carbon dioxide - A viable greenhouse gas mitigation option. Energy, 30(11-12 SPEC. ISS.), 2318–2333. doi:10.1016/j.energy.2003.10.023.

Holloway, S., (2008). Sequestration: the underground storage of carbon dioxide. Climate Change and Energy Pathways for the Mediterranean, 61–88.

Holloway, S., Savage, D., (1993). The potential for aquifer disposal of carbon dioxide in the UK. Energy Convers Manage 1993; 34:941–8.

Hossain, M.A., Ngo, H.H., Guo, W.S., and Setiadi, T., (2012). Adsorption and desorption of copper (II) ions onto garden grass. Bio resource Technology, 121, 386-395.

Hovorka, S. D., Choi, J. W., Meckel, T. A., Trevino, R. H., Zeng, H., Kordi, M., Nicot, J. P., (2009). Comparing carbon sequestration in an oil reservoir to sequestration in a brine formation-field study. Energy Procedia, 1(1), 2051–2056.doi: 10. 1016/ j. egypro. 2009. 01.267.

Hovorka, SD., (2006) Measuring permanence of CO_2 storage in saline formations: The Frio experiment. Environ Geosci 13:105–121.

Ide, T.S., Jessen, K., Orr Jr., F.M., (2007). Storage of CO_2 in saline aquifers: effects of gravity, viscous, and capillary forces on amount and timing of trapping. International Journal of Greenhouse Gas Control 1, 481–491.

IEA Greenhouse Gas R&D Programme., (2000). Barriers to Overcome in Implementation of CO2 Capture and Storage (1) Storage in Disused Oil and Gas Fields. Report Number PH3/22.

IEA GHG, (2009). "CO_2 Storage in Depleted Oil Fields", IEA-GHG technical study report no. 2009/12. Available at: www.ieaghg.org.

Iglauer, S., Pentland, C.H., and Busch, A., (2015), CO_2 wettability of seal and reservoir rocks and the implications for carbon geo-sequestration, Water Resour. Res., 51, 729–774, doi:10.1002/ 2014WR015553.

Iijima, M., Nagayasu, T., Kamijyo, T., Nakatani, S., (2011). MHI's Energy Efficient Flue Gas CO_2 Capture Technology and Large Scale CCS Demonstration Test at Coal-fired Power Plants in USA. Mitsubishi Heavy Ind. Tech. Rev. 48, 26.

IPCC, (2005). International Panel on Climate Change (IPCC), Special report on carbon dioxide capture and storage. In: Metz, B., Davidson, O., De Connick, H.C., Loos, M., Meyer, L.A. (Eds.), Prepared by Working Group III of the Intergovernmental Panel on Climate Change. Cambridge University Press, Cambridge, UK/New York, NY, USA, 442 pp.

ISO, (1995). International Organization for Standardization. Guide to the expression of uncertainty in measurement, Printing, 1995, CH – 1211 Geneva.
Jarrell, P.M., Fox, C.E., Stein, M.H., and Webb, S.L., (2002). Practical Aspects of CO_2 Flooding, SPE Monograph Volume 22, Society of Petroleum Engineers, 2002.

Jenkins, C. R., Cook, P. J., Ennis-King, J., Undershultz, J., Boreham, C., Dance, T., Urosevic, M., (2012). Safe storage and effective monitoring of CO_2 in depleted gas fields. Proceedings of the National Academy of Sciences, 109(2), E35–E41. doi:10.1073/pnas.1107255108.

Jiang, J., Shao, Y., Younis, R., (2014). Development of a multi-continuum multicomponent model for enhanced gas recovery and CO_2 storage in fractured shale gas reservoirs. In: Paper SPE 169114 Presented at SPE Improved Recovery Symposium Held in Tulsa, Oklahoma, USA, 12-16 April.

Ji, L., Zhang, T., Milliken, K. L., Qu, J., and Zhang, X., (2012). Experimental investigation of main controls to methane adsorption in clay-rich rocks. Applied Geochemistry, 27(12), 2533–2545. doi:10.1016/j.apgeochem.2012.08.027.

Jin, Z., and Firoozabadi, A., (2014). Effect of water on methane and carbon dioxide sorption in clay minerals by Monte Carlo simulations. Fluid Phase Equilibria, 382, 10–20. doi:10.1016/j.fluid.2014.07.035.

Jordan, P., and Doughty, C., (2009). Sensitivity of CO_2 migration estimation on reservoir temperature and pressure uncertainty. Energy Procedia, 1(1), 2587–2594. doi: 10.1016/j.egypro.2009.02.024.

Joubert, J.I., Grein, C.T., Bienstock, D., (1973). Sorption of methane in moist coal. Fuel 52, 181-185.

Joubert, J.I., Grein, C.T., Bienstock, D., (1974). Effect of moisture on the methane capacity of American coals. Fuel 53, 186–191.

Juanes, R., Spiteri, EJ, Orr, Jr. FM., Blunt, MJ, (2006). Impact of relative permeability hysteresis on geological CO_2 storage. Water Resource Res 2006; 42(W12418). doi:10.1029/2005WR004806.

Jung, J.W., Wan, J., (2012). Supercritical CO2 and ionic strength effects on wettability of silica surfaces: equilibrium contact angle measurements. Energy Fuels 26, 6053–6059.

Kalantari-Dahaghi, A., (2010). Numerical simulation and modelling of enhanced gas recovery ad CO_2 sequestration in shale gas reservoirs: a feasibility study. In: Paper SPE 139701 Presented at the SPE International Conference on CO_2 Capture, Storage, and Utilization Held in New Orleans, Louisiana, USA, 10-12 November.

Kalantari-Dahaghi, A., Mohaghegh, S., and He, Q., (2013). CO_2-Driven Enhanced Gas Recovery and Storage in Depleted Shale Reservoir- A Numerical Simulation Study. Carbon Management Technology Conference Proceedings.

Kaldi, JG., Gibson-Poole, C M., (2008) Storage Capacity Estimation, Site Selection and Characterization for Carbon Dioxide Storage Projects. CO_2-CRC, Canberra, Australia. Report No: RPT08-1001.

Kang, S.M., Fathi, E., Ambrose, R.J., Akkutlu, I.Y., Sigal, R.F., (2010). Carbon dioxide storage capacity of organic-rich shales. SPE 134583.Presented at the Annual Technical Conference and Exhibition, Florence, Italy. 16(04), pp. 842–855. doi: 10.2118/134583-pa.

Karadag, D., Koc, Y., Turan, M., Ozturk, M., (2007). A comparative study of linear and nonlinear regression analysis for ammonium exchange by clinoptilolite zeolite, J. Hazard. Mater. 144 (2007) 432–437.

Kharaka, Y.K., Cole, D.R., Thordsen, J.J., Kakouros, E., Nance, H.S., (2006). Gas-water-rock interactions in sedimentary basins: CO_2 sequestration in the Frio formation, Texas, USA. J. Geochem. Explor. 89, 183–186.

Kharroubi, K., Layan, B., and Cordelier, P., (2004). Influence of Pore Pressure Decline on the on the permeability of North Sea sandstones. International Symposium of the Society of Core Analysts, c, 1–6.

Khosrokhavar, R., Griffiths, S., and Wolf, K. H., (2014). Shale Gas Formations and Their Potential for Carbon Storage: Opportunities and Outlook. Environmental Processes, 1(4), 595–611. doi:10.1007/s40710-014-0036-4.

Khosrokhavar, R., Wolf, K. H., and Bruining, H., (2014). Sorption of CH_4 and CO_2 on a carboniferous shale from Belgium using a manometric setup. International Journal of Coal Geology, 128-129, 153–161. doi: 10.1016/j.coal.2014.04.014.

Kikuta, K., Hongo, S., Tanase, D., Ohsumi, T., (2005). Field test of CO_2 injection in Nagaoka, Japan. Proceedings of the Seventh International Conference on Greenhouse Gas Control Technologies, eds ES Rubin, DW Keith, and CF Gilboy (Elsevier, Amsterdam), pp 1367–1372.

Klusman RW, (2003). Rate measurements and detection of gas micro seepage to the atmosphere from an enhanced oil recovery/sequestration project, Rangely, CO. App Geochem 18:1839–1852.

Knauss, K.G., Johnson, J.W., Steefel, C.I., (2005). Evaluation of the impact of CO_2, Co-contaminant gas, aqueous fluid, and reservoir rock interactions on the geologic sequestration of CO_2. Chemical Geology 217, 339–350.

Knox, P. R., Hovorka, S. D., and Oldenburg, C. M., (2002), Potential new uses for old gas fields: sequestration of carbon dioxide: Gulf Coast Association of Geological Societies Transactions, v. 52, p. 563–571. GCCC Digital Publication Series #02-02.

Koide, H., Y. Tazaki, Y., Noguchi, M., Iijima, K., Ito, and Y, Shindo., (1993). Underground storage of carbon dioxide in depleted natural gas reservoirs and in useless aquifers: Engineering Geology, v. 34, p. 175.

Koide, H., Tazaki, Y., Noguchi, Y., Nakayama, S., Iijima, M., Ito, K., (1992). Subterranean containment and long-term storage of carbon dioxide in unused aquifers and depleted natural gas reservoirs. Energy Convers Manage 1992; 33:619–26.

Kongsjorden, H., Karstad O, Torp T. (1997). Saline aquifer storage of carbon dioxide in the Sleipner project. Waste Manage 1997; 17:303–8.

Korbol R, Kaddour A. Sleipner V (1995). CO_2 disposal-injection of removed CO_2 into the Utsira formation. Energy Convers Manage 1995; 36:509–12.

Kosuge, K., (1994). Layered polysilicate gas adsorption properties and dispersion of the particles. Journal of the Clay Science Society of Japan 33, 215–222.

Krooss, B.M., Van Bergen, F., Gensterblum, Y., Siemons, N., Pagnier, H.J., David, P., (2002). High-Pressure Methane and Carbon Dioxide Adsorption on Dry and Moisture equilibrated Pennsylvanian Coals. International Journal of Coal Geology, 51 (2), 69–92.

Kühn, M., Nakaten, N., Streibel, M., and Kempka, T., (2014). CO_2 geological storage and utilization for a carbon neutral “power-to-gas-to-power” cycle to even out fluctuations of renewable energy provision. Energy Procedia, 63, 8044–8049. doi: 10.1016/j.egypro.2014.11.841.

Kurniawan, Y., Bhatia, S.K., Rudolph, V., (2006). Simulation of binary mixture adsorption of methane and CO2 at supercritical conditions in carbons. AIChE J. 52 (3), 957-967.

Kuila, U., (2011). Surface Area and Pore-size Distribution in Clays and Shales. Presented at the SPE Annual Technical Conference and Exhibition Held in Denver, Colorado, USA, 30 October–2 November 2011, (November), SPE 146869, 146869. doi:10.2118/146869-ms.

Kunz. O., Wagner, W., and Jaeschke, M., (2007). The GERG-2004 Wide-Range Reference Equation of State for Natural Gases, GERG Technical Monograph 15. Dusselkorf, Germany: VDL-Verlag.

Kumar. K.V., (2006). Comparative analysis of linear and non-linear method of estimating the sorption isotherm parameters for malachite green onto activated carbon, J. Hazard. Mater. 136 (21), 197–202.

Kumar. K.V., (2007). Optimum sorption isotherm by linear and non-linear methods for malachite green onto lemon peel, Dyes and Pigments 74, 595–597.

Kumar. K.V, Porkodi. K, (2006). Relation between some two- and three-parameter isotherm models for the sorption of methylene blue onto lemon peel, J. Hazard. Mater. 138; 633–635.

Kumar, K.V, Sivanesan. S., (2006). Pseudo second order kinetics and pseudo isotherms for malachite green onto activated carbon: comparison of linear and nonlinear regression methods, J. Hazard. Mater. B136 (2006) 721–726.

Lackner, KS, Wendt, CH., Butt, DP, Joyce, EL., Sharp DH, (1995). Carbon dioxide disposal in carbonate minerals. Energy 1995; 20:1153–70.

Lagneau, V., Pipart, A., Catalette, H., (2005). Reactive transport modelling of CO_2 sequestration in deep saline aquifers. Oil Gas Sci Technol 2005; 50:231–47.

Langmuir, I., (1916). The Constitution and Fundamental Properties of Solids and Liquids. Part I. Solids: Journal of the American Chemical Society, v. 38, p. 2221-2295.

Law, DSH, Bachu, S., (1996). Hydrogeological and numerical analysis of CO_2 disposal in deep aquifers in the Alberta Sedimentary Basin. Energy Convers Manage 1996; 37:1167–74.

Levy, B.M., Ozdemir, J., Pan, E., Robinson, Z., Schroeder, R.L., Sudibandriyo, K., White, C.M., (2004). An inter-laboratory comparison of CO_2 isotherms measured on 500 argonne premium coal samples. Energy Fuels 2004, 18, 1175–1182.

Levy, J.H., Day, S.J., Killingley, J.S., (1997). Methane capacities of Bowen Basin coals related to coal properties. Fuel 76, 813–819.

Li, T., and Wu, C., (2015). Research on the abnormal isothermal adsorption of shale. Energy and Fuels, 29(2), 634–640. doi:10.1021/ef5024274.

Li, X. L. F., Watson, A. T., and Texas, A., (1995). Adsorption Studies of Natural Gas Storage in Devonian Shales. SPE Formation Evaluation, (June).

Li, Y., Pu, H., and In-Petro Technology Inc., (2015). Modelling Study on CO_2 Capture and Storage in Organic-Rich Shale. Presented at the Carbon Management Technology Conference Held in Sugarland, Texas, USA, 17–19 November 2015. This, CMTC-43956(November), 17–19.

Li, Y., and Pu, H., (2015). Modelling Study on CO_2 Capture and Storage in Organic-Rich Shale, CMTC-439561-MS, (pp. 17–19).

Li, Z., Dong, M., Li, S., and Huang, S., (2006). CO_2 sequestration in depleted oil and gas reservoirs-caprock characterization and storage capacity. Energy Conversion and Management, 47(11-12), 1372–1382. doi:10.1016/j.enconman.2005.08.023.

Liner, C. L., (2010). Carbon capture and sequestration: overview and offshore aspects" in Proceedings of the Offshore Technology Conference (OTC '10), pp. 3511–3514, May 2010.

Lindberg, E., (1999). Escape of CO_2 from aquifers. Energy Convers Manage 1997;38: S235–40. Rudnicki JI, Wawersik WR. Report looks at sequestering CO_2 beneath earth surface. EOS Trans AGU 1999; 80:607–8.

Liu, D., Yuan, P., Liu, H., Li, T., Tan, D., Yuan, W., and He, H., (2013). High-pressure adsorption of methane on montmorillonite, kaolinite and illite. Applied Clay Science, 85(1), 25–30. doi: 10.1016/j.clay.2013.09.009.

Liu, F., Ellett, K., Xiao, Y., Rupp, J.A., (2013). Assessing the feasibility of CO_2 storage in the New Albany Shale (Devonian-Mississippian) with potential enhanced gas recovery using reservoir simulation. Int. J. Greenh. Gas Control 17, 111–126.

Liu, Y., Wilcox, J., (2012). Effects of surface heterogeneity on the adsorption of CO_2 in microporous carbons. Environmental Science and Technology 46 (3), 1940–1947.

Loucks, R. G., Reed, R. M., Ruppel, S. C., and Jarvie, D. M., (2009). Morphology, Genesis, and Distribution of Nanometer-Scale Pores in Siliceous Mudstones of the Mississippian Barnett Shale. Journal of Sedimentary Research, 79(12), 848–861. doi:10.2110/jsr.2009.092.

Loizzo, M., Lecampion, B., Berard, T., Harichandran, A., Jammes, L., (2009). Reusing Oil and Gas depleted reservoirs for CO_2 storage: Pros and cons. SPE Offshore Europe Oil and Gas Conference, Aberdeen (Society of Petroleum Engineers, Richardson, TX), 10.2118/ 124317-MS.

Lu, X., Li, F., and Watson, A. T. (1993). Adsorption Measurement in Devonian Shale. Presented at the SCA Conference, 9302.

Lu, X.C., Li, F.C., Watson, A.T., (1995). Adsorption measurements in Devonian shales. Fuel 74 (4), 599–603.

Lu, J., Kharaka, Y. K., Thordsen, J. J., Horita, J., Karamalidis, A., Griffith, C., Hovorka, S. D., (2012). CO_2-rock-brine interactions in Lower Tuscaloosa Formation at Cranfield CO_2 sequestration site, Mississippi, U.S.A. Chemical Geology, 291, 269–277.doi: 10.1016/j.chemgeo.2011.10.020.

Lu, J., Kordi, M., Hovorka, S. D., Meckel, T. A., and Christopher, C. A., (2013). Reservoir characterization and complications for trapping mechanisms at Cranfield CO2

injection site. International Journal of Greenhouse Gas Control, 18, 361–374. doi:10.1016/j.ijggc.2012.10.007.

Liu. Y, and Wang. Z, (2008). Uncertainty of pseset-order kinetic equations in the description of biosorption data, Bioresource Technol., vol. 99, pp. 3309-3312, 2008.

Luo, S., Xu, R., Jiang, P., (2012). Effect of reactive surface area of minerals on mineralization trapping of CO_2 in saline aquifers. Pet. Sci. 9, 400–407.

MacRoberts, D. T., (1962). Abandonment pressure of gas wells. In SPE Petroleum Economics and Valuation Symposium, SPE-260-MS.

Mair, RW, Cory, DG, Peled, S., Tseng, C.H., Patz, S., Walsworth, L., (1998). Pulsed-field-gradient measurements of time-dependent gas diffusion. J Mag Res; 135:478–86.

Malbrunot, P., Vidal, D., Vermesse, J., Chahine, R., and Bose, T., (1997). Adsorbent Helium Density Measurement and Its Effect on Adsorption Isotherms at High Pressures," Langmuir, 13, 539–544 (1997).

Maldal, T., Tappel, MI., (2004). CO_2 underground storage for Snøhvit gas field development. Energy 29:1403–1411.

Mamora, DD., Seo, J.G., (2002). Enhanced Recovery by Carbon Dioxide Sequestration in Depleted Gas Reservoirs. Society of Petroleum Engineers. SPE-77347, SPE Annual Technical Conference and Exhibition, San Antonio, Texas, USA, 29 September–2 October. 2002. 1–9. doi:10.2118/77347-MS.

Mathias, S. A., Gluyas, J. G., González Martínez De MigueL, G. J., Bryant, S. L. and Wilson, D., (2013). On relative permeability data uncertainty and CO_2 injectivity estimation for brine aquifers. Intl J. Greenh. Gas Control 12, 200–212.

Mathias, S. A., McElwaine, J. N., and Gluyas, J. G., (2014). Heat transport and pressure buildup during carbon dioxide injection into depleted gas reservoirs. Journal of Fluid Mechanics, 756(September), 89–109. doi:10.1017/jfm.2014.348.

Mazumder, S., Van Hemert, P., Busch, A., Wolf, K.H.A.A., and Tejera-Cuesta, P., (2006). Flue gas and pure CO_2 sorption properties of coal: A comparative study. International Journal of Coal Geology, 67(4): 267-279.

Meckel, TA, Hovorka, SD., (2009). Results from continuous downhole monitoring (PDG) at a field-scale CO_2 sequestration demonstration project, Cranfield, MS. SPE International Conference on CO_2 Capture, Storage, and Utilization (Society of Petroleum Engineers, Richardson, TX), 10.2118/127087-MS.

Merey, S., and Sinayuc, C., (2016). Gas-in-place calculations in shale gas reservoirs using experimental adsorption data with adsorption models. Canadian Journal of Chemical Engineering, 94(9), 1683–1692. doi:10.1002/cjce.22538.

Merkel, A., Gensterblum, Y., Krooss, B. M., and Amann, A., (2015). International Journal of Coal Geology Competitive sorption of CH_4, CO_2 and H_2O on natural coals of different rank. International Journal of Coal Geology, 150-151, 181–192. doi: 10.1016/j.coal.2015.09.006.

Metz, B., Davidson, O., De Coninck, H., Loos, M., Meyer, L., (2005). IPCC Special Report on Carbon Dioxide Capture and Storage; Cambridge University Press for the Intergovernmental Panel on Climate Change: Cambridge, U.K., 2005.

Michael, K., Golab, A., Shulakova, V., Ennis-King, J., Allinson, G., Sharma, S., and Aiken, T., (2010). Geological storage of CO_2 in saline aquifers-A review of the experience from existing storage operations. International Journal of Greenhouse Gas Control, 4(4), 659–667. doi:10.1016/j.ijggc.2009.12.011.

Milliken, K.L., Esch, W.L., Reed, R.M., Zhang, T., (2012). Grain assemblages and strong diagenetic overprinting in siliceous mudrocks, Barnett Shale (Mississippian), Fort Worth Basin, Texas. Am. Assoc. Petrol. Geol. Bull. 96, 1553–1578.

Milliken, K. L., Rudnicki, M. D., and Awwiller, D. N., (2012), Form and distribution of organic matter-hosted pores, Marcellus Formation (Devonian), Pennsylvania, USA. Third EAGE Shale Workshop, Shale Physics and Shale Chemistry: New Plays, New Science, New Possibilities, Barcelona, Spain, January 2012.

Moghaddam, N. D., (2013). Sorption of Methane and Ethane on Belgian Black Shale Using a Manometric Setup. Technical University of Delft.

Mohammad, S., Fitzgerald, J., Robinson, R. L., and Gasem, K. A. M., (2009). Experimental uncertainties in volumetric methods for measuring equilibrium adsorption. Energy and Fuels, 23(5), 2810–2820. doi:10.1021/ef8011257.

Morris, JP, Hao, Y., Foxall, W., McNab, W., (2010). A study of injection induced mechanical deformation at the Salah CO storage project. ARMA10-307. 44th U.S. rock mechanics symposium and 5th U.S.–Canada rock mechanics symposium, 27–30 June 2010, Salt Lake City, Utah.

Myers, A. L., and Monson, P. A., (2002). Adsorption in Porous Materials at High Pressure: Theory and Experiment. Langmuir, 18(9), 10261–10273.

Mulders, FMM, (2003). Modelling of stress development and fault slip in and around a producing gas reservoir (PhD Thesis). Delft, the Netherlands: Delft University of Technology; 2003.

Mukhopadhyay, S., Yang, S. Y., and Yeh, H. D., (2012). Pressure build up during supercritical carbon dioxide injection from a partially penetrating borehole into gas reservoirs. Transp. Porous Med. 91, 889–911.

Mathias, S.A., and McElwaine, J.N., and Gluyas, J.G., (2014). Heat transport and pressure build up during carbon dioxide injection into depleted gas reservoirs. Journal of Fluid mechanics, 756. pp. 89-109.

Mazumder, S., van Hemert, P., Busch, A., Wolf, K.H.A.A., and Tejera-Cuesta, P., (2006). Flue gas and pure CO_2 sorption properties of coal: A comparative study. International Journal of Coal Geology, 67(4): 267-279.

Morrissey, F.A., Grismer, M.E., (1999). Kinetics of volatile organic compound sorption/desorption on clay minerals. Journal of Contaminant Hydrology 36, 291–312.

Majewska, Z., Ceglarska-Stefanska, G., Majewski, S. and Zietek, J., (2009). Binary gas sorption/desorption experiments on a bituminous coal: Simultaneous measurements on

sorption kinetics, volumetric strain and acoustic emission. International Journal of Coal Geology, 77(1-2): 90-102.

Mohammad, S., Fitzgerald, J., Robinson, R.L., Gasem, K.A.M., (2009). Experimental uncertainties in volumetric methods for measuring equilibrium adsorption. Energy Fuel 23 (5), 2810–2820.

Mavor, MJ, Gunter, WD., Robinson, JR., Law, DHS, Gale, J., (2002). Testing for CO_2 sequestration and enhanced methane production from coal. SPE 75683, SPE gas technology symposium, 30 Apr– 2 May 2002, Calgary, Alberta, Canada.

Mengal, S. A., and Wattenbarger, R. A., (2013). Accounting for Adsorbed Gas in Shale Gas Reservoirs. SPE Conference, (September), 25–28. doi:10.2118/141085-MS.

Merkel, A., Fink, R., and Littke, R., (2015). The role of pre-adsorbed water on methane sorption capacity of Bossier and Haynesville shales. International Journal of Coal Geology, 147-148, 1–8. doi: 10.1016/j.coal.2015.06.003.

Max, F. Daarnhouwer., (2013). Assessing the potential of depleted gas fields for geothermal energy (Unpublished bachelor thesis). Department of Geoscience & Engineering Delft, University of Technology, the Netherlands.

Mamora, D. D., and Seo, J. G., (2002). Enhanced Recovery by Carbon Dioxide Sequestration in Depleted Gas Reservoirs. SPE Annual Technical Conference and Exhibition, 1–9. doi:10.2118/77347-MS.

Mane, V.S., Mall, I.D., Srivastava, V.V., (2007). Kinetic and equilibrium isotherm studies for the adsorptive removal of Brilliant Green dye from aqueous solution by rice husk ash, J. Environ. Manage. 84 (2007) 390–400.

Matsuoka, T., and Azuma, H., (2014). Contributions of Rock Physics to Carbon Dioxide Capture and Sequestration. 8th Asian Rock Mechanics Symposium, (October), 35–42.

Mosher, K., He, J., Liu, Y., Rupp, E., and Wilcox, J., (2013). Molecular simulation of methane adsorption in micro- and mesoporous carbons with applications to coal and gas shale systems. International Journal of Coal Geology, 109-110, 36–44. doi: 10.1016/j.coal.2013.01.001.

Myers. R. H., (1986). Classical and Modern Regression with Application, PWS and Kent Publisher: New York, 1986.

Myers, A.L., (2004). Thermodynamics of Adsorption. In: T.M. Letcher (Editor), Chemical Thermodynamics for Industry, Cambridge, UK.

Nagelhout, ACG, Roest, JPA, (1997). Investigating fault slip in a model of an underground gas storage facility. International Journal of Rock Mechanics and Mining Sciences 1997; 34(3-4).

Nghiem, L. X., Shrivastava, V. K., Tran, D., Kohse, B. F., Hassam, M. S., and Yang, C., (2009). Simulation of CO_2 Storage in Saline Aquifers. SPE/EAGE Reservoir Characterization and Simulation Conference, October 19-21 2009, Abu Dhabi, UAE. doi:10.2118/125848-MS.

Nicot, J.-P., (2008). Evaluation of large-scale CO_2 storage on fresh-water sections of aquifers: an example from the Texas Gulf Coast Basin. Int. J. Greenhouse Gas Control 2 (4), 582–593.

Nordbotten, JM., Celia, MA, Bachu S., (2005). Injection and storage of CO_2 in deep saline aquifers: analytical solution for CO_2 plume evolution during injection. Transport Porous Media 2005; 58:339–60.

Nuttall, Brandon C., Eble, Cortland F., Drahovzal, James A., Bustin, R. Marc., (2005). Analysis of Devonian Black Shales in Kentucky for Potential Carbon Dioxide Sequestration and Enhanced Natural Gas Production". Kentucky Geological Survey, Final Report, Geological Survey/University of Kentucky (DE-FC26-02NT41442). December 30, 2005.

Ojo, A. C., and Tse, A. C., (2016). Geological Characterisation of Depleted Oil and Gas Reservoirs for Carbon Sequestration Potentials in a Field in the Niger Delta, Nigeria. Journal of Applied Sciences and Environmental Management, 20(1), 45. doi:10.4314/jasem. v20i1.6.

Okwananke, A., Adeboye, B. Y., and Sulaimon, L. A., (2011). Evaluation and performance of natural gas storage in depleted gas reservoirs. Petroleum & Coal,53(4),324–332. Retrieved from http://www.vurup.sk/sites/vurup.sk/files/downloads/ pc_4_2011_okwananke_134.pdf.

Oldenburg, CM., Benson, SM., (2002). CO_2 injection for enhanced gas production and carbon sequestration. Society of Petroleum Engineers, SPE-74367, SPE International Petroleum Conference and Exhibition in Mexico, Villahermosa, Mexico, 10–12 February. 2002.

Oldenburg, CM., Pruess, K., Benson, SM., (2001). Process modelling of CO_2 injection into natural gas reservoirs for carbon sequestration and enhanced oil recovery. Energy Fuels 2001; 15:293–8.

Oldenburg, C. M., Stevens, S. H., and Benson, S. M., (2004). Economic feasibility of carbon sequestration with enhanced gas recovery (CSEGR). Energy, 29(9-10), 1413–1422. doi:10.1016/j.energy.2004.03.075.

Orlic, B., Wassing, BBT., (2013). A study of stress change and fault slip in producing gas reservoirs overlain by elastic and visco-elastic caprocks. Rock Mechanics and Rock Engineering 2013;46(3):421e35.

Orlic, B., Wassing, BBT., Geel, CR., (2013). Field scale geomechanical modelling for prediction of fault stability during underground gas storage operations in a depleted gas field in the Netherlands. In: Proceedings of the 47th US Rock Mechanics/Geomechanics Symposium. ARMA; 2013. Paper. No. ARMA 13-300.

Orr, F. M., (2004). Storage of carbon dioxide in geologic formations" Journal of Petroleum Technology, vol. 56, no. 9, pp. 90–97 (2004).

Osmari, T., Gallon, R., Schwaab, M., Barbosa-Coutinho, E., Severo, J., and Pinto, J., (2013). Statistical Analysis of Linear and Non-linear Regression for the Estimation of Adsorption Isotherm Parameters. Adsorption Science & Technology, 31(5), 433-458. doi:10.1260/0263-6174.31.5.433.

Ottiger, S., Pini, R., Storti, G. and Mazzotti, M., (2008). Competitive adsorption equilibria of CO_2 and CH4 on a dry coal. Adsorption, 14(4-5): 539-5.

Orlic, B., (2016). Geomechanical effects of CO_2 storage in depleted gas reservoirs in the Netherlands: Inferences from feasibility studies and comparison with aquifer storage. Journal of Rock Mechanics and Geotechnical Engineering, 8, 846–859. doi:10.1016/j.jrmge.2016.07.003.

Palomino, A. M., and Santamarina, J. C., (2005). Fabric map for kaolinite: Effects of pH and ionic concentration on behaviour. Clays and Clay Minerals, 53(3), 211–223. doi:10.1346/CCMN.2005.0530302.

Parimal, S., Prasad, M., and Bhaskar. U., (2010). Prediction of equilibrium sorption isotherm: Comparison of linear and nonlinear methods, Ind. Eng. Chem. Res., Vol. 49, pp. 2882-2888, 2010.

Paschke, T., Dreisbach, F., (2013). Investigation of Enhanced Coal Bed Methane (EBCM) Processes- Gravimetric Adsorption Measurements under Realistic Conditions. IsoSORP Application Note, (2), 1–2. Retrieved from http://www.rubotherm.com.

Passey, Q.R., Bohacs, K.M., Esch, W.L., Klimentidis, R., and Sinha., (2010). From Oil-Prone Source Rock to Gas-Producing Shale Reservoir- Geological and Petrophysical Characterization of Unconventional Shale-Gas Reservoir, SPE-131350, Paper presented at the CPS/SPE International Oil & Gas Conference and Exhibition in China, SPE, Beijing, China, June 8-10.

Passey, Q. R., Bohacs, K. M., Esch, W. L., Klimentidis, R., Sinha, S., and Upstream, E., (2010). From Oil-Prone Source Rock to Gas-Producing Shale Reservoir – Geologic and Petrophysical Characterization of Unconventional Shale-Gas Reservoirs. CPS/SPE International Oil & Gas Conference and Exhibition in China 2010, 1707–1735. doi:131350.

Paula, D., (1982). Distribution a N D Dispersal of Clay Minerals on the. Clays and Clay Minerals, 43(4), 474–477.

Pawar, R. J., Warpinski, N. R., Lorenz, J. C., Benson, R. D., Grigg, R. B., Stubbs, B. A., Svec, R. K., (2006). Overview of a CO_2 sequestration field test in the West Perl Queen reservoir, New Mexico. Environmental Geosciences, 13(3), 163–180. doi:10.1306/eg.10290505013.

Pei, D., Xu, J., Zhuang, Q., Tse, H.-F., and Esteban, M. A., (2010). Induced pluripotent stem cell technology in regenerative medicine and biology. Advances in Biochemical Engineering/biotechnology, 123(July 2015), 127–141. doi:10.1007/10.

Pentland, C.H., El-Maghraby, R., Iglauer, S., Blunt, M.J., (2011). Measurements of the capillary trapping of super-critical carbon dioxide in Berea sandstone. Geophysical Research Letters 38, L06401, http://dx.doi.org/10.1029/2011GL046683.

Petrusak R., Riestenberg D., Goad P. (2009). World class CO_2 sequestration potential in saline formations, oil and gas fields, coal, and shale: the US southeast regional carbon sequestration partnership has it all. In Proceedings of the SPE International Conference on CO_2 Capture, Storage, and Utilization, pp. 136–153, November 2009.

P.D., S., and Parmely, C. R., (1989). Gas Composition Shifts in Devonian Shales. SPE Reservoir Engineering, 4(3), 283–287. doi:10.2118/17033-PA.

Pini, R., (2014). Assessing the adsorption properties of mudrocks for CO_2 sequestration. Energy Procedia, 63, 5556–5561. doi:10.1016/j.egypro.2014.11.589.

Pruess, K., Xu, T., Apps, J., Garcı´a, J., (2003). Numerical modelling of aquifer disposal of CO_2. Soc. Pet. Eng. J., 49 – 59.

Pike, R., and Soc, R., (2006). The Chemistry of Carbon Capture and Storage. Journal of Petroleum Technology.

P.D. Schettler Jr., C.R. Parmely., (1991). Contributions to total storage capacity in Devonian shales, in: SPE, J, SPE 23422, 1991.

Pini, R., Ottiger, S., Burlini, L., Storti, G. and Mazzotti, M., (2010). Sorption of carbon dioxide, methane and nitrogen in dry coals at high pressure and moderate temperature. International Journal of Greenhouse Gas Control, 4(1): 90-101.

Pini, R., (2014). Assessing the adsorption properties of burdocks for CO_2 sequestration. Energy Procedia, 63, 5556–5561. doi: 10.1016/j.egypro.2014.11.589.

Poomisitiporn, K., Rangsunvigit, P., Kitiyanan, B., Kulprathipanja, S., (2016), Competitive adsorption of methane and carbon dioxide on different activated carbons, Chemical Engineering Transactions, 52, 121-126 DOI:10.3303/CET1652021.

Predescu, L., Teze,l FH., Chopra, S., (1996). Adsorption of nitrogen, methane, carbon monoxide, and their binary mixtures on aluminosilicate molecular sieves. Adsorption 1996; 3:7–25.

Preston, C., Monea, M., Jazrawi, W., Brown, K., Whittaker, S., White D., (2005). IEA GHG Weyburn CO_2 monitoring and storage project. Fuel Process Technology 2005; 86:1547–68.

Pruess, K, Garcia, J., (2002). Multiphase flow dynamics during CO_2 disposal into saline aquifers. Environ. Geol. 2002; 42:282–95.

Pruess, K., (2004). Numerical simulation of CO_2 leakage from a geological disposal reservoir, including transition from super to sub-critical conditions, and boiling of liquid CO_2. SPE J 2004; 9:237–48.

Qi, R., LaForce, T., and Blunt, M. J. (2008). Design of carbon dioxide storage in oil fields. SPE Annual Technical Conference and Exhibition, (September), 21–24. Retrieved from https://www.onepetro.org/conference-paper/SPE-115663-MS.

Rani, S., Prusty, B. K., and Pal, S. K., (2015). Comparison of void volume for volumetric adsorption studies on shales from India. Journal of Natural Gas Science and Engineering, 26, 725–729. doi: 10.1016/j.jngse.2015.07.012.

Redlich, O., and Peterson, D.L., (1959). A useful adsorption isotherm, J. Phys. Chem.63 (1959) 1024.

Regan, M., (2007). A Review of the Potential for Carbon Dioxide (CO_2) Enhanced Gas Recovery in Australia, Cooperative Research Centre for Greenhouse Gas Technologies, Canberra (CO_2CRC Publication No: RPT07-0802. 39 pp.).

Rexer, T., (2014). Nanopore Characterisation and Gas Sorption Potential of European Gas Shales (Ph.D. Thesis). Newcastle University.

Ringot, D., Lerzy, B.L., Chaplain, K., Bonhoure, J., Auclair, E., and Larondelle. Y., (2007). In vitro biosorption of ochratoxin A on the yeast industry by-products: Comparison of isotherm models", Bioresource Technol., vol. 98, pp. 1812-1821, 2007.

Ringrose, P., Atbi, M., Mason, D., Espinassous, M., Myhrer, Ø, Iding, M., Mathieson, A., Wright, I., (2009). Plume development around well KB-502 at the in Salah CO_2 storage site. First Break 27:85–89.

Roest, JPA, Kuilman, W., (1994). Geomechanical analysis of small earthquakes at the Eleveld gas reservoir. In: Proceedings of EUROCK Symposium, Delft, the Netherlands. Society of Petroleum Engineers; 1994. p. 573-80.

Renard, F., Park, A., Ortoleva, P., Gratier, J.P., (1999). An integrated model for transitional pressure solution in sandstones. Tectonophysics 312, 97–115.

Romanov, V., Soong, Y., and Schroeder, K., (2006). Volumetric effects in coal sorption capacity measurements. Chemical Engineering and Technology, 29(3), 368–374. doi:10.1002/ceat.200500242.

Ross, D.J.K., Bustin, R.M., (2007). Shale gas potential of the Lower Jurassic Gordondale Member, north eastern British Columbia, Canada. Bull. Can. Petrol. Geol. 55 (1), 51–75.

Ross, D. J. K., and Marc Bustin, R., (2007). Impact of mass balance calculations on adsorption capacities in microporous shale gas reservoirs. Fuel, 86(17-18), 2696–2706. doi: 10.1016/j.fuel.2007.02.036.

Ross, D.J.K., Bustin, R.M., (2008). Characterizing the shale gas resource potential of Devonian– Mississippian strata in the Western Canada sedimentary basin: application of an integrated formation evaluation. AAPG Bull. 92 (1), 87–125.

Ross, D. J. K., and Marc Bustin, R., (2009). The importance of shale composition and pore structure upon gas storage potential of shale gas reservoirs. Marine and Petroleum Geology, 26(6), 916–927. doi:10.1016/j.marpetgeo.2008.06.004.

Rouquerol, F., Rouquerol, J., and Sing, K., (1999). Front Matter. In Adsorption by Powders and Porous Solids (p. iii –). London: Academic Press. doi:http://dx.doi.org/10.1016/B978-0-12-598920-6.50017-8.

Roy, W.R., Krapac, I.G., Chou, S.F.J., Griffin, R.A., (1992). Batch-type Procedures for Estimating Soil Adsorption of Chemicals. U.S. Environmental Protection Agency, Washington, DC, EPA/530/SW-87/006-F.

Rutqvist, J., Birkholzer, J., Cappa, F., Tsang, CF., (2007). Estimating maximum sustainable injection pressure during geological sequestration of CO_2 using coupled fluid flow and geomechanical fault-slip analysis. Energy Convers Manage 48:1798–1807.

Rutqvist, J., Vasco, DW., Myer, L., (2009). Coupled reservoir geomechanical analysis of CO_2 injection at InSalah, Algeria. Energy Procedia 1:1847–1854.

Saadatpoor, E., (2009). Effect of capillary heterogeneity on buoyant plumes: new trapping mechanism in carbon sequestration, M.S. Thesis. The University of Texas at Austin, http://www.pge.utexas.edu/theses09/saadatpoor.pdf.

Saini, D., and Jimenez, I., (2014). Evaluation of CO_2-EOR and Storage Potential in Mature Oil Reservoirs. SPE International, SPE-169555(April), 16–18.

Sakurovs, R., Day, S., Weir, S., Duffy, G., (2009). Temperature dependence of sorption of gases by coals and charcoals. Int. J. Coal Geol. 77 (1–2), 16–22.

Sakurovs, R., Day, S., Weir, S., (2009). Causes and consequences of errors in determining sorption capacity of coals for carbon dioxide at high pressure, Int. J. Coal Geol. 77 (2009), 16–22.

Salmachi, A., (2013). Thermally Enhanced Gas Recovery and Infill Well Placement Optimisation in Coalbed Methane Reservoirs. The University of Adelaide.

Sandor, G., (1977). A Study of Sorption Characteristics of Oil and Gas Bearing Sands Stones. Applied Chemistry, 311–315.

Saripalli, KP., McGrail BP., (2002). Semi-analytical approaches to modelling deep well injection of CO_2 for geologic sequestration. Energy Convers Manage 2002; 43:185–98.

Schaef, H. T., Davidson, C. L., Owen, A. T., Miller, Q. R. S., Loring, J. S., Thompson, C. J., McGrail, B. P., (2014). CO_2 utilization and storage in shale gas reservoirs: Experimental results and economic impacts. Energy Procedia, 63, 7844–7851. doi:10.1016/j.egypro.2014.11.819.

Schaef, H.T., Glezakou, V.A., Owen, A.T., Ramprasad, S., Martin, P.F., McGrail, B.P., (2014). Surface Condensation of CO_2 onto Kaolinite, Environmental Science & Technology Letters, 1, 142-145.

Schaef, H. T., Davidson, C. L., Owen, A. T., Miller, Q. R. S., Loring, J. S., Thompson, C. J., McGrail, B. P., (2014). CO_2 utilization and storage in shale gas reservoirs: Experimental results and economic impacts. Energy Procedia, 63, 7844–7851.doi: 10.1016/j.egypro.2014.11.819.

Schepers, K.C., Nuttall, B.C., Oudinot, A.Y., Gonzalez, R.J., (2009). Reservoir modelling and simulation of the Devonian Gas Shale of Eastern Kentucky for Enhanced Gas Recovery and CO_2 storage. In: Paper SPE 126620, Presented at the SPE International Conference on CO_2 Capture Storage and Utilization Held in San Diego, California, USA, 10-11 November.

Schettler, P.D., Parmely, C.R., (1991). Contributions to total storage capacity in Devonian shales. SPE Eastern Regional Meeting, Lexington, Kentucky. Society of Petroleum Engineers Journal (SPE-23422).

Schilling, F., Borm, G., Würdemann, H., Möller, F., Kühn, M. and CO_2SINK Group (2009): Status Report on the First European on-shore CO_2 Storage Site at Ketzin (Germany). Energy Procedia 1, 2029-2035.

Schumacher, M. M., (1980). Enhanced recovery of residual and heavy oils (2d ed.). Noyes Data Corp, Park Ridge, N.J.

Seo, J.G., and Mamora, D.D., (2003). Experimental and Simulation of Supercritical Carbon Dioxide in Depleted Reservoirs, SPE Paper 81200 presented at the SPE/EPA/DOE Exploration and Production Environmental Conference held in San Antonio, Texas, USA, 10-12 March 2003.

Shafeen, A., Croiset, E., Douglas, P. L., and Chatzis, I., (2004). CO_2 sequestration in Ontario, Canada. Part I: Storage evaluation of potential reservoirs. Energy Conversion and Management, 45(17), 2645–2659. doi:10.1016/j.enconman.2003.12.003.

Shi, J., Zhang, L., Li, Y., Yu, W., He, X., Liu, N., Wang, T., (2013). Diffusion and Flow Mechanisms of Shale Gas through Matrix Pores and Gas Production Forecasting. Presented at the SPE Unconventional Resources Conference-Canada Held in Calgary, Alberta, Canada, 5–7 November 2013., SPE 167226.

Shi, JQ., Sinayuc, C., Durucan, S., Korre, A., (2012). Assessment of carbon dioxide plume behaviour within the storage reservoir and the lower caprock around the KB- 502 injection well at InSalah. International Journal of Greenhouse Gas Control 2012; 7:115-26.

Shtepani, E., (2006). CO_2 sequestration in depleted gas/condensate reservoirs. Proceedings- SPE Annual Technical Conference and Exhibition.

Siemons, N. and Busch, A., (2007). Measurement and interpretation of supercritical CO_2 sorption on various coals. International Journal of Coal Geology, 69(4): 229-242.

Sinayuç, C., and Gümrah, F., (2008). Modelling of ECBM recovery from Amasra coalbed in Zonguldak Basin, Turkey. In Proceedings of the Canadian International Petroleum Conference, Alberta, Canada, 2008.

Singh, A. K., Baumann, J., Henninges, J., Goerke, U. J., and Kolditz, O., (2012). Numerical analysis of thermal effects during carbon dioxide injection with enhanced gas recovery: A theoretical case study for the Altmark gas field. Environ. Earth Sci. 67, 497–509.

Singh, A. K., Goerke, U. J., and Kolditz, O., (2011). Numerical simulation of non-isothermal compositional gas flow: Application to carbon dioxide injection into gas reservoirs. Energy 36, 3446–3458.

Sing, K.S., (1985). Reporting physisorption data for gas/solid systems with special reference to the determination of surface area and porosity. Pure Appl. Chem.57 (4), 603-619.

Sing, K. S. W., Everett, D. H., Haul, R. A. W., Moscou, L., Pierotti, R. A., Rouquérol, J., and Siemieniewska, T., (1982). International union of pure commission on colloid and surface chemistry including catalysis reporting physisorption data for gas / solid systems with Special Reference to the Determination of Surface Area and Porosity. Pure & Appl. Chem., 54(11), 2201–2218. doi:10.1351/pac198557040603.

Sircar, S., (2001). Measurement of Gibbsian Surface Excess, AIChE J.,47(5), 1169–1176 (2001).

Sloss, L. L., (2015). Potential for enhanced coalbed methane recovery. IEA Clean Coal Centre.

Sondergeld, C.H., Ambrose, R.J., Rai, C.S., Moncrieff, J., (2010). Micro-structural studies of gas shales: SPE Unconventional Gas Conference.

Stalkup, Jr., (1983). Miscible Displacement, SPE Monograph Volume 8, Society of Petroleum Engineers, 1983.

Stein, M.H., Premium Petroleum Consulting., Ghotekar, A.L., Avasthi & Associates, inc., and Avasthi, S.M., (2010), Paper presented at the SPE EUROPEC/EAGE Annual Conference and Exhibition, 14 –17 June, 2010.

Stevens, S. H., Spector, D., and Riemer, P., (1998). Enhanced coalbed methane recovery using CO_2 injection: worldwide resource and CO_2 sequestration potential, in Proceedings of the 6th International Oil & Gas Conference and Exhibition in China (IOGCEC '98), pp. 489–501, Beijing, China, November 1998.

Sobers, L. E., Frailey, S. M., and Lawal, A. S., (2004). Geological Sequestration of Carbon Dioxide in Depleted Gas Reservoirs. Carbon. SPE 89345.

Sondergeld, C.H., Ambrose, R.J., Rai, C.S., Moncrieff, J., (2010). Micro-structural studies of gas shales. In: Paper SPE 131771 Presented at the SPE Unconventional Gas Conference Held in Pittsburgh, Pennsylvania, USA, 23-25 February.

Stoessell, R.K., Byrne, P.A., (1982). Methane solubilities in clay slurries. Clays and Clay Minerals, Vol. 30, 67–72.

Streit, JE., Hillis, RR., (2004). Estimating fault stability and sustainable fluid pressures for underground storage of CO_2 in porous rock. Energy 29:1445–1456.

Starzewski, P., Grillet, Y., (1989). Thermochemical studies of adsorption of He and CO2 on coals at ambient temperature. Fuel 68, 375-379.

Strapoc, D., Mastalerz, M., Schimmelmann, A., Drobniak, A., Hasenmueller, N.R., (2010). Geochemical constraints on the origin and volume of gas in the New Albany Shale (Devonian–Mississippian), eastern Illinois Basin. AAPG Bull. 94 (11), 1713–1740.

Sudibandriyo, M., Pan, Z., Fitzgerald, J.E., Robinson Jr., R.L., Gasem, K.A.M., (2003). Adsorption of methane, nitrogen, and carbon dioxide, and their binary mixtures on dry activated carbon at 318.2K and pressures up to 13.6 Mpa. Langmuir 19, 5323–5331.

Tan, J., Weniger, P., Krooss, B., Merkel, A., Horsfield, B., Zhang, J., Tocher, B.A., (2014). Shale gas potential of the major marine shale formations in the Upper Yangtze Platform, South China, Part II: methane sorption capacity. Fuel 129, 204–218.

Thomas, S. (2008). Enhanced oil recovery-an overview. Oil & Gas Science and Technology-Revue …, 63(1), 9–19. doi:10.2516/ogst.

Tian, H., Pan, L., Xiao, X., Wilkins, R.W.T., Meng, Z. and Huang, B., (2013). A preliminary study on the pore characterization of Lower Silurian black shales in the

Chuandong Thrust Fold Belt, south western China using low pressure N_2 adsorption and FE-SEM methods. Marine and Petroleum Geology, 48(0): 8-19.

Tian, L., Xiao, C., Xie, Q., Yang, Y., Zhang, Y., and Wang, Y., (2016). Quantitative determination of abandonment pressure for CO 2 storage in depleted shale gas reservoirs by free-simulator approach. Journal of Natural Gas Science and Engineering, 36, 519–539. doi:10.1016/j.jngse.2016.10.051.

U.S. Department of Energy., (1999). Carbon Sequestration Research and Development: Office of Fossil Energy, Office of Science, Washington, D.C., December, p195 U.S. Department of Energy, 2004, Carbon Sequestration Technology Roadmap and Program Plan: National Energy Technology Laboratory, P24.

U.S. Department of Energy., (2005). Carbon Sequestration, Technology Roadmap and Program Plan 2005: National Energy Technology Laboratory, P26.

Van der Meer, LGH, (1992). Investigation regarding the storage of carbon dioxide in aquifers in the Netherlands. Energy Convers Manage 1992; 33:611–8.

Van der Meer, LGH., (2004). Re-injecting CO2 into an offshore gas reservoir at a depth of nearly 4000 m subsea. Proceedings of the 7th International Conference on Greenhouse Gas Control Technologies Vancouver, Canada. http://uregina.ca/ghgt7/ PDF/papers/ nonpeer/534.pdf.

Van der Meer, B., (2005). Carbon Dioxide Storage in Natural Gas Reservoir. Oil & Gas Science and Technology, 60(3), 527–536. doi:10.2516/ogst:2005035.

Van der Meer, L.G.H., Kreft, E and Geel, C., (2005). K12-B Test Site for CO_2 Storage and Enhanced Gas Recovery. SPE Paper 94128, SPE Europec/EAGE Annual Conference, Madrid, Spain, 13- 16 June, 2005.

Van der Meer, L. G. H., and Yavuz, F., (2009). CO_2 storage capacity calculations for the Dutch subsurface. Energy Procedia, 1(1), 2615–2622. doi: 10.1016/j.egypro.2009.02.028.

Van Eijs, RMHE., Mulders FMM., Nepveu, M., Kenter, CJ., Scheffers, BC., (2006). Correlation between hydrocarbon reservoir properties and induced seismicity in the Netherlands. Engineering Geology 2006;84(3-4):99-111.

Van Wees, JD., Buijze, L., Van Thienen-Visser, K., Nepveu, M., Wassing, BBT., Orlic, B., Fokker, PA., (2014). Geomechanics response and induced seismicity during gas field depletion in the Netherlands. Geothermics 2014; 52:206-19.

Van Hemert, P. V., Bruining, H., Rudolph, E. S., Wolf, K. A., and Maas, J. G., (2009). Improved manometric setup for the accurate determination of supercritical carbon dioxide sorption. Review of Scientific Instruments, 80(3), 035103. doi:10.1063/1.3063064.

Vermylen, J. P., (2011). Geomechanical Studies of the Barnett Shale, Texas, USA. Stanford University. PhD Thesis.

Vilarrasa, V., Carrera, J., (2015). Geologic carbon storage is unlikely to trigger large earthquakes and reactivate faults through which CO_2 could leak. Proceedings of the National Academy of Sciences of the United States of America 2015;112(19):5938-43.

Walker Jr., P.L., Verma, S.K., Rivera-Utrilla, J., Davis, A., (1988). Densities, porosities and surface areas of coal macerals as measured by their interaction with gases, vapours and liquids. Fuel, 67: 1615-1623.

Wang, S., Dong, M., and Li, Z., (2009). Parameter Evaluation of CO_2 Sequestration Capacity in Depleted Oil Reservoirs — Coreflood Tests and Numerical Simulation. Canadian International Petroleum Conference (CIPC) 2009, Calgary, Alberta, Canada, 16-18 June 2009., 1–8.

Wang, X., and Qin, Y., (2005). Equilibrium sorption isotherms for of Cu^{2+} on rice bran, Process Biochem., vol. 40, pp. 677-680, 2005.

Weaver, C. E., (1956). A Discussion on the Origin of Clay Minerals in Sedimentary Rocks. Clays and Clay Minerals, 5(1), 159–173. doi:10.1346/CCMN.1956.0050113.

Weniger, P., Kalkreuth, W., Busch, A, Krooss, B.M., (2010). High-pressure methane and carbon dioxide sorption on coal and shale samples from the Paraná Basin, Brazil. International Journal of Coal Geology, 84: 190-205.

White, S.P., Allis, R.G., Moore, J., Chidsey, T., Morgan, C., Gwynn, W., Adams, M., (2005). Simulation of reactive transport of injected CO_2 on the Colorado Plateau, Utah. Chemical Geology 217, 387–405.

White, CM., Strazisar, BR., Granite, EJ., Hoffman, JS., Pennline, HW., (2003) Separation and capture of CO_2 from large stationary sources and sequestration in geological formations—coalbeds and deep saline aquifers. J Air Waste Manage Assoc 53:645–715.

White, DJ., Furrowes, G., Davis, T., Hajnal, Z., Hirsche, K., Hutcheon, I., Majer, E., Rostron, B., Whittaker, S., (2004). Greenhouse gas sequestration in abandoned oil reservoirs: The International Energy Agency Weyburn pilot project. GSA Today 14(7):4–10.

Whittaker, S., White, D., Law, D., Chalaturnyk, R., (2004). IEAGHG, Weyburn CO_2 monitoring and storage project summary report 2000–2004. (Petroleum Technology Research Centre, Regina, SK, Canada), Available at: http://www.ptrc.ca/weyburn_first.php.

William, Ampomah., Robert S. Balch., Reid B. Grigg., Zhenxue, Dai., and Feng, Pan., (2015). Compositional Simulation of CO_2 Storage Capacity in Depleted Oil Reservoirs. Paper presented at the Carbon Management Technology Conference held in Sugarland, Texas, USA. 17–19 November 2015.

Wollenweber, J., (2010). Experimental investigation of the CO_2 sealing efficiency of caprocks. International Journal of Greenhouse Gas Control, 4(2): 231-241.

Xu, T., Apps, JA., Pruess, K., (2003). Reactive geochemical transport simulation to study mineral trapping for CO_2 disposal in deep arenaceous formations. J Geophys Res 2003;108(B2). doi:10.1029/2002JB001979.

Xu, T., Apps, JA., Pruess, K., (2004). Numerical simulation of CO_2 disposal by mineral trapping in deep aquifers. Appl Geochem 2004; 19:917–36.

Xu, T., Sonnenthal, E., Spycher, N., Pruess, K., (2004). TOUGHREACT user's guide: a simulation program for non-isothermal multiphase reactive geochemical transport in variably saturated geologic media. In: Lawrence Berkeley National Laboratory Report LBNL-55460, Berkeley, CA.

Xu, T., Apps, J.A., Pruess, K., (2003). Reactive geochemical transport simulation to study mineral trapping for CO_2 disposal in deep arenaceous formations. Journal of Geophysical Research 108 (B2), 13, http://dx.doi.org/10.1029/2002JB001979.

Xu, T., Apps, J.A., Pruess, K., (2005). Mineral sequestration of carbon dioxide in a sandstone–shale system. Chemical Geology 217, 295–318.

Yang, R. T., (1997) Gas separation by adsorption processes, Imperial College Press, London, U.K.

Yu, H., Guo, W., Cheng, J., and Hu, Q., (2008). Impact of experimental parameters for manometric equipment on CO_2 isotherms measured: Comment on "Inter-laboratory comparison II: CO_2 isotherms measured on moisture-equilibrated Argonne premium coals at 55°C and up to 15MPa" by Goodman et al. (2007). International Journal of Coal Geology, 74(3-4), 250–258. doi:10.1016/j.coal.2007.12.002.

Yu, Z., Liu, L., Yang, S., Li, S., and Yang, Y., (2012). An experimental study of CO_2–brine–rock interaction at in situ pressure–temperature reservoir conditions. Chemical Geology, 326-327, 88–101. doi:10.1016/j.chemgeo.2012.07.030.

Yuan, W., Pan, Z., Li, X., Yang, Y., Zhao, C., Connell, L. D., He, J., (2014). Experimental study and modelling of methane adsorption and diffusion in shale. Fuel, 117(PART A), 509–519. doi:10.1016/j.fuel.2013.09.046.

Zerai, B., Saylor, B.Z., Matisoff, G., (2006). Computer simulation of CO_2 trapped through mineral precipitation in the Rose Run Sandstone, Ohio. Applied Geochemistry 21, 223–240.

Ziabaksh-Ganji, Z., and Kooi, O., (2014). Sensitivity of Joule–Thomson cooling to impure CO_2 injection in depleted gas reservoirs. Appl. Energy 113, 434–451.

Zhang, X. G., Ranjith, P. G., Perera, M. S. A., Ranathunga, A. S., and Haque, A., (2016). Gas Transportation and Enhanced Coalbed Methane Recovery Processes in Deep Coal Seams: A Review. Energy & Fuels, 30(11), 8832–8849. doi: 10.1021/acs.energyfuels.6b01720.

Zhang, T., Geology, E., Austin, U. T., Ellis, G. S., Ruppel, S. C., Milliken, K., Sun, X., (2013). Effect of Organic Matter Properties, Clay Mineral Type and Thermal Maturity on Gas Adsorption in Organic-Rich Shale Systems. Presented at the Unconventional Resources Technology Conference Held in Denver, Colorado, USA, 12-14 August 2013.SPE Conference, SPE 168862(1), 1–6. Doi: 10.1190/urtec2013-205.

Zoback, MD., Gorelick SM., (2012). Earthquake triggering and large-scale geologic storage of carbon dioxide. Proceedings of the National Academy of Sciences of the United States of America 2012; 109(26):10164e8.

Zweigel, P., Arts, R., Lothe, A.E. and Lindeberg, E.B.G., (2004). Reservoir geology of the Utsira Formation at the first industrial scale underground CO_2 storage site (Sleipner

area, North Sea). In: Baines, S.J., Worden, R.H. (Eds.) Geological Storage of Carbon Dioxide. Geological Society, London, Special Publications, 233, 165–180.

Zweigel, P., Hamborg, M., Arts, R., Lothe, AE., Sylta, O., and Tommeras A., (2000). Prediction of migration of CO_2 injected into an underground depository: Reservoir geology and migration modelling in the Sleipner case (North Sea), in Greenhouse Gas Control Technologies, Proceedings of the 5th International Conference on Greenhouse Gas Control Technologies, 13–16 August 2000, ed. by Williams D, Durie I, McMullan P, Paulson C and Smith A. CSIRO, Cairns, Australia, pp. 360 – 365 (2001).

8 APPENDIX

APPENDIX A-1: Dry Bandera and Scioto adsorption experimental adsorption results at 23°C and variable pressure.

	Excess Adsorbed (mmol/g)	
Pressure(psia)	**Bandera**	**Scioto**
50	0.010	0.012
100	0.019	0.022
150	0.025	0.033
200	0.031	0.043
250	0.037	0.051
300	0.043	0.058
350	0.047	0.067
400	0.051	0.072
450	0.057	0.077
500	0.061	0.082
550	0.065	0.086
600	0.068	0.090
650	0.072	0.094
700	0.075	0.097
750	0.079	0.101
800	0.082	0.103
850	0.085	0.105
900	0.087	0.108
950	0.089	0.110
1000	0.089	0.110
1050	0.089	0.110
1100	0.089	0.110
1150	0.089	0.110
1200	0.089	0.110
1250	0.089	0.110

APPENDIX A-2: Dry Bandera and Scioto adsorption isotherm data at 23°C and variable pressure.

	Excess Adsorbed (mmol/g)	
Pressure (psia)	**Bandera**	**Scioto**
50	0.010	0.012
100	0.019	0.022
150	0.025	0.033
200	0.031	0.043
250	0.037	0.051
300	0.043	0.058
350	0.047	0.067
400	0.051	0.072
450	0.057	0.077
500	0.061	0.082

APPENDIX A-3: Water-saturated Bandera and Scioto Methane (CH_4) experimental adsorption data at 23°C and variable pressure.

	Methane Adsorbed (mmol/g) (Scioto)				Methane Adsorbed (mmol/g) (Bandera)			
Pressure(psia)	Dry	water content			Dry	water content		
		33%	65%	91%		33%	65%	91%
50	0.012	0.005	0.003	0.001	0.010	0.007	0.005	0.002
100	0.022	0.012	0.007	0.006	0.019	0.013	0.009	0.007
150	0.033	0.017	0.013	0.011	0.025	0.019	0.015	0.010
200	0.043	0.023	0.018	0.016	0.031	0.025	0.021	0.018
250	0.051	0.025	0.023	0.019	0.037	0.029	0.024	0.020
300	0.058	0.030	0.028	0.024	0.043	0.034	0.030	0.025
350	0.067	0.035	0.033	0.029	0.047	0.037	0.032	0.028
400	0.072	0.042	0.038	0.034	0.051	0.046	0.041	0.035

APPENDIX A-4: Brine saturated Bandera and Scioto measured methane (CH_4) adsorption capacity at 23°C and variable pressure.

Pressure(Psia)	Methane Adsorbed (mmol/g)(Bandera)				Methane Adsorbed (mmol/g)(Scioto)			
	Dry	Brine Content at 20% NaCl Salinity			Dry	Brine Content at 20% NaCl Salinity		
		33%	65%	91%		33%	65%	91%
50	0.010	0.005	0.003	0.001	0.012	0.004	0.002	0.001
100	0.019	0.012	0.007	0.004	0.022	0.009	0.007	0.003
150	0.025	0.015	0.012	0.008	0.033	0.014	0.012	0.006
200	0.031	0.020	0.015	0.013	0.043	0.019	0.017	0.011
250	0.037	0.027	0.023	0.018	0.051	0.024	0.022	0.015
300	0.043	0.031	0.025	0.023	0.058	0.029	0.027	0.019
350	0.047	0.034	0.029	0.025	0.067	0.034	0.032	0.024
400	0.051	0.043	0.037	0.032	0.072	0.039	0.037	0.029

conferenceseries.com

Petroleum Engineering 2016

Young Researchers Forum

Mr/Ms. **Hayatu Bashir**

University of Salford, UK

for presenting the oral entitled

Theoretical fitting of experimental adsorption data from cored clay shale

at the "4th International Conference on Petroleum Engineering"
held during August 15-17, 2016 in London, UK

The award has been attributed in recognition of research paper quality, novelty and significance.

Srinu Babu Gedela
Conferenceseries LLC, USA


An ISO 9001:2008 certified journal
Thomson Reuters ResearcherId: P-8024-2015
The Board of
International Journal of Latest Trends in Engineering & Technology
is hereby awarding this certificate to
Hayatu Bashir
in recognition of the publication of the paper entitled
On void volume determination in clay rich shale
published In IJLTET Journal, Volume 7 Issue 2 July, 2016
ONLINE PEER REVIEWED JOURNAL
IJLTET
Dr. Priti Singla
Chief-Editor
Lucy Garg
Editor
IJLTET Board
International Journal of Latest Trends in Engineering & Technology
SN Education Society
www.ijltet.org
ISSN : 2278-621X (for online version)
ISSN : 2319-3778 (for printed version)


An ISO 9001:2008 certified journal
Thomson Reuters ResearcherId: P-8024-2015
The Board of
International Journal of Latest Trends in Engineering & Technology
is hereby awarding this certificate to
Hayatu Bashir
in recognition of the publication of the paper entitled
A comparative evaluation of adsoprtion isotherm in clay- dominated shale
published In IJLTET Journal, Volume 7 Issue 2 July, 2016
ONLINE PEER REVIEWED JOURNAL
IJLTET
Dr. Priti Singla
Chief-Editor
Lucy Garg
Editor
IJLTET Board
International Journal of Latest Trends in Engineering & Technology
SN Education Society
www.ijltet.org
ISSN : 2278-621X (for online version)
ISSN : 2319-3778 (for printed version)

STM JOURNALS
Journal of Petroleum Engineering & Technology
ISSN: 2231-1785(online), ISSN: 2321-5178(print)
Volume 6, Issue 3
www.stmjournals.com

Construction/Assembling of a Low Cost Adsorption Apparatus for Cored Clay Shales

H. Bashir, Y. Wang, A. Abbas*
School of Computing, Science and Engineering, University of Salford, Manchester, United Kingdom

Abstract

The secret to unlocking these reserves lies in accurate experimental data which in turn depends on the experimental method used. Recently many procedures such as manometric, volumetric and gravimetric have been developed to quantify adsorption. In this paper, we show how to construct/assemble a simple manometric adsorption apparatus for gas adsorption. The setup is inexpensive and can be built easily using part available in university laboratories. Furthermore, it can be used to measure adsorption capacity of different cored materials using different gases at low pressure (< 450 Psia). The laboratorial setup permits the measurement of gas adsorption equilibrium on cored samples with dimensions of 3-inch by 1.5 inch up to 450 Psia at laboratory temperature (23°C), and can also be used at higher temperatures (up to 45°C) by using a water bath.

Keywords: *Manometric apparatus, adsorption, clay rich shale*

****Author for Correspondence*** E-mail: h.b.bashir@edu.salford.ac.uk

INTRODUCTION

Since the inception of gas adsorption experiments till date, there have been a number of techniques used by various equipment vendors and laboratories (commercial or in-house manometric, gravimetric setup/instrument) and researchers (manometric, volumetric, gravimetric, chromatographic, temperature programmed desorption). The most widely used experimental method in shale adsorption is the manometric [1, 2, 3, 23] and volumetric method. [5, 10, 14] These methods are based on Boyle's law, and are very similar to porosity measurements using pycnometer [22].This technique is sometimes referred to as Sieverts method and can be designed as constant-volume (manometric) or constant pressure (volumetric) measurement [4]. They are widely used because of their simplicity and ease of construction. Commercial devices built based on these techniques include FY–KT 1000 isothermal adsorption apparatus based on the volumetric method [1] , automated Sieverts' apparatus known as the PCT-Pro-E&E from Setaram Instrumentation [5]. Adsorption apparatus based on other methods are the Rubotherm and Mettler-Toledo based on the gravimetric technique [6] and the mass balance [13,15].

Some laboratories apply in-house modifications to these devices and custom make them for specific experimental conditions like shale adsorption at high temperature [7, 16] and moisture equilibration [9]. Several studies have been conducted on such devices, for example in adsorption measurements using gravimetric techniques [8, 17, 18, 19].

In terms of modification and user designed equipment, several tactics were used by researchers [8, 11, 12 19, 20, 21]. Gasparik *et al*, 2012 modified their set up to enable sorption measurements at high temperatures, by separating the low-temperature zone (reference cell) and high temperature zone (sample cell) [8] . Li *et al.* (2015) however, developed a high-pressure gas adsorption–desorption instrument mounted on a constant-temperature oil bath [20]. Heller & Zoback, (2011) modified a conventional tri-axial machine to measure adsorption and gas permeability by incorporating a Quizix Series 1500 pump, using a method similar to volumetric adsorption principle, and an adsorption equipment where an isothermal multistep gas uptake process measures the storage capacity [11, 21]. For this purpose, adsorption equilibria of methane at 273 K at

